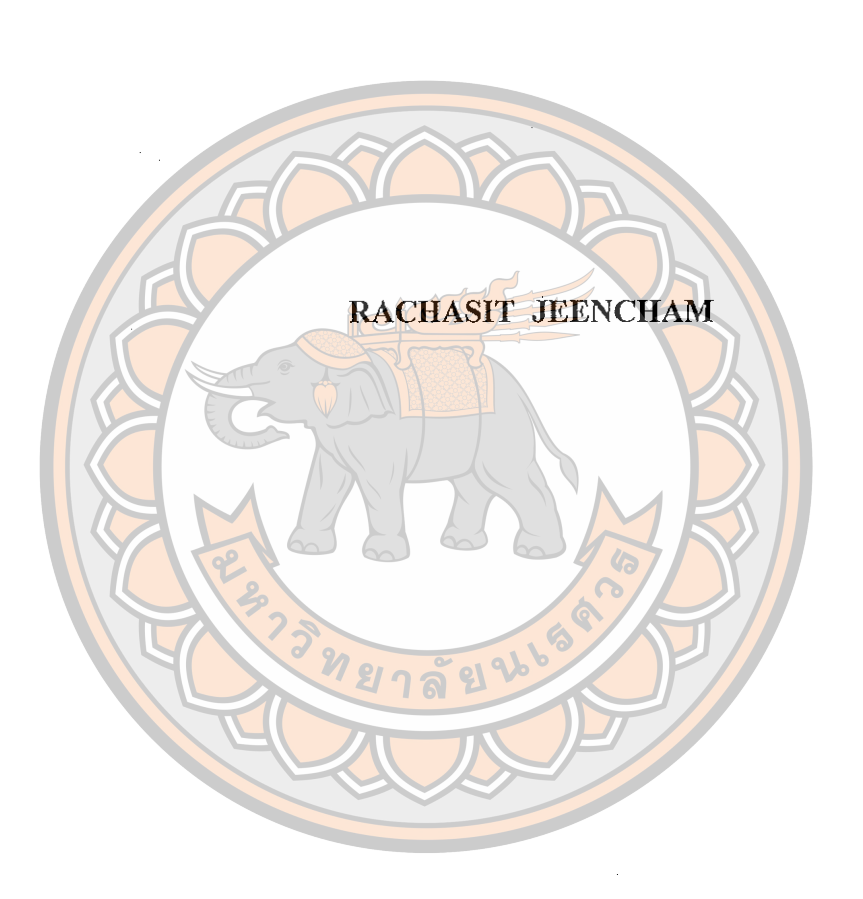
DEVELOPMENT OF SILK FIBROIN/CHITOSAN BLEND FILMS FOR CONTACT LENS-BASED OPHTHALMIC DRUG DELIVERY SYSTEM



A Thesis Submitted to the Graduate School of Naresuan University
in Partial Fulfillment of the Requirements
for the Doctor of Philosophy Degree in Pharmaceutical Sciences
July 2020

Copyright 2020 by Naresuan University

Thesis entitled "Development of silk fibroin/chitosan blend films for contact lensbased ophthalmic drug delivery system"

By Mr. Rachasit Jeencham

has been approved by the Graduate School as partial fulfillment of the requirements
for the Doctor of Philosophy Degree in Pharmaceutical Sciences
of Naresuan University

Oral Defense Committee
Nontaka Khorana Chair/External Examiner
(Associate Professor Nantaka Khorana, Ph.D.)
While Z. Advisor
(Associate Professor Waree Tiyaboonchai, Ph.D.)
Manda 5H H da Co-Advisor
(Associate Professor Magiote Sutheerawattananonda, Ph.D.)
Co-Advisor
(Professor Thomas Scheibel, Ph.D.)
Nordade l'apareles Internal Examiner
(Associate Professor Nanteetip Limpeanchob, Ph.D.)

Approved

(Professor Paisarn Muneesawang, Ph.D.)

Dean of the Graduate School

ACKNOWLEDGEMENT

I wish to express my deepest sincere appreciation to my advisor, Associate Professor Dr. Waree Tiyaboonchai, for her constructive guidance, patience, inspiring words, understanding and her insights in pharmaceutical sciences. I am thankful to my co-advisor, Associate Professor Dr. Manote Sutheerawattananonda (Suranaree University of Technology, Thailand) for his encouragement and invaluable advice. Also, I would like to acknowledge my co-advisor, Professor Dr. Thomas Scheibel from Universität Bayreuth (Germany), for his useful guidance, intellectual support, and his suggestions during the time I worked in Universität Bayreuth. Also, thank him for making the time and effort to continue this guidance after I got back to Naresuan University.

I acknowledge my supervisor, Dr. Martin Humenik, Germany for his generous guidance during the time I worked in Universität Bayreuth. His friendliness and responsibility helped me surviving in a faraway land.

I am also thankful to Associate Professor Dr.Nantaka Khorana (University of Phayao, Thailand) and Associate Professor Dr.Nanteetip Limpeanchob for their valuable suggestion to improve my work, and for being members of my external and internal examination committees, respectively.

I gratefully acknowledge the financial support by the financial support by Naresuan University and the Thailand Research Fund (TRF) under the Royal Golden Jubilee Ph.D. Program (Grant No. PHD/0044/2557). This research is also partially supported by the Center of Excellence for Innovation in Chemistry (PERCH-CIC), Commission on Higher Education, Ministry of Education, Thailand and German Academic Exchange Service (DAAD), Germany.

I am also thankful to all staff in all the related academic staff and technicians at the Naresuan University (Thailand), and Universität Bayreuth (Germany) for their helpful support throughout my study.

Lastly, but definitely not the least, I extend my sincere thanks to my parents for all their sacrifice in providing me the best possible education. Words are not enough to express my devotion and gratitude towards them and I hope I get same blessings, love and care from them for the rest of my life. Also, I have a great respect

and gratitude towards my friends from my graduate college, who have been a constant motivation and have been there with me during my tough times.

Rachasit Jeencham



Title DEVELOPMENT OF SILK FIBROIN/CHITOSAN BLEND

FILMS FOR CONTACT LENS-BASED OPHTHALMIC

DRUG DELIVERY SYSTEM

Author Rachasit Jeencham

Advisor Associate Professor Waree Tiyaboonchai, Ph.D.

Co - Advisors Associate Professor Manote Sutheerawattananonda, Ph.D.

Professor Thomas Scheibel, Ph.D.

Academic Paper Thesis Ph.D. in Pharmaceutical Sciences,

Naresuan University, 2019

Keywords Chitosan, Silk fibroin, Films, Contact lens, Ophthalmic drug

delivery system

ABSTRACT

More than 90% of currently marketed topical eye drops are in the form of solutions and suspensions because of their convenience and non-invasive application. However, a rapid drug clearance induced by a blink action leads to poor drug bioavailability with less than 5% of administered drugs entering the intraocular tissues. Therefore, to maintain therapeutic drug levels, frequent administration or large doses of eye drops are commonly required. However, this may reduce patient compliance, increase local and systemic side effects. In order to overcome this limitation of the low ocular bioavailability, chitosan/regenerated silk fibroin (CS/RSF) films a biomaterial for contact lenses-based ophthalmic drug delivery system were developed for a prolonged drug release by increasing the residence time of the drug on the ocular surface. CS/RSF films were prepared with polyethylene glycol 400 as a plasticizer by using a film casting technique. At optimal preparation conditions, CS/RSF films showed smooth surfaces with a highly visible light transparency of > 90%, which meet the visual requirement. CS/RSF films showed high water content, 59-65% by weight, good oxygen permeability (22-26 Barrers), and their Young's modulus and elongation at break were in the range of 3.8-6 Mpa and 113-135%, respectively. The CS/RSF films also could be sterilized by autoclave method as they possessed high thermal decomposition temperature of > 260°C which can be confirmed by both differential scanning calorimetry and thermogravimetric analysis. In addition, CS/RSF films showed no degradation in stimulated tear fluid containing lysozyme for 7 days and showed no cytotoxicity by MTT assay. CS/RSF films showed excellent physicochemical properties and non-cytotoxicity indicating their promising potential use as a biomaterial for daily disposable contact lenses.

Therefore, CS/RSF films were further developed and evaluated as a contact lenses-based ophthalmic drug delivery system; CS/RSF films coating with recombinant spider silk (RSS) and layer by layer (L-b-L) technique. Non-charged acetaminophen (APAP), negatively charged 5(6)-carboxyfluorescein (CF) and zwitterion rhodamine B (RB) were loaded as model drugs and their release was studies in vitro. Whereas non-charged APAP was not able to incorporate into the CS/RSF films, negatively charged CF and zwitterion RB were successfully loaded in the CS/RSF films. The CS/RSF ratio significantly affected the drug loading capacity and released characteristic profile of charged drug. 100CS/ORSF film showed the highest CF loading and prolonged CF release more than 12 h and 70CS/30RSF film showed the highest RB loading and prolonged RB release more than 12 h. Interestingly, RSS coatings made of the positively and negatively charged spider silk variants significantly increased the loading efficiency and prolonged drug release of negatively charged CF and zwitterion RB, respectively. Furthermore, L-b-L films made of CS and RSF also showed enhanced drug loading efficiency as well as prolonged release of RB for more than 12 h. However, these films revealed low oxygen permeability, thus being not appropriate for use as therapeutic contact lenses. Thus, RSS coated CS/RSF films is a benefit for increasing drug loading and prolong drug release efficiency of CS/RSF films.

In addition, we also investigated the drug loading capacity and drug release characteristic of hydrophilic drug. The diclofenac sodium (DS) is a nonsteroidal anti-inflammatory drug widely used to treat pain and inflammatory eye diseases. Therefore, DS was selected to load into the films by a soaking method. Due to the simplicity of films formation process, CS/RSF films were used for this study. The best conditions of DS loading are the loading time of 2 h and pH 6.5 of drug solution. The drug loading showed no effect on the intrinsic contact lens properties of CS/RSF films, which comply with the requirements for daily disposable contact lenses. The drug

loading capacity was found to be affected by the film RSF content and initial dug loading concentration. The higher the film RSF content or the dug loading concentration, the higher drug loading was achieved. With increasing of RSF content from 0 to 30% into the films, the amount of loaded DS increased from 12 to 23 µg. Furthermore, the prolong drug released within therapeutic level was obtained with increasing the film RSF content. Consequently, a fast released characteristic within a therapeutic level up to 3 h was observed with the 100CS/0RSF film. On the other hand, the 70CS/30RSF film demonstrated a significant prolonged drug release within therapeutic level up to 11 h. However, increasing the amount of loaded drug could not further prolong the DS release duration.

In conclusion, the CS/RSF films are promising as novel biomaterials for daily disposable contact lenses-based ophthalmic delivery, which is beneficial for reducing drug side effects and administration frequency as compared to eye drop and conventional contact lenses.

LIST OF CONTENTS

Chapte	er [.]	Page
I	INTRODUCTION	1
	Rationale of the study	1
	Objectives of the study	3
	Expected outputs of this study	3
	References	4
П	LITERATURE REVIEW	10
	Anatomy of the eye.	10
	Tears	11
	Lipid layer	12
	Aqueous layer	13
	Mucus layer	13
	Topical ocular administration	13
	Ocular barriers	14
	Precorneal barriers.	14
	High turnover rate	14
	Gel-like mucus layer	15
	Protein binding	15
	Cornea barrier.	15
	Blood-ocular barrier	16
	Ocular pharmacokinetics	16
	Ophthalmic drug delivery system	19
	Contact lenses based ophthalmic drug delivery system	20
	Definition of contact lenses	20
	Drug loading methods into daily disposable contact lenses	21
	Soaking of lens in drug solution	22
	Incorporation of drug-loaded colloidal nanoparticles	22

Chapter Chapte	Page
Copolymerization of the contact lens with functional	
monomers	22
Molecular imprinting	23
Ideal properties of daily disposable contact lenses-based	
ophthalmic drug delivery system	23
Lenses material for daily disposable contact lenses-based	
ophthalmic drug delivery system	24
Commercial contact lenses	24
New contact lenses material	27
Silk fibroin	28
Silk fibroin structure	28
Silk fibroin extraction	30
Silk fibroin characterization	
Films based silk fibroin	31
Chitosan	33
Chitosan structure	33
Chitosan extraction	33
Chitosan characterization.	34
Films based chitosan	35
Films formation	37
Films characterization	38
Model drugs	38
References	40

Chapter		Page
III PREPARATION A	ND CHARACTERIZATION OF	
CHITOSAN/RE	GENERATED SILK FIBROIN (CS/RSF)	
FILMS AS A BIO	OMATERIAL FOR CONTACT LENSES-	
BASED OPHTH	ALMIC DRUG DELIVERY SYSTEM	51
Abstract		51
Introduction		52
Materials and me	thods	53
		53
Preparation o	of RSF	54
Preparation o	f CS/RSF films	54
Thickness me	easurements	55
Morphology.		55
Light transpa	rency	55
Mechanical p	properties	55
	t	55
Thermal prop	Derties lity 0	56
Ion permeabi	lity 182	56
Oxygen perm	eability.	57
In vitro enzyi	natic degradation	57
Cytotoxicity	study	57
Statistical and	alysis	58
Results and discu	ssion	58
Appearances	and morphology of CS/RSF films	59
Light transpa	rency of CS/RSF films	59
Mechanical p	properties of CS/RSF films	62
Water conten	t of CS/RSF films	62
Thermal prop	perties of CS/RSF films	63
Ion permeahi	lity of CS/RSF films	65

Chapter	Page
Oxygen permeability of CS/RSF films	67
In vitro enzymatic degradation study	68
Cytotoxicity study	68
Conclusion	71
References	71
IV OPHTHALMIC DRUG DELIVERY SYSTEM BASED ON	
BIOGENIC MATERIALS	77
Abstract	77
Introduction	78
Materials and Methods	
Materials	
Preparation of CS/RSF films	80
Preparation of RSS coated CS/RSF films	80
Preparation of L-b-L films	81
Physicochemical characterization	
In vitro enzymatic degradation study	83
Drug loading procedure	
In vitro drug release	83
Statistical analysis	84
Results and discussion	84
CS/RSF films	84
Drug loading and in vitro release of CS/RSF films	84
Effect of drug loading on material properties	
of CS/RSF films	91
RSS-coated CS/RSF films	92
Material properties of RSS-coated CS/RSF films	92
Biodegradation of RSS-coated CS/RSF films	95

Chapter	Page
Drug loading and in vitro release of RSS-coated	
CS/RSF films	95
L-b-L films-based CS and RSF	98
Material properties of L-b-L films-based CS and RSF	98
Biodegradation of L-b-L films-based CS and RSF	100
Drug loading and in vitro release of L-b-L films-based	
CS and RSF	10
Conclusion	103
References	103
V DAILY DISPOSABLE CONTACT LENSE BASED ON	
CHITOSAN AND REGENERATED SILK FIBROIN	
FOR THE OPHTHALMIC DELIVERY OF	
DICLOFENAC SODIUM	110
Abstract	110
Introduction	11.
Materials and Methods	112
Materials	112
Preparation of CS/RSF films	112
Drug loading by soaking method	11:
In vitro drug release studies	113
Mathematical model for release kinetics and diffusion	
coefficient	114
Estimation of therapeutic dose	11
Physical properties of DS loaded CS/RSF films	11:
Statistical analysis	11:

Chapter	Page
Results and discussion	116
Drug loading capacity	116
In vitro drug release studies	119
Physical properties of DS loaded CS/RSF films	124
Conclusion	124
References	125
VI CONCLUSION	130 132

LIST OF TABLES

Table		Page
2.1	Ideal properties of daily disposable contact lenses-based	
	ophthalmic drug delivery system requirement	24
2.2	Commercial synthetic polymers contact lens	26
2.3	Amino acid composition of Bombyx mori silk fibroin	29
2.4	Basic films physicochemical properties and their corresponding	
	characterization methods	37
3.1	Light transparency of CS/RSF films	61
3.2	Mechanical properties and water content of CS/RSF films	63
3.3	Percentage of remaining weight of CS/RSF films after incubation	
	in STF Containing lysozyme	68
4.1	Effect of drug loading time on loading capacity of CS/RSF films	87
4.2	Effect of pH of drug solution on loading capacity of CS/RSF films	87
4.3	Physical properties of CS/RSF films and drug-loaded CS/RSF films	91
4.4	Properties of uncoated and RSS coated CS/RSF films	93
4.5	Drug loading into uncoated and RSS-coated CS/RSF films	96
4.6	Properties of L-b-L films-based CS and RSF	100
4.7	Drug loading into multilayer films-based CS and RSF	101
5.1	Effect of drug loading time on drug loading capacity	117
5.2	Effect of pH of drug solution on drug loading capacity	118
5.3	Effect of concentration of initial drug solution on drug loading	
	capacity	118
5.4	Drug release kinetic data of DS loaded CS/RSF films	121
5.5	Drug release kinetic data of 30CS/70RSF films with different loaded	
	DS content.	123
5.6	Physical properties of 30CS/70RSF films and DS-loaded	
	30CS/70RSF films	124

LIST OF FIGURES

rigures		Page
2.1	The human eye	10
2.2	Model of tear film	12
2.3	Model showing the movement of drug into the eye after topical	
	administration. (BAB, blood-aqueous barrier; BRB, blood-	
	retinal barrier)	14
2.4	The structure of cornea	15
2.5	Schematic presentation of the ocular structure showing	
	a summary of ocular pharmacokinetics	17
2.6	The permeation mechanisms across cornea. Passive paracellular	
	and transcellular permeation. Transporter mediated influx	
	and efflux across cell membrane in the apical (1 and 2) and	
	basolateral (3 and 4) side, respectively	19
2 <mark>.7</mark> <	Drug loading methods into daily disposable contact lenses	21
2.8	Schematic structure of a fibroin unit	29
2.9	The structure of chitosan	33
2.10	Chemical structures of CF, RB, APP and DS	39
3.1	SEM micrographs of surface and cross-section of CS/RSF films	
	(×1000 magnification)	60
3.2	Light transparency of CS/RSF films with indicated blend ratios	61
3.3	DSC curve of CS/RSF films with indicated blend ratios	64
3.4	TGA curve of CS/RSF films with indicated blend ratios,	
	(A) Original curve and (B) Adjusted curve after moisture	
	removal	66
3.5	The plots of NaCl concentration in the receiving chamber versus	
	time for CS/RSF films used in ion permeability study	67
3.6	Cell viability of HCECs after exposed to CS/RSF films for 24 h	69

LIST OF FIGURES (CONT.)

igures		rage
3.7	Optical micrographs of HCECs after 24 h incubation with film	
	and after 2 h incubation with MTT solution	
	(×4 magnification).	70
4.1	Formulation of L-b-L films-based CS and RSF	81
4.2	SEM micrographs of the surface and cross-section of negatively	
	charged CF loaded CS/RSF films, pH 6.5, for 3 h	
	(×3000 magnification)	88
4.3	SEM micrographs of the surface and cross-section of zwitterion	
	RB loaded CS/RSF films, pH 6.5, for 3 h	
	(×3000 magnification)	89
4.4	Cumulative release of CF (A) and RB (B) from	
	CS/RSF blended films.	90
4.5	Fluorescence micrographs of RSS coated CS/RSF films	
	(×10 magnification)	93
4.6	(A) Light transparency of uncoated and RSS-coated	
	CS/RSF films, SEM micrographs of cross-section of	
`	RSS-coated CS/RSF films: (B) eADF4(C16)-coated CS,	
	(C) eADF4(C16)-coated CS/RSF: 70/30, (D) eADF4(κ16)-	
	coated CS, (E) eADF4(κ16)-coated CS/RSF: 70/30	
	(×3000 magnification)	94
4.7	DSC curve of uncoated and RSS coated CS/RSF films	95
4.8	Cumulative release of CF (A) and RB (B) from uncoated and	
	RSS coated CS/RSF blended films	97
4.9	(A) SEM micrographs of surface and cross-section of L-b-L	
	films (×1000 magnification) (B) Light transparency of	
	L-b-L films	99
4.10	DSC curve of L-b-L films-based CS and RSF	100

LIST OF FIGURES (CONT.)

Figures		Page
4.11	Cumulative release of CF in (A) and RB in (B) from	
	the L-b-L films	102
5.1	SEM micrographs of the surface and cross-section of DS loaded	
	CS/RSF films, soaking in 125 µg/ml of DS solution,	
	pH 6.5, for 2 h (×5000 magnification)	119
5.2	Cumulative DS release from CS/RSF films	121
5.3	DS release from CS/RSF films compared with therapeutic level	122
5.4	Cumulative DS release from 30CS/70RSF films with different	
	loaded DS content	122
5.5	DS release from 70CS/30RSF films with different loaded DS	
	content compared with therapeutic level	123

ABBREVIATIONS

% = percentage

°C = degree Celsius

μg = microgram μl = microliter

 $\mu m = micrometer$

ANOVA = analysis of variance

APAP = acetaminophen

ASTM = American Society for Testing and Materials

BPE = bovine pituitary extract

CaCl₂ = calcium chloride

Ca(No₃)₂ calcium nitrate

CF = 5(6)-carboxyfluorescein

CS = chitosan

CO₂ = carbon dioxide

D = diffusion coefficient

Da dalton

DI water = deionized water

DMSO = dimethyl sulfoxide

DS = diclofenac sodium

DSC = differential scanning calorimetry

EtOH = ethanol

EGF = epidermal growth factor

FDA = Food and Drug Administration

FTIR = Fourier transform infrared spectroscopy

g = gram

GdmSCN = guanidinium isothiocynate

h = hour

HCECs = human corneal epithelial cells line

 H_2O = water

ABBREVIATIONS (CONT.)

kDa = kilodaltons

K-SFM = keratinocyte serum-free medium

kV = kilovolt

M = Molar

mg = milligram

min = minute

L-b-L = layer by layer

LWB = long-wavelength blue region

ml = milliliter

mm = millimeter

Mpa megapascal

MTT 3-(4,5-dimethylthiazol-2-yl)-2,5-diphenyltetrazolium bromide

MWCO = molecular weight cut-off

nm = manometer

NHS = succinimidyl ester

PBS = phosphate buffer saline

PEG400 = polyethylene glycol 400

pHEMA = poly (2-hydroxyethyl methacrylate)

POLTF = post-lens tear film

RO = reverse osmosis

rpm = revolutions per minute

RSF = regenerated silk fibroin

RSS = recombinant spider silk

RB = rhodamine B

s = second

SD = standard deviation

SiH = silicone based-hydrogel

SEM = scanning electron microscopy

STF = stimulated tear fluid

ABBREVIATIONS (CONT.)

SWB = short-wavelength blue region

Td = decomposition temperature

Tg = glass transition temperature

UV = ultraviolet

UV-VIS = Ultraviolet-visible

w/v = weight by volume

w/w = weight by weight



CHAPTER I

INTRODUCTION

Chapter I consists of three sections, including the rationale, the objectives, and the expected outputs of the study. The following sections give detailed information on each part.

Rationale of the study

Topical eye drops in the form of solutions and suspensions are a common approach to treat ocular disorders because of their convenient and non-invasive application (1-3). However, a rapid drug clearance induced by a blink action leads to poor drug bioavailability with less than 5% and 0.5% of administered lipophilic drugs and hydrophilic drugs, respectively, entering the intraocular tissues (2, 4-7). Therefore, to maintain sustained therapeutic drug levels, frequent administration or large doses of eye drops are commonly required. However, this may reduce patient compliance, increase local and systemic side effects (2, 8-10).

Recently, daily disposable contact lenses have been proposed as alternative ophthalmic drug delivery system (11-15). This approach offers several advantages including administration without any surgery, increased drug residence time on the ocular surface and reduced application frequency (13, 16-18). Prior studies focused on soaking commercial contact lenses in hydrophilic ocular drug solutions, such as diclofenac sodium, cysteamine, brimonidine, fluconazole, and moxifloxacin hydrochloride, followed by insertion into the eye (19-22). Contact lenses are placed directly on the cornea with a thin 5-10 micron thick post-lens tear film (POLTF) layer in between, which makes contacts a natural choice for delivering drugs to the cornea. The released drug by the contact towards the cornea surface is trapped in the POLTF for extended duration into the cornea leading to improved drug bioavailability, ~50% (23). However, these lenses have some limitations including low drug loading and a fast release characteristic within 1-3 h. This suggested that commercial contacts lenses are not ideal for drug delivery due to the short release durations which may necessitate

wearing multiple lenses each day, reducing the viability of this approach. Therefore, developing a new daily disposable contact lenses to effectively deliver the hydrophilic drug in a prolonged drug release pattern is still a challenging task.

To overcome the limitation of conventional contact lenses, we have proposed natural polymers as a potential biomaterial for contact lenses. This is due to their potential advantages of non-toxicity, good biocompatibility, low inflammatory, high oxygen permeability, high optical transparency, high wettability, and good chemical and mechanical stabilities that could meet the required properties of daily disposable contact lenses. Furthermore, they can be used as daily disposable therapeutic contact lenses (24-37). Chitosan (CS) and regenerated silk fibroin (RSF) are natural polymers of interest for creating the daily disposable contact lenses-based ophthalmic drug delivery system. CS is a natural polycationic linear polysaccharide derived from the deacetylation of chitin (38). RSF, which is derived from degumming of the Bombyx mori cocoons and dissolution of silk fibroin respectively, is a protein mainly comprised of amino acids glycine, alanine, and serine (39-40). CS films showed good flexibility, high light transparency and high water content but it is highly sensitive to lysozyme degradation (30-33, 41). RSF films offer the advantages of high oxygen permeability, non-toxicity, excellent biocompatibility, and also excellent wound healing properties, but it is quite brittle (24-29). Therefore, the blending between CS and RSF is a possible solution to improve properties of films for creating the materials of daily disposable therapeutic contact lenses. Moreover, the blending of CS with RSF shows a good compatibility between two different materials by hydrogen bonding interaction (34, 38).

To broader the applicability of the drug delivery system, negatively and positively charged recombinant spider silk (RSS) proteins were used to coat the CS/RSF films. The used RSS variants are based on the consensus sequence of the repetitive part of the dragline silk protein ADF4 of the European garden spider (Araneus diadematus) and possess a well-dominated excellent biocompatibility, non-toxicity, and non-immune reactivity (42-49). The negatively and positively charged RSS effectively accommodated oppositely charged drugs. The variant eADF4(C16) is polyanionic consisting of 16 repeats of module C (sequence: GSSAAAAAAAASGP GGYGPENQGPSGPGGYGPGGP). In contrast, eADF4(κ16) is polycationic consisting

of module κ (sequence: GSSAAAAAAAAASGPGGYGPKNQGPSGPGGYGPGGP) in which all glutamic acid residues are replaced by lysine ones (49-53). In addition, the development of the layer-by-layer (L-b-L) films-based CS and RSF was also investigated for contact lenses-based ophthalmic drug delivery system.

Nowadays, there are very few reports in published literatures of therapeutic contact lenses using combinations of natural polymers (33, 38). Furthermore, there were no reports on combinations of CS/RSF that have been used to produce the contact lenses. Therefore, the purpose of this study was to develop CS/RSF films as a new biomaterial for contact lenses-based ophthalmic drug delivery system. Typically, the topical ophthalmic drugs for the treatment of eye disease are hydrophilic substances (54-57). Consequently, the substances with various charged, non-charged acetaminophen (APAP), negatively charged 5(6)-carboxyfluorescein (CF) and zwitterion charged rhodamine B (RB) were used as a hydrophilic substance model. In addition, diclofenac sodium (DS), a hydrophilic anti-inflammatory agent was also used as a hydrophilic model drug. The physicochemical properties of CS/RSF films were investigated by measuring various properties such as thickness, morphology, chemical interaction, light transparency, mechanical properties, water content, oxygen permeability, thermal properties and enzyme degradation. In addition, cytotoxicity, drug lading and drug release characteristic were also studied.

Objectives of the study

- 1. To develop and characterize the processing parameters effecting the physicochemical properties of CS/RSF films and RSS coated CS/RSF films
 - 2. To investigate the cytotoxicity of CS/RSF films

ยาลัยง

- 3. To study the effects of drug loading parameters on drug loading capacity
- 4. To study in vitro drug release characteristics

Expected outputs of this study

The expected outputs of this study are to obtain the CS/RSF films as a new biomaterial for daily disposable contact lenses-based ophthalmic drug delivery system. The CS/RSF films can be enhanced the drug loading capacity and prolong the drugs

release, which is beneficial for reducing drug side effects and administration frequency as compared to eye drops and conventional contact lenses.

References

- 1. Bourlais CL, Acar L, Zia H, Sado PA, Needham T, Leverge R. Ophthalmic drug delivery systems. Progress Retinal Eye Research. 1998;17(1):33-58.
- 2. Lang JC. Ocular drug delivery conventional ocular formulations. Advanced Drug Delivery Reviews. 1995;16(1):39-43.
- 3. Ali M, Byrne ME. Challenges and solutions in topical ocular drug delivery systems. Expert Opinion on Drug Delivery. 2008;1(1):145-61.
- 4. Deshpande SG, Shirolkar S. Sustained release ophthalmic formulations of pilocarpine. Journal of Pharmacy and Pharmacology. 1989;41(3):197-200.
- 5. Geroski DH, Edelhauser HF. Drug delivery for posterior segment eye disease. Investigative Ophthalmology & Visual Science. 2000;41(5):961-4.
- 6. Hyun JJ, Anuj C. Ophthalmic drug delivery by contact lenses. Expert Review of Ophthalmology. 2012;7(3):199-201.
- 7. Zhang W, Prausnitz M, Edwards A. Model of transient drug diffusion across cornea. Journal of Controlled Release. 2004;99:241-58.
- 8. Winfield AJ, Jessiman D, Williams A, Esakowitz L. A study of the causes of non-compliance by patients prescribed eyedrops. British Journal of Ophthalmology. 1990;74(8):477-80.
- 9. Barbu E, Verestiuc L, Nevell TG, Tsibouklis J. Polymericmaterials for ophthalmic drug delivery: trends and perspectives. Journal of Materials Chemistry. 2006;16(36):3439-43.
- 10. Lin HR, Sung KC. Carbopol/pluronic phasechange solutions for ophthalmic drug delivery. Journal of Controlled Release. 2000;69(3):379-88.
- 11. Maulvi FA, Soni TG, Shah DO. A review on therapeutic contact lenses for ocular drug delivery. Drug Delivery. 2016;23(8):3017-26.
- 12. Xinming L, Yingde C, Lloyd AW, Mikhalovsky SV, Sandeman SR, Howel CA, Liewen L. Polymeric hydrogels for novel contact lens-based ophthalmic drug delivery systems: a review. Cont Lens Anterior Eye. 2008;31(2):57-64.

- 13. Guzman-Aranguez A, Colligris B, Pintor J. Contact lenses: Promising devices for ocular drug delivery. Journal of Ocular Pharmacology and Therapeutics. 2013;29(2):189-99.
- 14. Gulsen D, Chauhan A. Dispersion of microemulsion drops in HEMA hydrogel: a potential ophthalmic drug delivery vehicle. International Journal of Pharmaceutics. 2005;292(1-2):95-117.
- 15. Tieppo A, Pate KM, Byrne ME. In vitro controlled release of an anti-inflammatory from daily disposable therapeutic contact lenses under physiological ocular tear flow. European Journal of Pharmaceutics and Biopharmaceutics. 2012;81(1):170-7.
- 16. Karlgard CCS, Wong NS, Jones LW, Moresoli C. In vitro uptake and release studies of ocular pharmaceutical agents by silicon-containing and p-HEMA hydrogel contact lens materials. International Journal of Pharmaceutics. 2003;257(1):141-51.
- 17. Lee D, Cho S, Park HS, Kwon I. Ocular drug delivery through pHEMA-hydrogel contact lenses co-loaded with lipophilic vitamins. Scientific Reports. 2016;6:34194.
- 18. McDermott ML, Chandler JW. Therapeutic uses of contact lenses. Survey of Ophthalmology. 1989;33(5):381-94.
- 19. Hsu K-H, Fentzke RC, Chauhan A. Feasibility of corneal drug delivery of cysteamine using vitamin E modified silicone hydrogel contact lenses. European Journal of Pharmaceutics and Biopharmaceutics. 2013;85(3, Part A):531-40.
- 20. Peng CC, Kim J, Chauhan A. Extended delivery of hydrophilic drugs from silicone-hydrogel contact lenses containing vitamin E diffusion barriers. Biomaterials. 2010;31(14):4032-47.
- 21. Sharma J. Moxifloxacin loaded contact lens for ocular delivery an in vitro study; 2018.
- 22. Hu X, Hao L, Wang H, Yang X, Zhang G, Wang G, Zhang X. Hydrogel contact lens for extended delivery of ophthalmic drugs. International Journal of Polymer Science. 2011;2011:814163.

- 23. Gause S, Hsu KH, Shafor C, Dixon P, Powell KC, Chauhan A. Mechanistic modeling of ophthalmic drug delivery to the anterior chamber by eye drops and contact lenses. Advances in Colloid and Interface Science. 2016;233:139-54.
- 24. Minoura N, Tsukada M, Nagura M. Fine structure and oxygen permeability of silk fibroin membrane treated with methanol. Polymer. 1990;31(2):265-9.
- 25. Minoura N, Tsukada M, Nagura M. Physico-chemical properties of silk fibroin membrane as a biomaterial. Biomaterials. 1990;11(6):430-4.
- 26. Sashina ES, Golubikhin AY, Novoselov NP, Tsobkallo ES, Zaborskii M, Goralskii Y. Study of a possibility of applying the films of the silk fibroin and its mixtures with synthetic polymers for creating the materials of contact lenses. Russian Journal of Applied Chemistry. 2009;82(5):898-904.
- 27. Liu TL, Miao JC, Sheng WH, Xie YF, Huang Q, Shan YB, Yang JC. Cytocompatibility of regenerated silk fibroin film: a medical biomaterial applicable to wound healing. J Zhejiang Univ Sci B. 2010;11(1):10-6.
- 28. Ju HW, Lee OJ, Lee JM, Moon BM, Park HJ, Park YR, Lee MC, Kim SH, Chao JR, Ki CS, et al. Wound healing effect of electrospun silk fibroin nanomatrix in burn-model. International Journal of Biological Macromolecules. 2016;85:29-39.
- 29. Li M, Lu S, Wu Z, Tan K, Minoura N, Kuga S. Structure and properties of silk fibroin–poly(vinyl alcohol) gel. International Journal of Biological Macromolecules. 2002;30(2):89-94.
- 30. Caner C, Vergano PJ, Wiles JL. Chitosan film mechanical and permeation properties as affected by acid, plasticizer, and storage. Journal of Food Science. 1998;63(6):1049-53.
- 31. Luangbudnark W, Viyoch J, Laupattarakasem W, Surakunprapha P, Laupattarakasem P. Properties and biocompatibility of chitosan and silk fibroin blend films for application in skin tissue engineering. ScientificWorldJournal. 2012;2012:697201.
- 32. Kweon H, Ha HC, Um IC, Park YH. Physical properties of silk fibroin/chitosan blend films. Journal of Applied Polymer Science. 2001;80(7):928-34.
- 33. Shi X-Y, Tan T-W. New Contact Lens Based on Chitosan/Gelatin Composites. Journal of Bioactive and Compatible Polymers. 2004;19(6):467-79.

- 34. Moraes MAd, Nogueira GM, Weska RF, Beppu MM. Preparation and characterization of insoluble silk fibroin/chitosan blend films. Polymers. 2010;2(4):719.
- 35. Dalia MNA, Ahmed Abd E-b, Samia HS, Mohamed AEN. Chitosan mucoadhesive buccal films: Effect of different casting solvents on their physicochemical properties. International Journal of Pharmacy and Pharmaceutical Sciences. 2016;8(9):231-6.
- 36. Preethi GB, Prashanth K. Design and evaluation of controlled-release ocular inserts of brimonidine tartrate and timolol maleate. International Journal of Pharmacy and Pharmaceutical Sciences. 2016;9(1): 79.
- 37. Aya MD, Hamdy MD, Amal SMAE-e, Maha KAK. Fabrication of bioadhesive ocusert with different polymers: Once a day dose. International Journal of Applied Pharmaceutics. 2018;10(6):309.
- 38. Sashina ES, Janowska G, Zaborski M, Vnuchkin AV. Compatibility of fibroin/chitosan and fibroin/cellulose blends studied by thermal analysis. Journal of Thermal Analysis and Calorimetry. 2007;89(3):887-91.
- 39. Bini E, Knight DP, Kaplan DL. Mapping Domain Structures in silks from insects and spiders related to protein assembly. Journal of Molecular Biology. 2004;335(1):27-40.
- 40. Mukhamedzhanova MY, Takhtaganova DB, Pak TS. Properties of concentrated solutions of fibroin and its derivatives. Chemistry of Natural Compounds. 2001;37(4):377-80.
- 41. Verheul RJ, Amidi M, van Steenbergen MJ, van Riet E, Jiskoot W, Hennink WE. Influence of the degree of acetylation on the enzymatic degradation and in vitro biological properties of trimethylated chitosans. Biomaterials. 2009;30(18):3129-35.
- 42. Römer L, Scheibel T. Spinnenseidenproteine: Grundlage für neue Materialien. Chemie in unserer Zeit. 2007;41(4):306-14.
- 43. Vollrath F, Barth P, Basedow A, Engstrom W, List H. Local tolerance to spider silks and protein polymers in vivo. In Vivo. 2002;16(4):229-34.
- 44. Leal-Egana A, Scheibel T. Silk-based materials for biomedical applications. Biotechnol Appl Biochem. 2010;55(3):155-67.

- 45. Allmeling C, Jokuszies A, Reimers K, Kall S, Choi CY, Brandes G, Kasper C, Scheper T, Guggenheim M, Vogt PM. Spider silk fibres in artificial nerve constructs promote peripheral nerve regeneration. Cell Prolif. 2008;41(3):408-20.
- 46. Spiess K, Lammel A, Scheibel T. Recombinant spider silk proteins for applications in biomaterials. Macromol Biosci. 2010;10(9):998-1007.
- 47. Humenik M, Smith A, Thomas S. Recombinant spider silks-biopolymers with potential for future applications Polymers. 2011;3:640-61.
- 48. Slotta U, Tammer M, Kremer F, Koelsch P, Scheibel T. Structural analysis of spider silk films. Supramolecular Chemistry. 2006;18(5):465-71.
- 49. Blüm C, Scheibel T. Control of drug loading and release properties of spider silk Sub-Microparticles; 2012.
- 50. Huemmerich D, Helsen CW, Quedzuweit S, Oschmann J, Rudolph R, Scheibel T. Primary structure elements of spider dragline silks and their contribution to protein solubility. Biochemistry. 2004;43(42):13604-12.
- 51. Lammel A, Schwab M, Hofer M, Winter G, Scheibel T. Recombinant spider silk particles as drug delivery vehicles. Biomaterials. 2011;32(8):2233-40.
- 52. Hofer M, Winter G, Myschik J. Recombinant spider silk particles for controlled delivery of protein drugs. Biomaterials. 2012;33(5):1554-62.
- 53. Doblhofer E, Scheibel T. Engineering of recombinant spider silk proteins allows defined uptake and release of substances. J Pharm Sci. 2015;104(3):988-94.
- 54. Lindell K, Engblom J, Engström S, Jonströmer M, Carlsson A. Influence of a charged phospholipid on the release pattern of timolol maleate from cubic liquid crystalline phases. In: Lindman B, Ninham BW, editors; Darmstadt (pp. 111-8). N.P.: Steinkopff; 1998.
- 55. Hirano T, Yasuda S, Osaka Y, Kobayashi M, Itagaki S, Iseki K. Mechanism of the inhibitory effect of zwitterionic drugs (levofloxacin and grepafloxacin) on carnitine transporter (OCTN2) in Caco-2 cells. Biochimica et Biophysica Acta (BBA) Biomembranes. 2006;1758(11):1743-50.
- 56. Suzuki T, Yamamoto T, Ohashi Y. The antibacterial activity of levofloxacin eye drops against staphylococci using an pharmacokinetic model in the bulbar conjunctiva. Journal of Infection and Chemotherapy. 2016;22(6):360-5.

57. Patidar N, Rathore MS, Sharma DK, Middha A, Gupta VB. Transcorneal permeation of ciprofloxacin and diclofenac from marketed eye drops. Indian journal of pharmaceutical sciences. 2008;70(5):651-4.



CHAPTER II

LITERATURE REVIEW

Anatomy of the eye

The human eye is a slightly asymmetrical globe, about an inch in diameter. It can be divided into the anterior and the posterior segments (1). The anterior segments include the cornea, pupil, lens, iris, sclera, ciliary body, and conjunctiva. The posterior segments comprise the choroid, retina, macular, fovea and vitreous body. Behind the eye, the optic nerve carries electrical impulses to the brain (Figure 2.1).

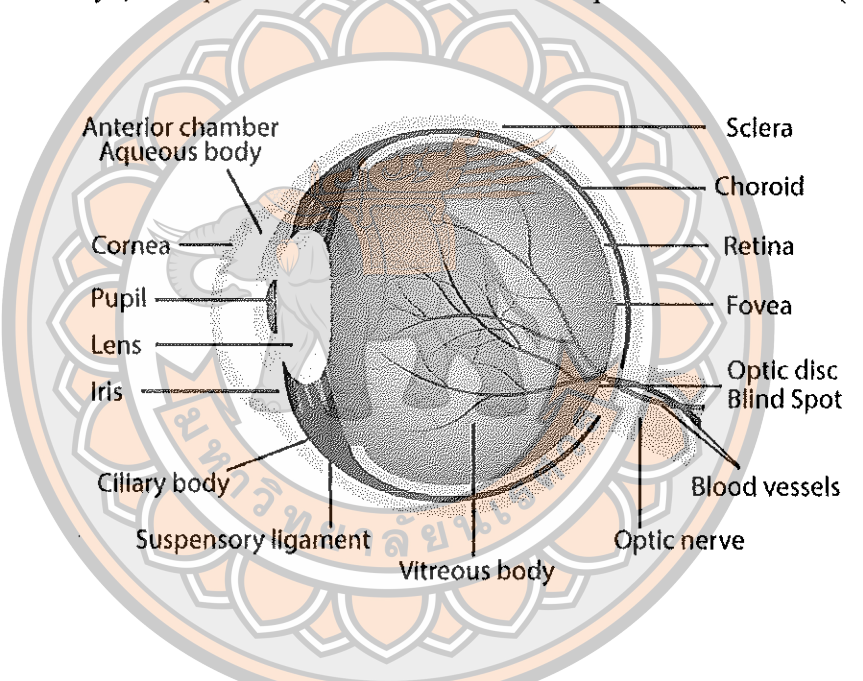


Figure 2.1 The human eye

The lacrimal functional unit includes the lacrimal glands, ocular surface (cornea and conjunctiva), eyelids, meibomian glands, and associated sensory and motor nerves. This unique physiology constrains such as the blinking reflex, lachrymal secretion and nasolacrimal drainage that are the barriers to remove the drug from the ocular surface for topical administration. The short residence time (only a few minutes) for drug absorption leading to ocular bioavailability is very low (less than 5%).

Tears

The tears, also known as tear film, are an extracellular fluid that cover the surface epithelial cell and forming the anterior component of the ocular surface. Under normal condition, the volume of tear fluid is around 5 - 10 µl and the secretion rate is about 1.2 µl per minute, with a turnover rate of approximately 16% per minute (2). The tears can be divided into three type including basal, reflex and crying tears. The basal tears are secreted by accessory lacrimal gland and distributed cover the cornea by blinking of the eye lid while the reflex tear is secreted by main lacrimal gland. The reflex tears is resulted from the corneal or blink reflex which occur at a rapid rate as 0.1s. The corneal or blink reflex is an involuntary blinking of the eyelid elicited by the stimulation of the cornea such as touching, foreign body, and foreign particle. The blink reflex is a true reflex, with a sensory afferent limb, intervening synapses, and a motor efferent. The afferent limb of the blink reflex is mediated by sensory fiber of the supraorbital branch of the ophthalmic division of the trigeminal nerve (cranial nerve V1) and the efferent limb by motor fibers of the facial nerve (cranial nerve VII). Just as with the corneal reflex, ipsilateral electrical stimulation of the supraorbital branch of the trigeminal nerve elicits a facial nerve (eye blink) response bilaterally. Stimulation of the ipsilateral supraorbital nerve results in an afferent volley along the trigeminal nerve to both the main sensory nucleus of V (mid-pons) and the nucleus of the spinal tract of V (lower pons and medulla) in the brainstem (3).

Although small in volume, the tear fluid is an extremely complex biological mixture containing proteins/peptides, electrolytes, lipids, mucin, and small molecule metabolites. The sources for the tears include the main and accessory lacrimal glands, ocular surface epithelial cells, Meibomian glands, goblet cells, and an ultrafiltrate of blood all contribute to the composition of the tear fluid. Thus, an extensive literature exists reporting various substances (inflammatory mediators, cytokines, growth factors, invading white cells, remodelling enzymes, mucin, and complement component) that have been detected in tears in various disorders (2, 4).

Generally, the tear film is composed of three layers: the outermost lipid layer, the middle aqueous layer, and the innermost mucus layer (Figure 2.2). Each layer contains various macromolecules that have specific role and assist in maintaining ocular health and function of the eye.

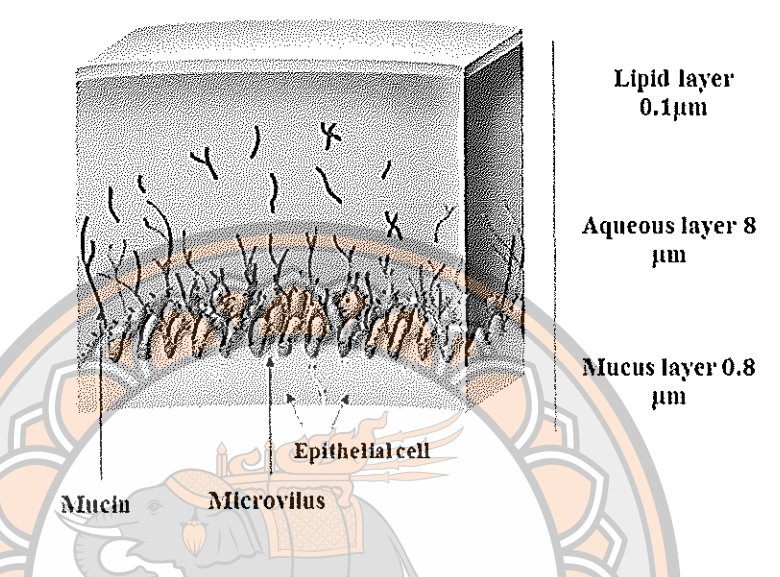


Figure 2.2 Model of tear film

Lipid layer

The lipid layer is the outermost layer that consists of polar and non-polar lipid which produced by meibomian gland in the eye. These meibomian glands are lined in the parallel to each other in the upper and lower tarsal plates, perpendicular to the lid margins (5). The polar lipid, which is closest to the external environment, is composed of phospholipids such as phosphatidylcholine, phosphatidylethanolamine and sphingosine, and makes up less than 10% of lipid layer. In contrast, the non-polar lipid, which is located closest to the aqueous layer and forms the major component of the lipid layer, is composed of cholesterol, cholesterol ester, mono-di-triglyceride and hydrocarbon. This layer is approximately 0.1µm thick that serves as a protective barrier for both the eye and the tear film from foreign contaminants. In addition, it provides stability for the tear film as it prevents the evaporation of tears when eyelids are opened, as well as maintaining a smooth tear film for the refraction of incoming light. Lastly, the lipid layer acts as a lubricant which assists in eyelid movement during the process of blinking.

Aqueous layer

The aqueous layer is the middle layer that produced by the lacrimal gland in the eye. The aqueous layer makes up the bulk of the tear film, with a thickness of about 6-8 µm and is composed of water and various water-soluble proteins, vitamins, cytokines, immunoglobulins, hormones, electrolytes and metabolites (4). The various electrolytes present in the aqueous layer include sodium, potassium, calcium, magnesium, bicarbonates, chloride, and phosphate ions. These electrolytes regulate tear osmolality, as well as acting as a buffer to maintain the physiological pH of tears. In addition, more than 400 proteins have been identified in human tear fluid. These different proteins and antimicrobial agents in the aqueous layer are largely responsible for the prevention of viral and bacterial infections in the eye.

Mucus layer

The mucin innermost layer is 0.8-1.0 µm thick that contains immunoglobulins, enzymes, urea, salts, and glucose. Mucins are secreted from conjunctival goblet cells, which form the mucin layer to maintain a wettable of corneal surface. Mucins are large glycoproteins with molecular weights ranging from 3 × 10⁵ - 4 × 10⁷ kDa and are classified as transmembrane or secretory mucins. Transmembrane mucins form a protective barrier against pathogens at cell-tear film interface, whereas secretory mucins move within the tear film. Moreover, this layer can be lubricated the palpebral conjunctiva leading to smooth movement of the eyelid during blinking.

Topical ocular administration

Most ocular medications may be administered topically in order to treat ocular disorders. This route is often preferred for the management of various pathological diseases that affect the anterior chamber of the eye, for two main reasons including, it is more conveniently administered and provides a higher ratio of ocular to systemic drug level (6). Typically topical ocular drug administration is accomplished by eye drops, but they have only a short contact time on the eye surface that the result from precorneal barrier leading to low ocular bioavailability (Figure 2.3). The contact, and thereby duration of drug action, can be prolonged by formulation design (e.g. gels, ointments, and inserts). Usually, 1-5 % of the instilled dose is absorbed and only 1% reaches the aqueous humor.

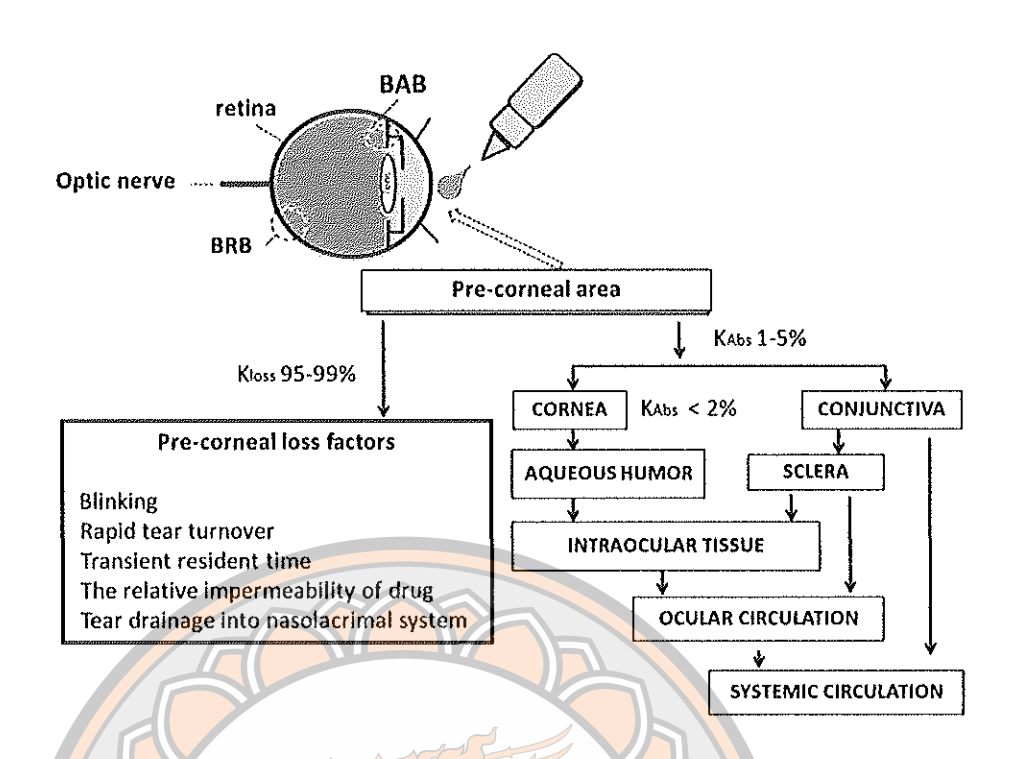


Figure 2.3 Model showing the movement of drug into the eye after topical administration. (BAB, blood-aqueous barrier; BRB, blood-retinal barrier)

Ocular barriers

Compared with drug delivery to the other part of the body, ocular drug delivery has significant challenges because they have various ocular barriers. The almost of these ocular barrier is occurred by the unique of ocular anatomy and physiology that a result of it a challenging task for drug delivery scientists. These barriers are specific depending upon the route of administration such as topical, systemic and injectable. The ocular barriers are divided into three parts including precorneal barrier, cornea barrier and blood ocular barrier.

Precorneal barriers

The loss of drug from the precorneal area is a result of drainage, tear secretion, non-corneal absorption and corneal absorption rate process. There are three possible of the precorneal barriers causing loss of drug.

High turnover rate

As the lacrimal functional unit function, the basal tear flow is $\sim 1.2 \mu l/min$ (0.5–2.2 $\mu l/min$). This results in a tear turnover rate of 16% per minute during waking

hours. Reflex stimulation might increase lachrymation 100-fold, up to 300 μ l/min. Topical administration, mostly in the form of eye drops, is quickly washed away by the tear film after application on the surface of the eye.

Gel-like mucus layer

Approximately 2–3 ml mucus is secreted daily. Mucin present in the tear film has a protective role by forming a hydrophilic gel layer that moves over the glycocalyx of the ocular surface and clears cell debris, foreign bodies and pathogens. At the same time, it acts as a barrier with a protective role that hinders drug diffusion to anterior chamber.

Protein binding

Protein binding of drugs in the tear fluid is a factor affecting drug bioavailability (7). Tear normally, contain about 0.7% protein and the protein level increase during infection or inflammation. When the drug-protein complex continuous to circulate, tears are replaced quickly thus removing both free and bound forms of the drug (8).

Cornea barrier

The cornea is a ~500-800 µm thick transparent collagenous structure. It provides the majority of the refractive power of the eye and is the primary barrier to topical drug absorption. The cornea is consisted of the 5 layers, epithelium, Bowman's membrane, stroma, Descemet's membrane and endothelium each of alternating polarity (Figure 2.4) (1).

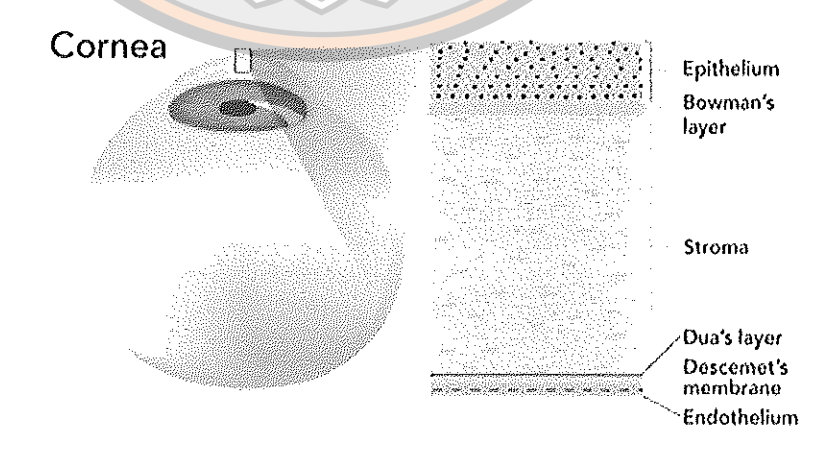


Figure 2.4 The structure of cornea

The corneal epithelium consists of 5-6 layers of cells packed closed by tight junctions that limit the paracellular drug permeation (9-11). The epithelium is impermeable to polar or hydrophilic compounds with molecular weight greater than 60-100 Da (8). Immediately underneath the epithelium is the Bowman's membrane, a thin homogeneous layer forming a transition toward the stroma and it's not considered to be a barrier to drug diffusion. The stroma makes up 90% of the corneal thickness. It consists of 75% water in a collagenous extracellular matrix. So it shows hydrophilic nature. Thus, the stroma allow hydrophilic molecule to pass through easily. However, it limits the penetration of highly lipophilic or large molecular weight compound. Descemet's membrane is a tough, homogeneous band supporting the endothelium, a single layer of cells important to keeping the hydration of the stroma constant. Finally, the corneal endothelium, this layer is a leaky monolayer that is easier permeated than epithelium. In addition, it maintains an effective barrier between the stroma and aqueous humor. In the conclusion, these layers make cornea a crucial barrier to most lipophilic and hydrophilic drugs. To penetrate the cornea, optimal lipophilicity for the permeant corresponds to log P values of 2-3 (9).

Blood-ocular barrier

The eye is protected from the xenobiotics in the blood stream by blood-ocular barriers. These barriers have two parts; blood-aqueous barrier and blood-retina barrier. The blood-aqueous barrier, locate in anterior segment, is composed of the endothelial cells in the uvea. This barrier prevents the access of plasma albumin into the aqueous humor, and limits also the access of hydrophilic drugs from plasma into the aqueous humor. The blood-retina barrier, locate in posterior segment between blood stream and eye is comprised of retinal pigment epithelium (RPE) and the tight walls of retinal capillaries. Unlike retinal capillaries the vasculature of the choroid has extensive blood flow and leaky walls. Drugs easily gain access to the choroidal extravascular space, but thereafter distribution into the retina is limited by the RPE and retinal endothelia.

Ocular pharmacokinetics

The main routes of drug administration and elimination from the eye have been shown schematically in Figure 2.5. For topical administration, the ocular routes of

absorption are divided into corneal and non-corneal. For the corneal route, the drug go to the systemic circulation by across the cornea to aqueous humor and intraocular circulation while the non-corneal route the drug go to the systemic circulation by conjunctiva and sclera (Figure 2.5).

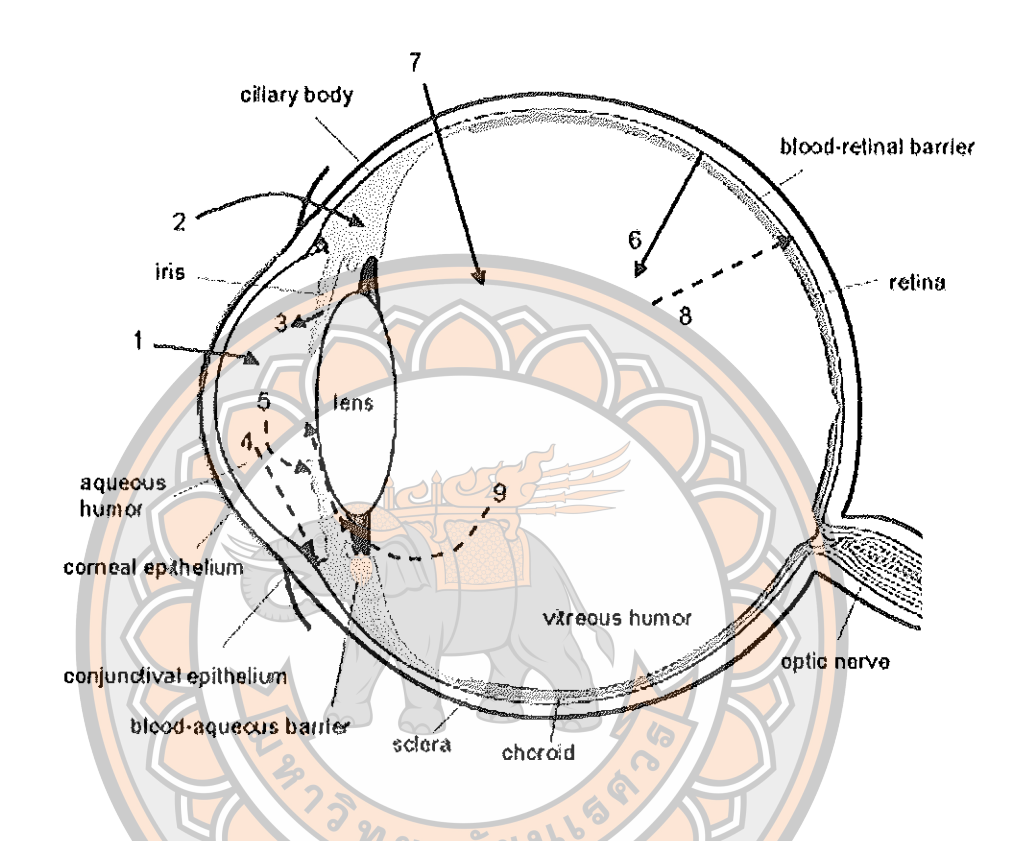


Figure 2.5 Schematic presentation of the ocular structure showing a summary of ocular pharmacokinetics

The numbers refer to following processes: 1) transcorneal permeation from the lachrymal fluid into the anterior chamber, 2) non-corneal drug permeation across the conjunctiva and sclera into the anterior uvea, 3) drug distribution from the bloodstream via the blood-aqueous barrier into the anterior chamber, 4) elimination of drug from the anterior chamber by aqueous humour passage into the trabecular meshwork and Sclemm's canal, 5) drug elimination from the aqueous humor into the systemic circulation across the blood-aqueous barrier, 6) drug distribution from the blood into the posterior eye across the blood-retina barrier, 7) intravitreal drug administration, 8) drug elimination from the vitreous via the posterior route across the

blood-retina barrier, and 9) drug elimination from the vitreous via the anterior route to the posterior chamber (10).

Corneal route is the most common pathway of drug absorption across cornea. Major permeation mechanism across the cornea including passive transport and active transport (Figure 2.6). There are three mechanisms of passive transport including passive transcellular, passive paracellular, and facilitated diffusion. Passive transcellular and paracellular is not dependent on transporter proteins, but it is dependent on drug properties that we can determine the partitioning and diffusion of the molecule in the lipid bilayer of the cell membrane. The drugs can move from higher to lower concentration to maintain equilibrium in cells. Passive transcellular permeability of drugs across the cornea is influenced by various factors, such as lipophilicity (i.e. partition coefficient), molecular weight, charge, and degree of ionization. In particular, lipophilicity is a major factor in corneal drug penetration. Passive paracellular diffuse via the spaces between the cells. These spaces are limited by the tight junctions in the cornea epithelium. There are many reported that the intercellular spaces are smaller than 3 nm. Only small drugs of MW < 350 Da and ions can permeate through the paracellular route. In addition, facilitate diffusion or called carrier-mediated diffusion, requires expression of transporters in the corneal epithelium. Many large molecules such as glucose will bind with a specific carrier proteins and then move through the cell membrane. The drugs move down the concentration gradient and don't use ATP (cellular energy) to move. Active transport requires ATP to move the drugs across the cell membrane in the direction against their concentration gradient. Other types of transporters perform efflux of drugs from the cells. The efflux transporters such as MRP, P-gp, and BCRP express on the corneal epithelium that facilitate the export of drug from the cell.

Although the corneal route is the primary route of enter drug into the eye, studies have also shown that absorption can occur via the non-corneal (conjunctival-sceral) route, particularly for large hydrophilic molecule such as protein and peptide. The conjunctiva is composed of 3 layers include outer epithelium, stroma and submucosa. It is more permeable or leaky than the cornea and allows drugs to permeate through the paracellular as well as transcellular route. The conjunctiva is highly vascularized so drug absorption often results in systemic distribution of the

drug away from the eye. The sclera is the white eye which outer coat of the eye. Sclera anatomy is similar to corneal stroma. Thus, drug permeation through the sclera occurs via the aqueous intercellular space between the collagen fibers. The sclera is more permeable (10 times) than cornea and half permeable as the conjunctiva such as drug with a MW of more than 1 kDa are almost impermeable through the cornea whereas dextran (40 kDa) and albumin (69 kDa) have good permeability through the sclera.

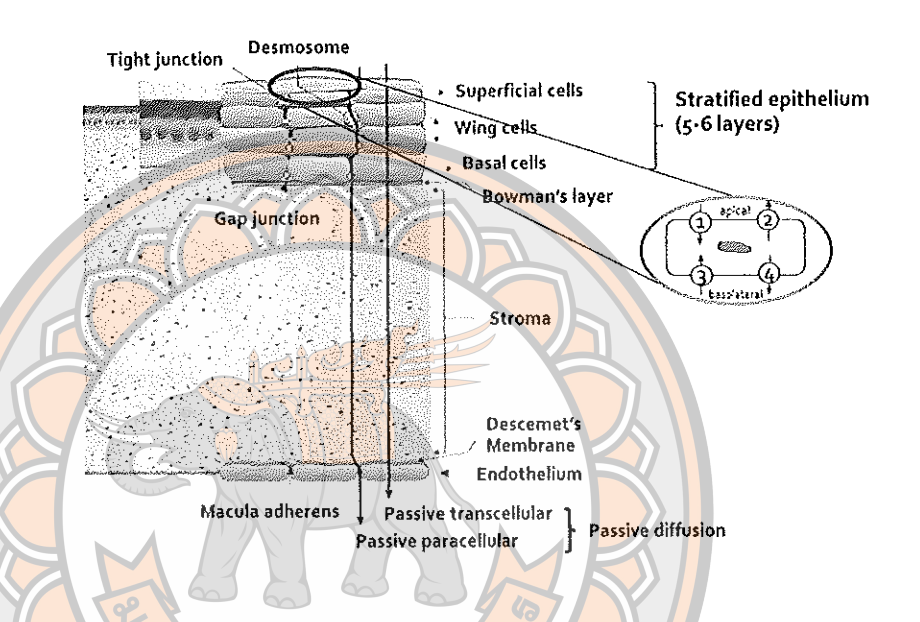


Figure 2.6 The permeation mechanisms across cornea, Passive paracellular and transcellular permeation, Transporter mediated influx and efflux across cell membrane in the apical (1 and 2) and basolateral (3 and 4) side, respectively

Ophthalmic drug delivery system

One of the major problems encountered with topical administration is the rapid precorneal loss caused by nasolacrimal drainage and high tear fluid turnover, which leads to drug concentrations of typically less than 5% of the applied drug. The concept of development of ocular drug delivery systems are increasing of the bioavailability and the duration of the therapeutic action of ocular drugs that divided into two categories. The first one is based on the use of sustained drug delivery systems, which provide the controlled and continuous delivery of ophthalmic drugs. The second involves maximizing corneal drug absorption and minimizing precorneal

drug loss by increasing the corneal contact time. This can be achieved by effective adherence to corneal surface. So to overcome these problems newer pharmaceutical ophthalmic formulations such as in-situ gel, nanoparticles, nanosuspensions, microemulsions, liposomes and contact lens have been developed to increase the bioavailability of the ocular drug. In this context, soft contact lenses are gaining an increasing attention as new vehicle for ophthalmic drug delivery. The use of soft contact lens for ophthalmic drug delivery can overcome several of the drawbacks associated with eye drops and previous ophthalmic drug delivery devices. The advantages of using contact lens are that drugs are released directly to the cornea, while protected from corneal removal mechanisms. Furthermore, contact lens can be engineered to deliver drugs over extended time periods, which simplifies dosing regimens (11-16).

Contact lenses based ophthalmic drug delivery system Definition of contact lenses

Contact lenses are thin lenses placed directly on the surface of the eyes. Contact lenses are medical devices used by over 150 million people worldwide (17) and they can be worn to correct vision or for cosmetic or therapeutic reasons (18). Rigid and soft contact lenses are the two main types of contact lenses available today. Rigid contact lenses are made of gas-permeable materials that they provide very crisp, clear vision and allow oxygen to reach the cornea more than soft contact lenses. Soft contact lenses are made of soft and very flexible plastics that absorb water that they are more flexible than rigid lenses, and can be gently rolled or folded without damaging the lens. While rigid lenses require a period of adaptation before comfort is achieved, soft lens wearers typically report lens awareness rather than pain or discomfort (18). In addition, soft contact lenses are classified in daily-wear lenses, extended-wear lenses and disposable lenses, respectively. Daily-wear soft lenses are removed and cleaned at night and reinserted in the morning. Extended-wear lenses can be worn day and night. After several days, wearers take them out, clean them, and wear them again. Disposable soft lenses are designed to be worn day and night for 1 day (daily disposable contact lenses) and 1 week (weekly disposable contact lenses) and then discarded.

Recently, daily disposable contact lenses have been proposed as alternative ophthalmic drug delivery systems for increased ocular bioavailability (11, 19-22). The benefit of using daily disposable therapeutic contact lenses would be a lower risk for infection (23) and the delivery of correct medication dose at an approximately constant rate, thereby eliminating the frequent application of topical eye drops and, more importantly, leading to better benefit to the patient with substantially increased efficacy.

Drug loading methods into daily disposable contact lenses

The drug loading methods into daily contact lenses are including soaking of contact lens in drug solution, incorporation of drug-loaded colloidal nanoparticles, copolymerization of the contact lens with functionalized monomers and molecular imprinting as shown in Figure 2.7 (24).

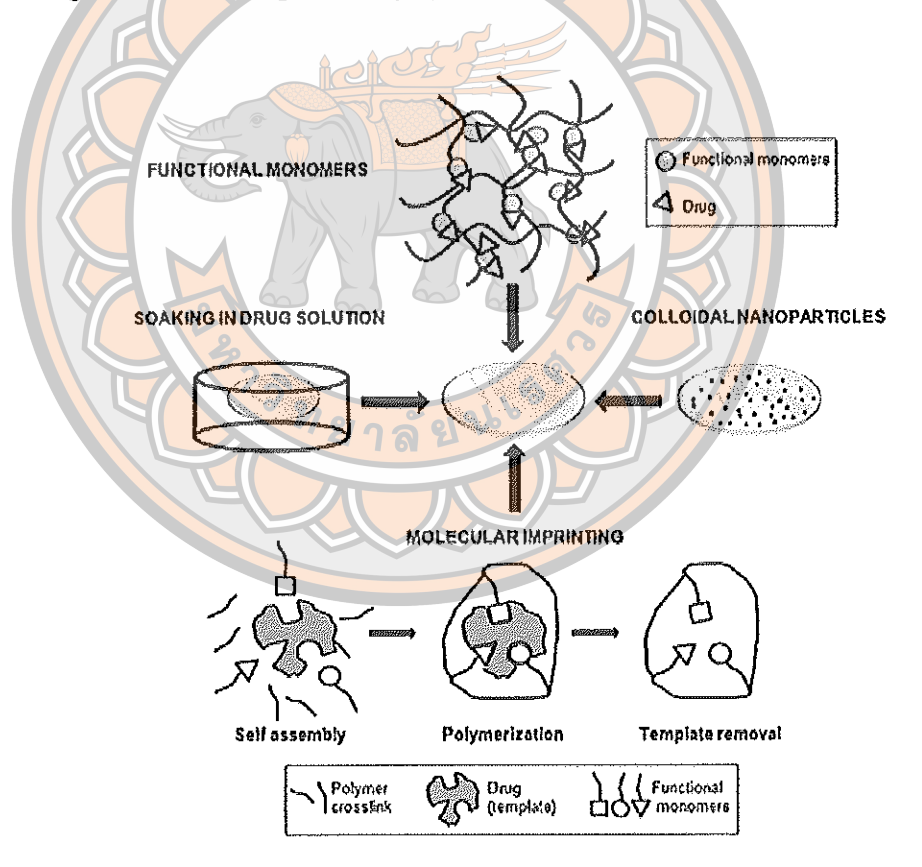


Figure 2.7 Drug loading methods into daily disposable contact lenses

Soaking of lens in drug solution

One of the most conventional ways of loading a therapeutic drug into the contact lenses is the soaking method due to its cost-effectiveness and simplicity (25-26). To this end, the preformed contact lenses are immersed in the drug solution and the drug molecules can be adsorbed into the lenses surfaces and/or inner core. The drug loading capacity depends on the water content and thickness of the lens drug, the molecular weight of the drug, loading time, pH of drug solution and concentration of initial drug solution (11, 26-28). The *in-vitro* release kinetics was dependent on the hydrogel composition (hydrophilic/hydrophobic monomers) of the contact lenses. The lenses showed sustained release was observed with increase in hydrophobic phase in the contact lens matrix (29).

Incorporation of drug-loaded colloidal nanoparticles

This method is based on incorporation of drug-loaded colloidal particles (micro-/nanoparticles, micro-/nanoemulsions, nanosuspensions, and liposomes) into the matrix of contact lenses. Drug-loaded colloidal particles entrap a large amount of drug, and then are dispersed in the lens material during polymerization. Nanocapsules prevent the interaction of drug molecules with the polymerization mixture and also provide additional resistance to drug release. The drug must first diffuse through the nanoparticles and penetrate the particle surface to reach the hydrogel matrix. Thus, it is expected that colloidal particle-loaded contact lenses can deliver drugs at a slow rate for a long period of time. However, there are some drawbacks of using colloid laden hydrogel contact lenses. The colloid laden hydrogel contact lenses exhibited the rough surface lead to high bacteria composition and corneal irritation (30-32). One is the instability of the colloid-laden hydrogel during preservation and transportation because the loaded drugs diffused from the hydrogel matrix into packaging solution (11).

Copolymerization of the contact lens with functional monomers

The monomers act as drug binding points for protonizable or hydrophobic molecules, and communicate functionality to the contact lenses (33). The incorporation of ionic/hydrophobic monomer would increase the interaction between contact lenses and drugs so that the drugs had more difficulties diffusing from the contact lenses. However, if hydrophilic/hydrophobic ratio was improper, hydrophilic/hydrophobic copolymer hydrogel would become opaque because of phase separation.

Molecular imprinting

In this technique, the target drug is mixed with functional monomers, which rearrange and interact with drug molecules. After polymerization, the drug from contact lens is removed, which results in formation of tailored active sites or imprinted pockets called macromolecular memory sites, i.e. the 3D structure of drug is left behind within a flexible macromolecular network. The monomers in the hydrogel matrix are organized in such a way that high drug affinity molecular sites are created. These molecular imprinted sites mimic the drug's receptors or its structurally similar analogy, which increase drug loading capacity (34). Drug affinity and its release profile are therefore governed by the type of functional monomers used as well as their ratio in the polymeric matrix. Thus one can tailor the release pattern based on monomer composition. The limitation of molecular imprinting method is the highly cross-linked structure of hydrogel which affects the optical and physical performance of contact lens (35). The fall in water content (decrease in swelling) leads to an insufficient ion and oxygen permeability which limit the use of contact lenses (36).

Ideal properties of daily disposable contact lenses-based ophthalmic drug delivery system

The appropriate daily disposable soft contact lenses for ophthalmic drug delivery should be met the ideal properties of daily disposable therapeutic contact lenses requirement. The ideal properties requirement should be high physicochemical properties, visible light transparency, water content, mechanical properties, ion and oxygen permeability (37-44) as shown in Table 2.1. In addition, the lenses should be non-toxicity, and delivered drugs in a prolonged release pattern more than 3 h and up to 24 h (45-46).

Table 2.1 Ideal properties of daily disposable contact lenses-based ophthalmic drug delivery system requirement

Physicochemical properties	Value requirements
Visible light transparency (%)	≥ 90
Young's Modulus (Mpa)	≥ 0.5
Elongation at break (%)	≥ 50
Water content (%)	≥ 50
Ion permeability (mm²/min)	≥ 0.6
Oxygen permeability (Barrers)	≥ 10

Lenses material for daily disposable contact lenses-based ophthalmic drug delivery system

Commercial contact lenses

Currently, only synthetic polymers ware use for commercial daily disposable contact lenses which are shown in Table 2.2. Typically, commercial daily disposable contact lenses are usually made from two main types of synthetic polymers, poly (2-hydroxyethyl methacrylate) (pHEMA)-based hydrogel and silicone based hydrogel (SiH). SiH contact lenses, in contrast, have high oxygen permeability, but they are low in water content with a hydration ability of < 45% (38, 40, 42, 47-49). pHEMA-based hydrogel contact lenses provide high water content of up to 80% and softness that promotes comfortable wearing (42, 47, 50-51). Thus, prior studies focused on soaking pHEMA-based hydrogel contact lenses in hydrophilic ocular drug solutions, such as diclofenac sodium, cysteamine, brimonidine, fluconazole, and moxifloxacin hydrochloride, followed by insertion into the eye (52-55). From the previous report, the commercial pHEMA-based hydrogel contact lenses exhibited excellent optical light transparency (>95%) and high water content (50-80 % by weight) (53). Their Young's modulus and elongation at break in the range of 0.3-1.5 MPa and \geq 50%. respectively. They showed high ion and oxygen permeability of 0.6 to 26×10^{-3} mm²/min and 10-33 Barrers, respective (42-44). Furthermore, commercial pHEMAbased hydrogel contact lenses showed no cytotoxicity. Although in the majority of the

cases, a higher bioavailability of the drug delivered via pHEMA-based hydrogel contact lenses was observed compared with eye drops (e.g., combination of *in vitro* experiments with modeling of the *in vivo* behavior showed that at least 20% of the drug timolol that was entrapped in pHEMA-based hydrogel contact lenses entered the cornea, which is larger than the fractional uptake recorded using eye drops) (56). The corticosteroid prednisolone, the glaucoma drug pilocarpine, and the antibiotic ciprofloxacin were released from pHEMA-based hydrogel contact lenses within 1 to 3 h (57). *In vitro* experiments have shown complete release of ketotifen fumarate from drug-soaked pHEMA contact lens in ~3 h (58). A significant release of ketotifen fumarate was detected initially at 10-15 min, and then reaching release plateaus from 1 to 3 h. which suggested that commercial contacts lenses may require multiple exchanges per day, reducing the viability of this approach.

Therefore, the development of new daily disposable contact lenses to effectively deliver drugs in a prolonged release patterns is still a demanding as well as challenging task.

Table 2.2 Commercial synthetic polymers contact lens

USAN/ISO name Filcon la	le Filcon la	Vificon A	Etaficon A	Filcon 3a	Nelfecon A	Lotrafilcon A Lotrafilcon B Balafilcon A Senoficon A Galyfilcon A	Lotrafilcon B	Balafilcon A	Senoficon A	Galyfilcon A
Brad name	Vistagel	Focus	Acuvue	Vistagel	Focus	Night	Air Optix	PureVision	AcuvueOsays	Acuvue
)	Monthlies	1 Day	65	Dailies	& Day				
Monomers	HEMA	HEMA,	HEMA,	HEMA,	modified	DMA,	DMA,	NVP,	mPPMS,	mPDMS,
		MA PVP	MA	NVP	PVA	TRIS,	TRIS,	TPVC,	HEMA,	HEMA,
				1		Siloxane	Siloxane	NCVE,	DMA	DMA
				200				PBVC		
EWC (%)	38	55	58	3 65	69	24	33	36	38	47
Ionicity	Neutral	Anionic	Anionic	Neutral	Neutral	Neutral	Neutral	Mildly	Neutral	Neutral
•			>	ล้		2	\sim	ionic		
Surface C (%)	•	•	人	21		6.69	71.1	62.2	67.5	67.3
Surface N (%)	ı	ı		96	7	10.6	10.1	7.5	5.2	5
Surface O (%)	1	•		6		13.8	12.5	19.3	18.1	18.6
Surface Si (%)	•	ı		9:		2.5	1.8	9.4	9.2	9.1
Bulk C (%)	53.5	58.3	53.2	59.0	54.0	54.9	59.1	63.3	62.8	64.8
Bulk N (%)	< 0.1	9.4	< 0.1	9.2	< 0.1	5.3	5.1	9.4	9.2	9.1
Bulk O (%)	Ca 38	Ca 24	Ca 38	Ca 23.5	Ca 36	12	11.6	12.7	15	14.3
	(H=8.1)	(H=8.3)	(H=7.9)	(H=8.2)	(H=8.9)					
Bulk Si (%)	t	1	1	_		19.6	17.3	17.8	16.7	15.5

DMA: N'N-dimethylacrylamide; HEMA: hydroxyethyl methacrylate; mPPMS: monofunctionalpoly(dimethylsiloxane); MA: methacrylic tristrimethylsiloxysilylpropylvinylcabamate; EWC: equilibrium water content; LogD of repeat unit structure: HEMA(0.4); NVP (0.38): poly(dimethysiloxy)disilylbutanolbisvinylcarbamate; NVP: N-vinyl pyrrolidone; TRIS: trimethylsiloxysilane; TPVC: acid; NCVE: N-carboxyvinyl ester; PVA: poly(vinyl alcohol); PVP: poly(vinyl pyrrolidone); PBVC:

MA (-2.8 at pH7, 074 at pH 4): PVA (-0.2): siloxane monomer (1.1-2.5).

New contact lenses material

Nowadays, there are very few reports in published literatures of new materials for therapeutic contact lenses and there are not many studies analyzing in depth all contact lenses properties. Srisuwan et al. (2013) studied tetracycline hydrochloride loaded-regenerated silk fibroin (RSF) or alginate or RSF/alginate films (59). Films containing the model drug were prepared by casting method. They found that the visible light transparency of drug loaded-alginate film was 75%. On the other hand, the visible light transparency of drug loaded-RSF film and drug loaded-RSF/alginate films of > 90%. The film transparency of the blend films slightly decreased with increasing alginate film content. Drug loaded-alginate film incubated with distilled water at 37°C for 24 h showed film degradation, with weight loss of 90%. The degradation of blend films significantly decreased with increasing RSF content. The alginate film showed a fast release characteristic with nearly 95% drug released within 3 h whereas the RSF film and all RSF/alginate films prolonged release more than 24 h. Essentially, RSF film showed the lowest drug release. For RSF/alginate blend films, the drug release rates from the films were decreased with increasing RSF ratio (59). This indicated that RSF is a possible to develop as daily disposable therapeutic contact lenses materials. From the previous reports, RSF films also offer the advantages of high oxygen permeability, non-toxicity, excellent biocompatibility, and also excellent wound healing properties, but it is quite brittle (60-65). Chitosan (CS) films showed the prolong release pattern for long time, good flexibility, high light transparency and high water content but it is highly sensitive to lysozyme degradation (66-70). Therefore, the blending between RSF and CS is a possible solution to improve properties of films for creating the materials of daily disposable therapeutic contact lenses. Moreover, the blending of RSF with CS shows a good compatibility between two different materials by intermolecular interaction (71-72).

Silk fibroin

Silk fibroin structure

Silk fibroin is the structural protein of *Bombyx mori* silkworm cocoons and is insoluble in water (73). Figure 2.8 (74) illustrates the schematic structure of a fibroin molecule. Silk fibroin is a large protein macromolecule made up of more than 5000 amino acids, it accounts for about 75 wt% of total silkworm cocoons. The proportions of amino acids in silk fibroin are show in Table 2.3(75). Fibroin composes of two subunits, a heavy chain (molecular weight (MW) of ~390 kDa) and a light chain (MW ~ 26 kDa) which are linked by disulfide bond (76). Another component of silk fibroin is glycoprotein P25 (~30 kDa), which is attached by non-covalent interactions to the covalently bonded heavy and light chain complex. In terms of amino acid composition, Bombyx mori fibroin consists mainly of Gly (45%), Ala (26%), and Ser (12%). The heavy chain composes of 12 major hydrophobic domains linking together by 11 minor hydrophilic sections. Each hydrophobic domain contains repetitive sequences of Gly-Ala-Gly-Ala-Gly-Ser and several repeats of Gly-X, with X = Ala, Ser, Thr, Tyr, or Val. The hydrophilic sections have random amino acid sequences. The hydrophilic sections have random amino acid sequences. By utilizing intra- and intermolecular hydrogen bonds (mostly between Gly and Ala) and van der Waals forces, the heavy chain can form stable anti-parallel β-sheet crystallites (77). On the other hand, the light chain consists of a different proportions of amino acids, 15% Asp. 14% Ala, 11% Gly, 11% Ser, and a trace of cysteine. With non-repetitive amino acid sequences, the light chain is more hydrophilic and has low water resistance ability, ultimately contributing to the fibroin elasticity. Silk fibroin comprises both a crystalline region (~66%) and an amorphous (~33%) region. Therefore, fibroin is a semi-crystalline structure that has stiffness, strength and hygroscopic properties (78).

Table 2.3 Amino acid composition of Bombyx mori silk fibroin

Glycine	44.7	
	44.7	
Alanine	25.7	
Serine	11.9	
Tyrosine	5.4	
Valine	2.4	
Aspartic acid	1.6	
Phenylalanine	1.6	
Glutamic acid	1.1	
Threonine	1.0	
Isoleucine	0.6	
Leucine	0.5	
Proline	0.5	
Arginine	0.5	
Lysine	0.4	
Histidine	0.2	

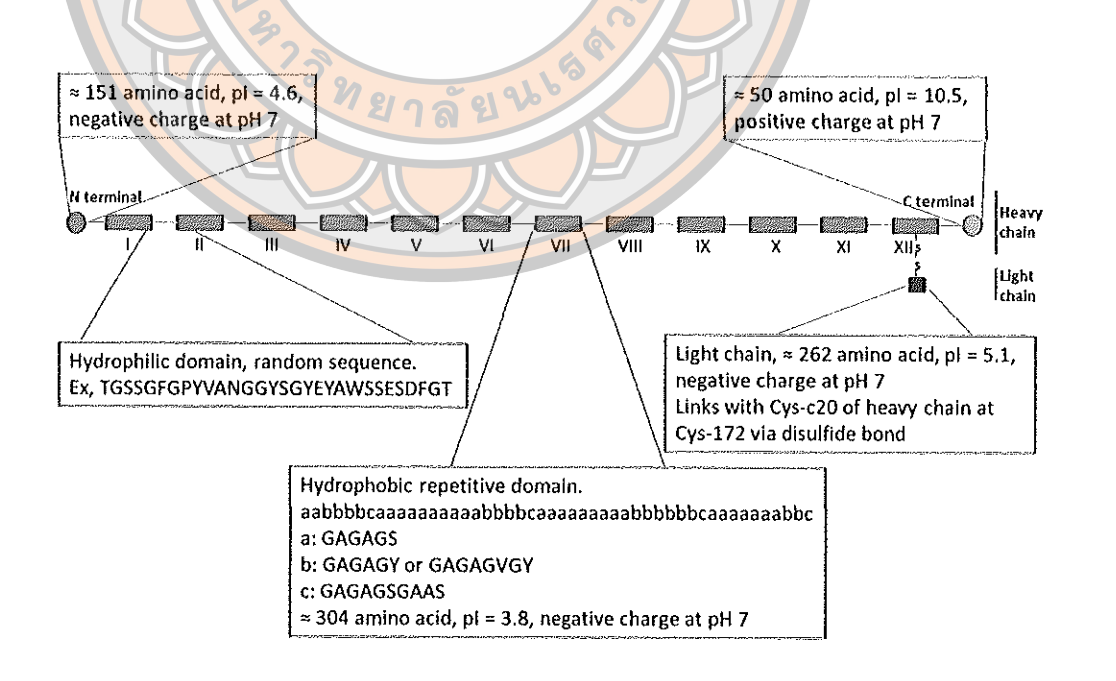


Figure 2.8 Schematic structure of a fibroin unit

Silk fibroin extraction

Typically, the silk fibroin is extracted from the silkworm cocoon by removal of sericin and is then purified (79-80). One of the most widely used procedures for the removal of sericin is Na₂CO₃ boiling (degumming) and neutralize (80). After that the degummed silk fibroin is washed for three times and dried. Unethically, without the need of degumming, silk fibroin can be extracted directly from the worm posterior glands by dissecting the mature fifth instar silkworm larvae. In this case, silk fibroin is in liquid water soluble form and is regarded as silk I. But, the degummed silk fiber consists of insoluble silk fibroin (silk II), and thus, requires further treatment to be transformed back to soluble silk fibroin (silk I). The product of this process is commonly called regenerated silk fibroin (RSF). The degummed silk fibroin is extracted by dissolving in a concentrated solution of LiBr or calcium-alcohol solvents such as Ca(NO₃)₂·4H₂O-methanol, Ca(NO₃)₂·4H₂O-ethanol, CaCl₂/methanol/H₂O and CaCl₂/ethanol/H₂O followed by heating to 60-90 °C (81-83). The viscous silk fibroin liquid is then dialyzed against deionized water for 48-72 h, and centrifuged at 4°C for 30 min to remove calcium chloride, smaller molecules, and some impurities. The supernatant is the soluble regenerated fibroin, which can be preserved at 4°C for at least one month before becoming irreversible gel. For long-term storage, fibroin solutions should be lyophilized and the resulting powder will be stable for several years at temperature -80 °C.

Silk fibroin characterization

The surface morphology of lyophilized RSF was observed with a scanning electron microscope (SEM). From the previous report (82, 83), the silk fibroins treated with LiBr, Ca(NO₃)₂·4H₂O-methanol, Ca(NO₃)₂·4H₂O-ethanol, CaCl₂/methanol/H₂O and CaCl₂/ethanol/H₂O solution were separately dissolved. After lyophilized, the surface morphology of RSF was observed with SEM. The regenerated silk fibroins were spherical and irregular shapes. This shape may have resulted from the merger of smaller micelles that occurred in the aqueous solutions. The RSF is generally analyzed determined by sodium dodecyl sulfate polyacrylamide gel electrophoresis (SDS-PAGE) to determine the corresponding molecular weights of the protein. The use of SDS-PAGE technique largely eliminates the influence of the structure and charge. The silk fibroin is separated solely based on polypeptide chain length. It uses sodium

dodecyl sulfate (SDS) molecules to help identify and isolate protein molecules. RSF solution was resolved on 12% acrylamide gel and 4% condensing gel, and protein bands were visualized by staining with 0.25% Coomassie Brilliant Blue R-250 (82). The RSF treated with LiBr showed molecular weight of 30-200 kDa. RSF treated Ca(NO₃)₂·4H₂O-methanol had a molecular weight of 95-170 KDa, but RSF treated with Ca(NO₃)2.4H₂O-ethanol gave a molecular weight of 100-170 KDa. The molecular weight of RSF treat with CaCl₂/methanol/H₂O is ranged of 140-170 kDa, while the molecular weight of RSF treat with CaCl₂/methanol/H₂O fibroins is ranged of 100-300 kDa. This indicated that the solvent of CaCl₂/methanol/H₂O appeared to be sufficiently gentle to produce silk fibroins with less obvious damage to the secondary bonds. Thus, the CaCl₂/methanol/H₂O solution may be superior to the other solutions in its ability to protect the integrity of the fibroin secondary structure which enhanced the stability mechanical properties. In addition, the isoelectric point (PI) of RSF varies in the range pH 3.6-5.2, depending on the conditions of solution preparation (84). Below pH 5 the RSF particles aggregated into non-dispersible clusters due to dominating intermolecular hydrogen bonding, which correlates with the theoretical PI of RSF (85). RSF obtained from the silkworm cocoon is reported to be non-toxic. The results of safety evaluation of RSF solution (5% w/v) in the rabbit eye test showed no effect on lacrimation and no signs of irritation to cornea, iris and conjunctiva. The skin irritation test revealed absence of any kind of inflammatory response, edema or erythema (redness), indicating the non-allergic, non-irritant property and safety for human use (86).

Films based silk fibroin

Sashina et al. (2007) developed the RSF blending with synthesis polymer, polymethyl methacrylate (PMMA), poly-3-hydroxybutyric acid (P3HB), polylactic acid (PLA). They observed that RSF film gave light transparency reaching 88-90% toward the light with the wavelength 380-700 nm. With increasing the blend ratio between RSF and synthesis polymer, the film light transparency were deceased. They suggested that at the growth of the content of synthetic polymer, the mixture becomes heterogeneous with the macrophase separation. Actually, films become less transparent, their ability of light transmitting falls (72). In addition, they observed that

with increasing the synthetic component content, the oxygen permeability of the blend films decreases (72).

Lloyd et al. (2001) found that the RSF film was characterized by the high oxygen permeability, which at 25°C reaches (90-95) x 10^{-11} cm² of O_2 s⁻¹ mm⁻¹ Hg. On the other hand, they observed that contemporary fluorosilicone materials of rigid contact lenses have the oxygen permeability at the level (60–64) x 10^{-11} cm² of O_2 s⁻¹ mm⁻¹ Hg (51).

Kweon et al. (2001) studied the mechanical properties of RSF/CS films with varying chitosan contents. In wet state, the tensile strength of silk fibroin film was 4.5 MPa, while that of chitosan film was 30 MPa. The RSF film is very brittle in dry conditions, but the elongation increases as the film absorbs water in the wet state. The elongation at break in wet state of RSF was 10% while The CS film has excellent breaking elongation of 100%, as well as tensile strength. In RSF/CS films, the tensile strength and elongation at break increased with increasing the chitosan content. (87).

Luangbudnark et al. (2012) studies the properties of CS/RSF blend film. They found that the flexibility, swelling index, and enzyme degradation were increased by the chitosan content of the blend films. In addition, biocompatibility of the blend films was determined by cultivation with fibroblast cells. All RSF/CS films showed no cytotoxicity by XTT assay. Fibroblast cells spread on CS/RSF films via dendritic extensions, and cell-cell interactions were noted. Cell proliferation on CS/RSF films was also demonstrated (67).

Prasong (2011) studied methylene blue as a model drug-loaded RSF/CS (1:1) blend films. The condition of the *in vitro* drug release of the film samples were soaking in 20 ml of phosphate buffer solution (pH=7.4) for 72 h. They found that methylene blue was released the highest in the initial 30 min of study. The methylene blue release content was increased until 10 h. and then gradually increased even the last time of 72 hr (88).

Zheng et al. (2017) developed RSF film for wound dressing. From *In vivo* rabbit full-thickness skin defect study, the RSF film effectively reduced the wound healing time with better skin regeneration compared with the commercial wound dressings. Subsequent assessment in porcine model confirms its long-term safety and effectiveness for full-thickness skin defects. Moreover, a randomized single-blind

parallel controlled clinical trial with 71 patients shows that the silk fibroin film significantly reduced the time to wound healing and incidence of adverse events compared to commercial dressing (89).

Chitosan

Chitosan structure

CS is a cationic linear copolymer polysaccharide made up of random distribution of β (1 \rightarrow 4) linked 2- amino- 2- deoxy- D- glucose (D-glucosamine) and 2- acetamido- 2- deoxy- D- glucose (N- acetyl- D- glucosamine) units. The structure is shown in Figure 2.9 and it is very similar to cellulose, in which the C-2 hydroxyl groups are replaced by acetamido residue. However owing to the presence of large percentage of nitrogen (6.89%), chitosan shows much commercial interest than synthetically substituted cellulose (1.2%). This provides chitosan chelating properties.

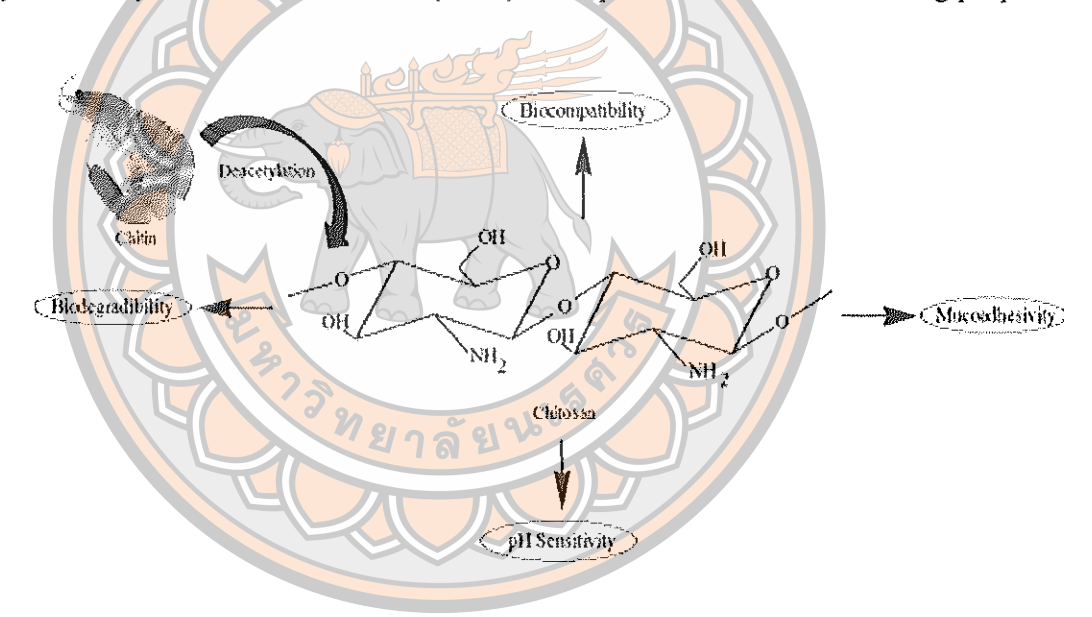


Figure 2.9 The structure of chitosan

Chitosan extraction

CS is typically obtained by extensive deacetylation of chitin, an abundant polysaccharide found in crustacean shells. Deacetylation process of synthesis of chitosan from chitin is generally done by hydrolysis under alkali condition at high temperature. There are four steps in the preparation method i.e. deproteinization, demineralization, decolouration and deacetylation (90). Deproteinization involves overnight alkaline treatment with 3-5% aqueous NaOH (w/v) solution at room

temperature. The inorganic ingredients are then removed by treating with 3-5% aqueous HCl (w/v) solution at room temperature for 5 h. After that, crude chitosan is obtained, which is then purified by precipitating the chitosan from its acetic acid solution by NaOH and washing with distilled water till neutralization. Commercially chitosan is obtained with different molecular weight (MW) and degree of deacetylation (DD) depending on the percentage of primary amino groups present in the polymer backbone (91).

Chitosan characterization

Typically, the molecular weight of CS was measured by Gel permeation Chromatography (GPC). The molecular weight of CS is typically between 300-1000 kDa depending on the source of chitin. The DD denotes the removal of acetyl group from the long chain of chitin and it plays a substantial role in deciding the precise application of chitosan (92). The DD is an important parameter to be considered for physical and chemical properties of chitosan including solubility, adsorption, chemical reactivity, covalent linking, encapsulation and biodegradability (93). Degree of deacetylation (DD) refers to the removal of acetyl group from the chain which is determined by potentiometric titration. Homogenous solution of chitosan was prepared using HCl solution which was titrated against NaOH solution. The end point is determined by the inflections of the pH values. Two inflections were mainly considered out of which first one corresponds to neutralization of HCl and second one to neutralization of ammonium ions from chitosan. The difference between two points gives the amount of amino groups in the chitosan it was also referred as degree of deacetylation (94). DD of chitosan may range from 30% to 95% depending on the source of chitin, and concentration of acid and alkaline used, time and temperature in deacetylation procedure (95). The solubility of CS is one of the important parameters for quality of CS, where higher solubility will produce a better chitosan. There are several critical factors affecting chitosan solubility including temperature and time of deacetylation, alkali concentration and prior treatments applied to chitin isolation, ratio of chitin to alkali solution and particle size. Solubility of chitosan to estimate the solubility nature of extracted chitosan was determined according to Fernandez-Kim (96). The chitosan powder sample was taken in centrifuge tube and dissolved in acetic acid solution and kept in incubated shaker. The solution was immersed in boiling water bath and cooled to room temperature followed by centrifuge and the supernatant was discarded. The undissolved particles were thoroughly washed using distilled water by centrifuging and the supernatant was discarded. The undissolved pellets were dried. At the end the dried particles were weighed and the solubility percentage was calculated (94). The solubility, however, is controlled by the degree of deacetylation and it is estimated that DD must be at least 85% complete in order to achieve the desired solubility (97). Proportionally increase in solubility was observed with increasing deacetylation degree. Brine and Austin, suggested that the incomplete removal of protein and acetyl group leads to lower solubility (98). Since solubility of chitosan depends on the removal of acetyl group from chitin, therefore the lower DD value could adversely interfere with the results. Chitosan, unlike chitin has high content of highly protonated free amino group that very well attracts ionic compounds. This could be the reason for its solubility in mild inorganic acid (99). The amino group of CS has a pKa value of ~6.5; hence, chitosan is positively charged and is soluble in weakly acidic solutions with a charge density (100).

Films based chitosan

Yuan et al. (2004) developed CS/gelatin blend film from 0-50% of gelatin content. They observed that the visible light transparency of all film ratio were > 90%. The tensile strength and elongation at break of the CS/gelatin films with various from 0-50% of gelatin content were between 3.71-6.25 Mpa and 90-120%, respectively and were generally higher than those of the PMMA commercial contact lens. The mechanical properties of the films increased with increasing CS film content. Moreover, they investigated the cytotoxicity of CS/gelatin films compared with PMMA contact lens by investigating biocompatibility of RSF/CS films with 0%, 10%, 25%, 33% and 50% gelatin content. The control sample was the commercial contact lens which was mainly composed of PMMA. The CS and CS/gelatin film had good biocompatibility. The biocompatibility of CS and CS/gelatin films were evaluated by cell culture methods. They found that the diploid fibroblast cell growth and their adhesion on CS and CS/gelatin films were better than on the commercial contact lens. The CS film appears to be the best for the cell growth and adhesion (101).

JJ et al. (2009) studied cytotoxicity of CS film as a drug sustained-release system. Osteoblasts derived from fetal rat calvarial were cultured on chitosan films. Cell proliferation was tested by MTT assay. The relative growth rate was calculated and the cytotoxicity was graded. The result showed the cytotoxicity grade was 0 suggesting that the CS film was free of cytotoxicity (102).

Fulgêncio et al. (2012) studied the CS film for ophthalmic drug delivery of timolol maleate (TM) (103). The CS films containing timolol maleate as model drug were prepared by casting method. In an in vitro drug release study, TM showed prolonged released over a 4 week period, in which 85% of the drug was released over the first 2 weeks. In addition, the drug loaded-chitosan film was evaluated for their pharmacodynamics in ocular normotensive albino rabbits, in which the intraocular pressure (IOP) was measured by means of applanation tonometer on alternative days (13 h) for 11 weeks. For 15 days, 0.5% TM commercial ophthalmic solution was administered twice a day (n=5) and compared to chitosan-coated TM (n=5). In the control group (n=5), saline was used twice a day. The maximum TM release time from chitosan films were also recorded. The film's release of TM lowered the in vivo IOP levels over a 10 week period. No significant difference in the lowering of IOP in rabbits treated with 0.5% TM commercial ophthalmic solution, as compared to those that received the films, could be observed. No signs of ocular discomfort or irritations could be identified upon ophthalmic examination by slit-lamp biomicroscopy. Ophthalmic structures that came in direct contact with the films revealed no alterations within the histopathological studies. Moreover, the animals showed no signs of ocular discomfort during the experimental assays. These findings suggest that the TM-loaded chitosan film is safe.

Waibel et al. (2011) studied the safety of CS film using as bandage in shellfish allergic patients. Patients who reported shellfish allergy were recruited. Initial assessment included a detailed history, IgE skin prick testing (SPT), and serum testing to shellfish allergens. Participants who demonstrated specific shellfish IgE underwent a bandage challenge. The participants had positive SPT and serum IgE testing to at least one shellfish, 80% of participants had shrimp positive SPT and 100% of participants demonstrated shrimp-specific IgE. Essentially, no participants had a

positive SPT to CS powder or experienced an adverse reaction during bandage challenges indicating that CS/RSF film is safe in shellfish allergic subjects (100).

Films formation

In development of new contact lenses material, the thin film form is typically use for properties characterization. Generally, 2 approaches, film casting and layer by layer commonly produced the films (104-105). Monolayers films were prepared by a casting method. Briefly, the ingredient solutions were mixed and then poured onto the polystyrene plates and dried in an oven. Multilayer films were prepared using layer-by-layer casting. Each of the solutions were then poured onto the polystyrene plates and dried until completely dried. After that the next solution were poured for the next layer.

Table 2.4 Basic films physicochemical properties and their corresponding characterization methods

Films properties	Characterization methods
Film thickness	Thickness gage
Morphology	Scanning electron microscope (SEM)
Mechanical properties	Universal testing machine
MEIT	Texture analyzer
Water content	Moisture analyzer
Oxygen permeability	Polarographic amplifier
	Oxygen transmission rate tester
Thermal properties	Differential scanning calorimeter (DSC)
	Thermogravimetric analysis (TGA)
Cytotoxicity	MTT or XTT assay
Enzymatic degradation	Weight loss determination
Drug loading capacity	Drug extraction and purification, followed by
	UV-Vis spectroscopy measurement
Drug release/dissolution profiles	Drug separation by centrifugation or filtration,
	followed by UV-Vis spectroscopy measurement

Films characterization

Physicochemical properties, drug loading and drug release characteristic are a significant consideration in the design and quality control of contact lens materials for drug delivery. There are many the properties measurements for studies analyzing of properties. Table 2.4 summaries the basic films physicochemical properties, in terms of drug delivery system, and their respective characterization methods.

Model drugs

Since drugs used for the treatment of eye diseases are several charged molecules (106-109). In this study, non-charged acetaminophen (APAP), negatively charged 5(6)-carboxyfluorescein (CF) and zwitterionic rhodamine B (RB) and diclofenac sodium salt (DS) were used as model drug. The structural formula of model drugs is shown in Figure 2.10.

APAP is a non-opioid analgesic and antipyretic widely used for a large variety of mild to moderate pain conditions in a large variety of patient populations. APAP has a core aromatic (benzene) ring substituted in para orientation by two groups: a hydroxyl and an acetamide (ethanamide). Multiple portions of the molecule are conjugated, including the benzene ring, the hydroxyl oxygen, the amide nitrogen, and the carbonyl carbon and oxygen. The molecular weight of APAP is 151.16 g/mol. The reported solubility of APAP (MW 151.16 g/mol) in water are11.3 mg/ml (20°C), 13.85 mg/ml (25°C), 20 mg/ml (37°C). The reported pKa values for APAP range from 9.011 to 9.5 (110). APAP showed absorption maximum wave length at 243 nm (111).

CF and RB is a fluorescent dye. CF is a commercially available mixture of 5-carboxyfluorescein and 6-carboxyfluorescein isomers. The molecular weight of CF is 376.32 g/mol. The solubility of CF has a pKa and solubility of 6.5 and 0.5 mg/ml, respectively. CF showed absorption maximum wave length at 493 nm (112). RB composed N-(9-(2-carboxyphenyl)-6-(diethylamino)-3H-xanthen-3-ylidene)-N-ethylethanaminium as the counterion. The molecular weight of RB is 479.02 g/mol. The solubility of RB has a pKa and solubility of 3.7 and 15 mg/ml, respectively (113). CF showed absorption maximum wave length at 553 nm (114).

Diclofenac sodium (DS) is one of non-steroidal anti-inflammatory drugs currently approved by US Food and Drug Administration for ocular use. DS is designated chemically as 2-((2,6-dichlorophenyl)amino) benzeneacetic acid, monosodium

salt, with an empirical formula of $C_{14}H_{10}Cl_2NO_2Na$. It can suppress arachidonic acid transformation catalysed by cyclooxygenase enzymes leading to inhibition of prostaglandins synthesis in eyes. The molecular weight of DS is 318.13 g/mol. The reported solubility of DS in water is 50 mg/ml. The reported pKa value for DS is 4.15. DS showed absorption maximum wave length at 276 nm (115).

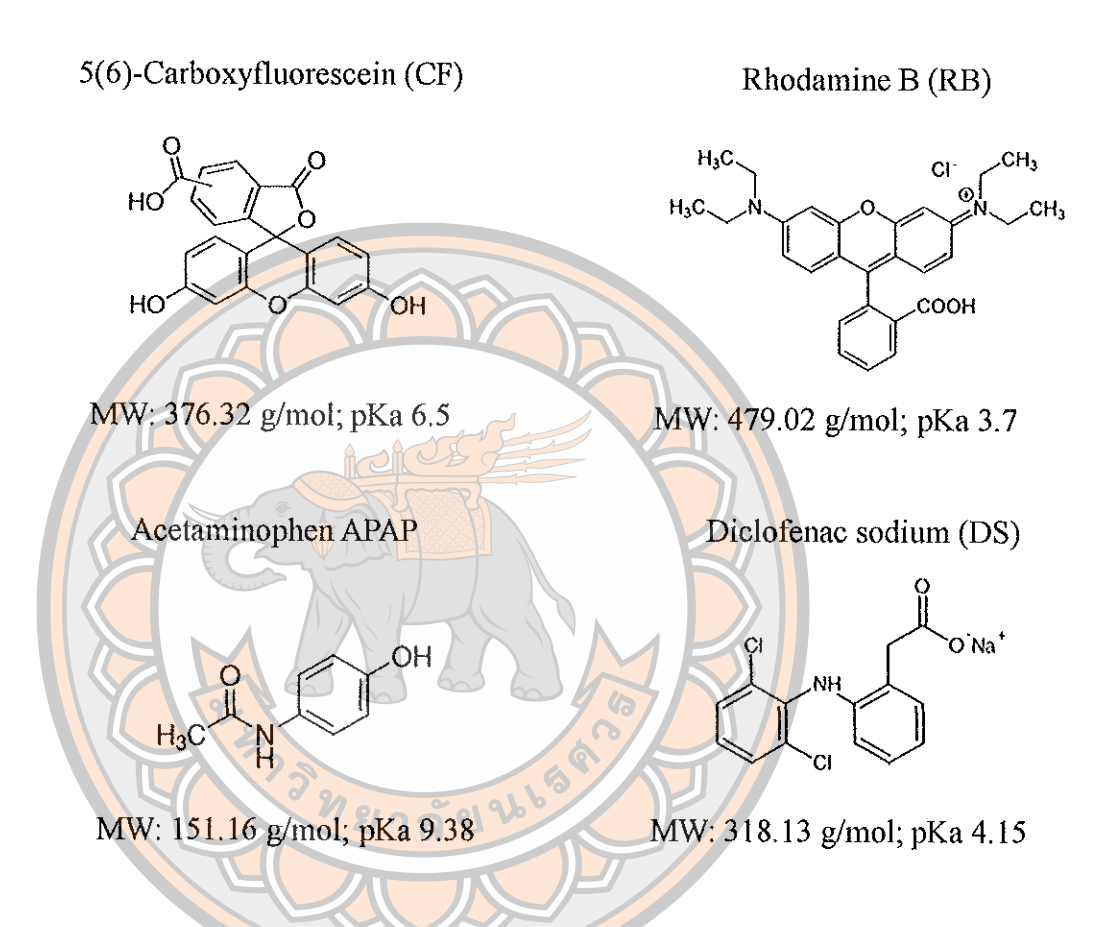


Figure 2.10 Chemical structures of CF, RB, APP and DS

References

- 1. Kim YC, Chiang B, Wu X, Prausnitz MR. Ocular delivery of macromolecules. J Control Release. 2014;190:172-81.
- 2. Zhou L, Beuerman RW. Tear analysis in ocular surface diseases. Prog Retin Eye Res. 2012;31(6):527-50.
- 3. Johnson ME, Murphy PJ. Changes in the tear film and ocular surface from dry eye syndrome. Prog Retin Eye Res. 2004;23(4):449-74.
- 4. Tiffany JM. Tears in health and disease. Eye (Lond), 2003;17(8):923-6.
- 5. Pucker A, Nichols J. Analysis of meibum and tear Llipids. The ocular surface. 2012;10:230-50.
- 6. Lallemand F, Felt-Baeyens O, Besseghir K, Behar-Cohen F, Gurny R. Cyclosporine A delivery to the eye: a pharmaceutical challenge. Eur J Pharm Biopharm. 2003;56(3):307-18.
- 7. Sasaki H, Yamamura K, Nishida K, Nakamura J, Ichikawa M. Delivery of drugs to the eye by topical application. Progress in Retinal and Eye Research. 1996;15(2):583-620.
- 8. Malhotra M, Majumdar DK. Permeation through cornea. Indian J Exp Biol. 2001;39(1):11-24.
- 9. Gan L, Wang J, Jiang M, Bartlett H, Ouyang D, Eperjesi F, Liu J, Gan Y. Recent advances in topical ophthalmic drug delivery with lipid-based nanocarriers. Drug Discov Today. 2013;18(5-6):290-7.
- 10. Urtti A. Challenges and obstacles of ocular pharmacokinetics and drug delivery. Adv Drug Deliv Rev. 2006;58(11):1131-5.
- 11. Xinming L, Yingde C, Lloyd AW, Mikhalovsky SV, Sandeman SR, Howel CA, Liewen L. Polymeric hydrogels for novel contact lens-based ophthalmic drug delivery systems: a review. Cont Lens Anterior Eye. 2008;31(2):57-64.
- 12. Willcox MDP, Harmis N, Cowell BA, Williams T, Holden BA. Bacterial interactions with contact lenses; effects of lens material, lens wear and microbial physiology. Biomaterials. 2001;22(24):3235-47.

- 13. Smolen VF, Vemuri R, Miya TS, Williams EJ. The Soflens® Contact Lens An Efficient, Corneal Loading, Drug Delivery System for Antiglaucoma Drugs. Drug Development Communications. 1974;1(6):479-94.
- 14. Ding S. Recent developments in ophthalmic drug delivery. Pharmaceutical Science & Technology Today. 1998;1(8):328-35.
- 15. McDermott ML, Chandler JW. Therapeutic uses of contact lenses. Surv Ophthalmol. 1989;33(5):381-94.
- 16. Hehl EM, Beck R, Luthard K, Guthoff R, Drewelow B. Improved penetration of aminoglycosides and fluorozuinolones into the aqueous humour of patients by means of Acuvue contact lenses. Eur J Clin Pharmacol. 1999;55(4):317-23.
- 17. Moreddu R, Vigolo D, Yetisen AK. Contact Lens Technology: From Fundamentals to Applications. Advanced Healthcare Materials. 2019;8(15):1900368.
- 18. Farandos NM, Yetisen AK, Monteiro MJ, Lowe CR, Yun SH. Contact lens sensors in ocular diagnostics. Adv Healthc Mater. 2015;4(6):792-810.
- 19. Maulvi FA, Soni TG, Shah DO. A review on therapeutic contact lenses for ocular drug delivery. Drug Deliv. 2016;23(8):3017-3026.
- 20. Guzman-Aranguez A, Colligris B, Pintor J. Contact Lenses: Promising Devices for Ocular Drug Delivery. Journal of Ocular Pharmacology and Therapeutics. 2013;29(2):189-199.
- 21. Gulsen D, Chauhan A. Dispersion of microemulsion drops in HEMA hydrogel: a potential ophthalmic drug delivery vehicle. Int J Pharm. 2005;292(1-2):95-117.
- 22. Tieppo A, Pate KM, Byrne ME. In vitro controlled release of an anti-inflammatory from daily disposable therapeutic contact lenses under physiological ocular tear flow. European Journal of Pharmaceutics and Biopharmaceutics. 2012;81(1):170-177.
- 23. Cope JR, Collier SA, Rao MM, Chalmers R, Mitchell GL, Richdale K, Wagner H, Kinoshita BT, Lam DY, Sorbara L et al. Contact Lens Wearer Demographics and Risk Behaviors for Contact Lens-Related Eye Infections--United States, 2014. MMWR Morb Mortal Wkly Rep. 2015;64(32):865-70.

- 24. Guzman-Aranguez A, Colligris B, Pintor J. Contact Lenses: Promising Devices for Ocular Drug Delivery. Journal of ocular pharmacology and therapeutics: the official journal of the Association for Ocular Pharmacology and Therapeutics. 2012;29.
- 25. Bengani LC, Hsu KH, Gause S, Chauhan A. Contact lenses as a platform for ocular drug delivery. Expert Opin Drug Deliv. 2013;10(11):1483-96.
- 26. Peterson RC, Wolffsohn JS, Nick J, Winterton L, Lally J. Clinical performance of daily disposable soft contact lenses using sustained release technology. Contact Lens and Anterior Eye. 2006;29(3):127-134.
- 27. Chow Edwin PY, Yang Yi Y; Polymer having interconnected pores for drug delivery and method. Singapore: Agency for science, technology and research; 2004.
- 28. Schrader S, Wedel T, Moll R, Geerling G. Combination of serum eye drops with hydrogel bandage contact lenses in the treatment of persistent epithelial defects.

 Graefe's Archive for Clinical and Experimental Ophthalmology. 2006;244(10):1345-9.
- 29. Maulvi FA, Soni TG, Shah DO. A review on therapeutic contact lenses for ocular drug delivery. Drug Delivery. 2016;23(8):3017-26.
- 30. Maria J, Giraldez E, Yebra-Pimentel E. Hydrogel Contact Lenses Surface Roughness and Bacterial Adhesion. London: Headquarters IntechOpen: 2012.
- 31. Baguet J, Sommer F, Claudon-Eyl V, Duc TM. Characterization of lacrymal component accumulation on worn soft contact lens surfaces by atomic force microscopy. Biomaterials. 1995;16(1):3-9.
- 32. Vermeltfoort PB, van der Mei HC, Busscher HJ, Hooymans JM, Bruinsma GM. Physicochemical factors influencing bacterial transfer from contact lenses to surfaces with different roughness and wettability. J Biomed Mater Res B Appl Biomater. 2004;71(2):336-42.
- 33. hu X, Hao L, Wang H, Yang X, Zhang G, Wang G, Zhang X. Hydrogel Contact Lens for Extended Delivery of Ophthalmic Drugs. International Journal of Polymer Science. 2011;2011:1-9.
- 34. Alvarez-Lorenzo C, Hiratani H, Gómez-Amoza JL, Martínez-Pacheco R, Souto C, Concheiro A. Soft contact lenses capable of sustained delivery of timolol. J Pharm Sci. 2002;91(10):2182-92.

- 35. White CJ, Tieppo A, Byrne ME. Controlled drug release from contact lenses: a comprehensive review from 1965-present. Journal of Drug Delivery Science and Technology. 2011;21(5):369-84.
- 36. Byrne ME, Salian V. Molecular imprinting within hydrogels II: progress and analysis of the field. Int J Pharm. 2008;364(2):188-212.
- 37. Lai C-F, Li J-S, Fang Y-T, Chien C-J, Lee C-H. UV and blue-light antireflective structurally colored contact lenses based on a copolymer hydrogel with amorphous array nanostructures. RSC Advances. 2018;8(8):4006-13.
- 38. Horst CR, Brodland B, Jones LW, Brodland GW. Measuring the modulus of silicone hydrogel contact lenses. Optom Vis Sci. 2012;89(10):1468-76.
- 39. Tranoudis I, Efron N. Tensile properties of soft contact lens materials. Contact Lens and Anterior Eye. 2004;27(4):177-91.
- 40. Tighe BJ. A decade of silicone hydrogel development: surface properties, mechanical properties, and ocular compatibility. Eye Contact Lens. 2013;39(1):4-12.
- Hutter J, Green J, Eydelman M. Proposed Silicone Hydrogel Contact Lens Grouping System for Lens Care Product Compatibility Testing. Eye & contact lens. 2012;38.
- 42. Lee SE, Kim SR, Park M. Oxygen permeability of soft contact lenses in different pH, osmolality and buffering solution. Int J Ophthalmol. 2015;8(5):1037-42.
- 43. Gavara R, Compan V. Oxygen, water, and sodium chloride transport in soft contact lenses materials. J Biomed Mater Res B Appl Biomater. 2017;105(8):2218-31.
- 44. Selby A, Maldonado-Codina C, Derby B. Influence of specimen thickness on the nanoindentation of hydrogels: measuring the mechanical properties of soft contact lenses. J Mech Behav Biomed Mater. 2014;35:144-56.
- 45. Bodaghi B. Diclofenac sodium 0.1% ophthalmic solution: update on pharmacodynamics, clinical interest and safety profile. Expert Review of Ophthalmology. 2008;3(2):139-48.
- 46. Jones LW, Jones DA. Non-inflammatory corneal complications of contact lens wear. Contact Lens and Anterior Eye. 2001;24(2):73-9.
- 47. Alava J, Garagorri N, Briz N, Mendicute J. Effects of bacterial adhesion with respect to the type of material, structure and design of intraocular lenses. Journal of Materials Science: Materials in Medicine. 2005;16(4):313-7.

- 48. Ho CH, Hlady V. Fluorescence assay for measuring lipid deposits on contact lens surfaces. Biomaterials. 1995;16(6):479-82.
- 49. Fornasiero F, Prausnitz JM, Radke CJ. Post-lens tear-film depletion due to evaporative dehydration of a soft contact lens. Journal of Membrane Science. 2006;275(1):229-43.
- 50. Henry VA, DeKinder JO. Soft lens material selection. In: Bennett ES, Henry VA, ed. Clinical Manual of Contact Lenses.: Lippincott, Williams & Wilkins; 2014.
- 51. Lloyd AW, Faragher RGA, Denyer SP. Ocular biomaterials and implants. Biomaterials. 2001;22(8):769-85.
- Hsu K-H, Fentzke RC, Chauhan A. Feasibility of corneal drug delivery of cysteamine using vitamin E modified silicone hydrogel contact lenses. European Journal of Pharmaceutics and Biopharmaceutics. 2013;85(3, Part A):531-40.
- 53. Peng CC, Kim J, Chauhan A. Extended delivery of hydrophilic drugs from silicone-hydrogel contact lenses containing vitamin E diffusion barriers.

 Biomaterials. 2010;31(14):4032-47.
- 54. Sharma J. Moxifloxacin loaded contact lens for ocular delivery an in vitro study; 2018.
- Lee D, Cho S, Park HS, Kwon I. Ocular Drug Delivery through pHEMA-Hydrogel Contact Lenses Co-Loaded with Lipophilic Vitamins. Scientific Reports. 2016;6:34194.
- 56. Li CC, Chauhan A. Ocular transport model for ophthalmic delivery of timolol through p-HEMA contact lenses. Journal of Drug Delivery Science and Technology. 2007;17(1):69-79.
- 57. Ruben M, Watkins R. Pilocarpine dispensation for the soft hydrophilic contact lens. The British journal of ophthalmology. 1975;59(8):455-8.
- 58. Karlgard CC, Wong NS, Jones LW, Moresoli C. In vitro uptake and release studies of ocular pharmaceutical agents by silicon-containing and p-HEMA hydrogel contact lens materials. Int J Pharm. 2003;257(1-2):141-51.
- 59. Srisuwan Y, Baimark Y. Preparation of Biodegradable Silk Fibroin/Alginate Blend Films for Controlled Release of Antimicrobial Drugs. Advances in Materials Science and Engineering, 2013;2013:6.

- 60. Minoura N, Tsukada M, Nagura M. Fine structure and oxygen permeability of silk fibroin membrane treated with methanol. Polymer. 1990;31(2):265-9.
- 61. Minoura N, Tsukada M, Nagura M. Physico-chemical properties of silk fibroin membrane as a biomaterial. Biomaterials. 1990;11(6):430-4.
- 62. Sashina ES, Golubikhin AY, Novoselov NP, Tsobkallo ES, Zaborskii M, Goralskii Y. Study of a possibility of applying the films of the silk fibroin and its mixtures with synthetic polymers for creating the materials of contact lenses. Russian Journal of Applied Chemistry. 2009;82(5):898-904.
- 63. Liu TL, Miao JC, Sheng WH, Xie YF, Huang Q, Shan YB, Yang JC. Cytocompatibility of regenerated silk fibroin film: a medical biomaterial applicable to wound healing. J Zhejiang Univ Sci B. 2010;11(1):10-6.
- 64. Ju HW, Lee OJ, Lee JM, Moon BM, Park HJ, Park YR, Lee MC, Kim SH, Chao JR, Ki CS et al. Wound healing effect of electrospun silk fibroin nanomatrix in burn-model. International Journal of Biological Macromolecules. 2016;85:29-39.
- 65. Li M, Lu S, Wu Z, Tan K, Minoura N, Kuga S. Structure and properties of silk fibroin-poly(vinyl alcohol) gel. International Journal of Biological Macromolecules. 2002;30(2):89-94.
- Caner C, Vergano PJ, Wiles JL. Chitosan film mechanical and permeation properties as affected by acid, plasticizer, and storage. Journal of Food Science 1998;63(6):1049-53.
- 67. Luangbudnark W, Viyoch J, Laupattarakasem W, Surakunprapha P, Laupattarakasem P. Properties and biocompatibility of chitosan and silk fibroin blend films for application in skin tissue engineering. ScientificWorldJournal. 2012;2012:697201.
- 68. Kweon H, Ha HC, Um IC, Park YH. Physical properties of silk fibroin/chitosan blend films. Journal of Applied Polymer Science. 2001;80(7):928-34.
- 69. Shi X-Y, Tan T-W. New Contact Lens Based on Chitosan/Gelatin Composites. Journal of Bioactive and Compatible Polymers. 2004;19(6):467-79.
- Verheul RJ, Amidi M, van Steenbergen MJ, van Riet E, Jiskoot W, Hennink WE. Influence of the degree of acetylation on the enzymatic degradation and in vitro biological properties of trimethylated chitosans. Biomaterials. 2009;30(18):3129-35.

- 71. Moraes MAd, Nogueira GM, Weska RF, Beppu MM. Preparation and Characterization of Insoluble Silk Fibroin/Chitosan Blend Films. Polymers. 2010;2(4):719.
- 72. Sashina ES, Janowska G, Zaborski M, Vnuchkin AV. Compatibility of fibroin/chitosan and fibroin/cellulose blends studied by thermal analysis. Journal of Thermal Analysis and Calorimetry. 2007;89(3):887-91.
- 73. Bini E, Knight DP, Kaplan DL. Mapping domain structures in silks from insects and spiders related to protein assembly. J Mol Biol. 2004;335(1):27-40.
- 74. Pham DT, Saelim N, Tiyaboonchai W. Crosslinked fibroin nanoparticles using EDC or PEI for drug delivery: physicochemical properties, crystallinity and structure. Journal of Materials Science. 2018;53.
- 75. Zafar MS, Al Samadani K. Potential use of natural silk for bio-dental applications. Journal of Taibah University Medical Sciences. 2014;9.
- 76. Inoue S, Tanaka K, Arisaka F, Kimura S, Ohtomo K, Mizuno S. Silk Fibroin of Bombyx mori Is Secreted, Assembling a High Molecular Mass Elementary Unit Consisting of H-chain, L-chain, and P25, with a 6:6:1 Molar Ratio. The Journal of biological chemistry. 2001;275:40517-28.
- 77. Motta A, Fambri L, Migliaresi C. Regenerated silk fibroin films: Thermal and dynamic mechanical analysis. Macromolecular Chemistry and Physics. 2002;203(10-11):1658-65.
- 78. Cao Y, Wang B. Biodegradation of silk biomaterials. Int J Mol Sci. 2009;10(4):1514-24.
- 79. Yamada H, Nakao H, Takasu Y, Tsubouchi K. Preparation of undegraded native molecular fibroin solution from silkworm cocoons. Materials Science and Engineering: C. 2001;14(1):41-6.
- 80. Akiyoshi A. Dissolution of silk fibroin with calcium chloride/ethanol aqueous solution. Journal of Sericology Science Japan. 1998;67(2):91-4.
- 81. Zhang H, Li L-l, Dai F-y, Zhang H-h, Ni B, Zhou W, Yang X, Wu Y-z. Preparation and characterization of silk fibroin as a biomaterial with potential for drug delivery. Journal of Translational Medicine. 2012;10(1):117.

- 82. Zhang H, Li L-L, Dai F-Y, Zhang H-H, Ni B, Zhou W, Yang X, Wu Y. Preparation and characterization of silk fibroin as a biomaterial with potential for drug delivery. Journal of translational medicine. 2012;10:117.
- 83. Zheng Z, Guo S, Liu Y, Wu J, Li G, Liu M, Wang X, Kaplan D. Lithium-free processing of silk fibroin. J Biomater Appl. 2016;31(3):450-63.
- 84. Freddi G, Pessina G, Tsukada M. Swelling and dissolution of silk fibroin (Bombyx mori) in N-methyl morpholine N-oxide. Int J Biol Macromol. 1999;24(2-3):251-63.
- 85. Foo CWP, Bini E, Hensman J, Knight DP, Lewis RV, Kaplan DL. Role of pH and charge on silk protein assembly in insects and spiders. Applied Physics A. 2006;82(2):223-33.
- 86. V D, Padamwar M, S P, Mahadik K. Moisturizing efficiency of silk protein hydrolysate: Silk fibroin. Indian Journal of Biotechnology. 2005;4:115-21.
- 87. Kweon H, Um IC, Park YH. Structural and thermal characteristics of Antheraea pernyi silk fibroin/chitosan blend film. Polymer. 2001;42(15):6651-6.
- 88. Srihanam P. Silk Fibroin/Chitosan Blend Films Loaded Methylene Blue as a Model for Polar Molecular Releasing: Comparison between Thai Silk Varieties.

 Journal of Applied Sciences. 2011;11.
- 89. Zheng W, Chen L, Chen J, Wang L, Gui X, Ran J, Xu G, Zhao H, Zeng M, Ji J et al. Silk Fibroin Biomaterial Shows Safe and Effective Wound Healing in Animal Models and a Randomized Controlled Clinical Trial. Advanced Healthcare Materials. 2017;6:1700121.
- 90. Rinaudo M. Chitin and chitosan: Properties and applications. Progress in Polymer Science. 2006;31(7):603-32.
- 91. Dutta P, Duta J, Tripathi VS. Chitin and Chitosan: Chemistry, properties and applications. Journal of Scientific and Industrial Research. 2004;63:20-31.
- 92. Puvvada Y, Vankayalapati S, Sukhavasi S. Extraction of chitin and chitosan from exoskeleton of shrimp for application in the pharmaceutical industry. International Current Pharmaceutical Journal. 2012;1.
- 93. di martino A, Liverani L, Rainer A, Salvatore G, Trombetta M, Denaro V. Electrospun scaffolds for bone tissue engineering. Musculoskeletal surgery. 2011;95:69-80.

- 24. Zhang Y, Zhang X, Ding R, Zhang J, Liu J. Determination of the degree of deacetylation of chitosan by potentiometric titration preceded by enzymatic pretreatment. Carbohydrate Polymers. 2011;83(2):813-7.
- 95. Pochanavanich P, Suntornsuk W. Fungal chitosan production and its characterization. Letters in Applied Microbiology. 2002;35(1):17-21.
- 96. Fernandez-Kim S-O. Physicochemical and Functional Properties of Crawfish Chitosan as Affected by Different Processing Protocols; 2004.
- 97. No HK, Meyers SP. Preparation and Characterization of Chitin and Chitosan—A Review. Journal of Aquatic Food Product Technology. 1995;4(2):27-52.
- 98. Brine CJ, Austin PR. Chitin variability with species and method of preparation. Comparative Biochemistry and Physiology Part B: Comparative Biochemistry. 1981;69(2):283-6.
- 99. Tarafdar A, Biswas G. Extraction of Chitosan from Prawn Shell Wastes and Examination of its Viable Commercial Applications. International Journal on Theoretical and Applied Research in Mechanical Engineering. 2013;2:2319-3182.
- Waibel KH, Haney B, Moore M, Whisman B, Gomez R. Safety of chitosan bandages in shellfish allergic patients. Mil Med. 2011;176(10):1153-6.
- 101. Yuan Y, Lee TR. Contact Angle and Wetting Properties. In: Bracco G, Holst B, editors. Surface Science Techniques. Berlin, Heidelberg: Springer Berlin Heidelberg. 2013;3-34.
- 102. Ji JJ, Ding ZJ, Yang XL. (Preparation and properties of chitosan film as a drug sustained-release system). Hua Xi Kou Qiang Yi Xue Za Zhi. 2009;27(3): 248-51.
- 103. Fulgêncio G, Viana F, Ribeiro R, Yoshida M, Faraco A, Silva-Cunha A. New Mucoadhesive Chitosan Film for Ophthalmic Drug Delivery of Timolol Maleate: In Vivo Evaluation. Journal of ocular pharmacology and therapeutics: the official journal of the Association for Ocular Pharmacology and Therapeutics. 2012;28:350-8.
- Dalia MNA, Ahmed Abd E-b, Samia HS, Mohamed AEN. Chitosan mucoadhesive buccal films: Effect of different casting solvents on their physicochemical properties. International Journal of Pharmacy and Pharmaceutical Sciences. 2016;8(9):38-49.

- 105. Li K, Zhu J, Guan G, Wu H. Preparation of chitosan-sodium alginate films through layer-by-layer assembly and ferulic acid crosslinking: Film properties, characterization, and formation mechanism. International Journal of Biological Macromolecules. 2019;122:485-92.
- 106. Lindell K, Engblom J, Engström S, Jonströmer M, Carlsson A. Influence of a charged phospholipid on the release pattern of timolol maleate from cubic liquid crystalline phases. In: Lindman B, Ninham BW, editors; Darmstadt (pp. 111-8). N.P.: Steinkopff; 1998.
- 107. Hirano T, Yasuda S, Osaka Y, Kobayashi M, Itagaki S, Iseki K. Mechanism of the inhibitory effect of zwitterionic drugs (levofloxacin and grepafloxacin) on carnitine transporter (OCTN2) in Caco-2 cells. Biochimica et Biophysica Acta (BBA) Biomembranes, 2006;1758(11):1743-50.
- 108. Suzuki T, Yamamoto T, Ohashi Y. The antibacterial activity of levofloxacin eye drops against staphylococci using an in vitro pharmacokinetic model in the bulbar conjunctiva. Journal of Infection and Chemotherapy. 2016;22(6):360-5.
- 109. Patidar N, Rathore MS, Sharma DK, Middha A, Gupta VB. Transcorneal permeation of ciprofloxacin and diclofenac from marketed eye drops. Indian journal of pharmaceutical sciences. 2008;70(5):651-4.
- 110. Bernal V, Erto A, Giraldo L, Moreno-Piraján J. Effect of Solution pH on the Adsorption of Paracetamol on Chemically Modified Activated Carbons.

 Molecules. 2017;22:1032.
- 111. Patel DM, Sardhara BM, Thumbadiya DH, Patel CN. Development and validation of spectrophotometric method for simultaneous estimation of paracetamol and lornoxicam in different dissolution media. Pharmaceutical methods. 2012;3(2):98-101.
- Sun S, Błażewska KM, Kadina AP, Kashemirov BA, Duan X, Triffitt JT, Dunford JE, Russell RGG, Ebetino FH, Roelofs AJ et al. Fluorescent Bisphosphonate and Carboxyphosphonate Probes: A Versatile Imaging Toolkit for Applications in Bone Biology and Biomedicine. Bioconjugate chemistry. 2016;27(2):329-40.

- 113. Wang P, Cheng M, Zhang Z. On different photodecomposition behaviors of rhodamine B on laponite and montmorillonite clay under visible light irradiation.

 Journal of Saudi Chemical Society. 2014;18(4):308-16.
- 114. Jonderian A, Maalouf R. Formulation and In vitro Interaction of Rhodamine-B Loaded PLGA Nanoparticles with Cardiac Myocytes. Frontiers in pharmacology. 2016;7:458.
- 115. Torres-Luna C, Koolivand A, Fan X, Agrawal NR, Hu N, Zhu Y, Domszy R, Briber RM, Wang NS, Yang A. Formation of Drug-Participating Catanionic Aggregates for Extended Delivery of Non-Steroidal Anti-Inflammatory Drugs from Contact Lenses. Biomolecules. 2019;9(10):593.



CHAPTER III

PREPARATION AND CHARACTERIZATION OF CHITOSAN/ REGENERATED SILK FIBROIN (CS/RSF) FILMS AS A BIOMATERIAL FOR CONTACT LENSES-BASED OPHTHALMIC DRUG DELIVERY SYSTEM

This chapter was published in International Journal of Applied Pharmaceutics, volume 11, issue 4, page 275-284, accepted on 24 May 2019. It describes how to develop and characterize chitosan/regenerated silk fibroin (CS/RSF) films as a biomaterial for contact lenses-based ophthalmic drug delivery system.

Abstract

The aim of this study was to develop chitosan/regenerated silk fibroin (CS/RSF) films as a biomaterial for contact lenses-based ophthalmic drug delivery system. CS/RSF films were prepared with polyethylene glycol 400 as a plasticizer by using a film casting technique. Their physicochemical properties were investigated by measuring various properties such as thickness, morphology, chemical interaction. light transparency, mechanical properties, water content, oxygen permeability, thermal properties and enzyme degradation. In addition, cytotoxicity was also studied. At optimal preparation conditions, CS/RSF films showed smooth surfaces with a highly visible light transparency of > 90%, which meet the visual requirement. CS/RSF films showed high water content, 59-65% by weight, and their Young's modulus and elongation at break were in the range of 3.8-6 Mpa and 113-135%, respectively. The CS/RSF films also could be sterilized by autoclave method as they possessed high thermal decomposition temperature of > 260°C which can be confirmed by both differential scanning calorimetry and thermogravimetric analysis. In addition, CS/RSF films showed no degradation in stimulated tear fluid containing lysozyme for 7 days and showed no cytotoxicity by MTT assay. CS/RSF films showed excellent physicochemical properties and non-cytotoxicity indicating their promising potential use as a biomaterial for contact lenses-based ophthalmic drug delivery system.

Keywords: Chitosan, Regenerated silk fibroin, Films, Contact lenses, Ophthalmic drug delivery system, Cytotoxicity

Introduction

Topical drug administration is a common approach to treat ocular disorders. Currently, more than 90% of marketed topical eye drops are in the form of solutions and suspensions because of their convenience and ease of administration (1-3). However, eye drops are notorious for poor ocular bioavailability with less than 5% of administered drugs entering the anterior chamber and reaching the intraocular tissues (2, 4-6). A large part of the drugs is lost into the systemic circulation by blinking, rapid tear turnover rate and drainage into the nasal cavity. To maintain sustained therapeutic drug levels, frequent administration or large doses are often required. Consequently, this reduces patient compliance, increases local side effects, and also results in pronounced systemic exposure (2, 7-9). Recently, daily disposable contact lenses-based ophthalmic drug delivery systems have been proposed as alternative ophthalmic drug delivery systems for increased ocular bioavailability (10-14). These approaches can be administered without any surgery and have been demonstrated to produce sustained drug release for a prolonged period by increasing the residence time of the drug on the ocular surface (12, 15-17). The benefit of daily disposable therapeutic contact lenses would be the delivery of the correct medication dosage at an approximate constant rate, thereby eliminating the frequent application of topical eye drops and, more importantly, leading to more benefits to the patient with substantially increased efficacy. Typically, commercial daily disposable contact lenses are usually made from synthetic polymers, such as poly (2-hydroxyethyl methacrylate) (pHEMA)based hydrogel and silicone based-hydrogel (SiH). pHEMA-based hydrogel contact lenses provide high water content of up to 80% and softness that promotes comfortable wearing. Their main disadvantages are low in strength (18-21). SiH contact lenses, in contrast, have high oxygen permeability and low adhesion to the bacteria, but they are low in water content with a hydration ability of < 45% (20-25).

To overcome the limitation of synthetic polymer-based contact lenses, we have proposed natural polymers as a potential biomaterial for contact lenses. This is due to their potential advantages of non-toxicity, good biocompatibility, low

inflammatory, high oxygen permeability, high optical transparency, high wettability, and good chemical and mechanical stabilities that could meet the required properties of daily disposable contact lenses. Furthermore, they can be used as daily disposable therapeutic contact lenses (26-39). Chitosan (CS) and regenerated silk fibroin (RSF) are natural polymers of interest for creating the daily disposable contact lenses-based ophthalmic drug delivery system. CS is a natural polycationic linear polysaccharide derived from the deacetylation of chitin (40). RSF, which is derived from degumming of the Bombyx mori cocoons and dissolution of silk fibroin respectively, is a protein mainly comprised of amino acids glycine, alanine, and serine (41-42). CS films showed good flexibility, high light transparency and high water content but it is highly sensitive to lysozyme degradation (32-35, 43). RSF films offer the advantages of high oxygen permeability, non-toxicity, excellent biocompatibility, and also excellent wound healing properties, but it is quite brittle (26-31). Therefore, the blending between CS and RSF is a possible solution to improve properties of films for creating the materials of daily disposable therapeutic contact lenses. Moreover, the blending of CS with RSF shows a good compatibility between two different materials by hydrogen bonding interaction (36, 40).

Nowadays, there are very few reports in published literatures of therapeutic contact lenses using combinations of natural polymers (35, 40). Furthermore, there were no reports on combinations of CS/RSF that have been used to produce the contact lenses. Therefore, the purpose of this study was to develop CS/RSF films as the biomaterials for contact lenses-based ophthalmic drug delivery system. The physicochemical properties of CS/RSF films were investigated by measuring various properties such as thickness, morphology, chemical interaction, light transparency, mechanical properties, water content, oxygen permeability, thermal properties and enzyme degradation. In addition, cytotoxicity was also studied.

Materials and methods

Materials

CS (> 90% deacetylation with mean molecular weight of 890 kDa) was obtained from Marine Bio Resources Co., Ltd (Samutsakhon, Thailand). *Bombyx mori* raw silk yarns were purchased from Badin Thai-Silk Korat Co., Ltd (Nakhon

Ratchasima, Thailand). Polyethylene glycol 400 (PEG400) was purchased from Namsiang trading Co., Ltd (Bangkok, Thailand). Snakeskin pleated dialysis tube with molecular weight cut-off (MWCO) at 10,000 Da was obtained from Thermo Scientific Inc. (Illinois, USA). All other chemicals and solvents were of analytical grade. Keratinocyte serum-free medium (K-SFM) with bovine pituitary extract (BPE), and recombinant human epidermal growth factor (EGF) were purchased from Thermo Fisher Scientific Co., Ltd. (Bangkok, Thailand). Telomerase-immortalized human corneal epithelial cells line (HCECs) were a gift from Associate Professor Dr. Sangly P. Srinivas (School of Optometry, Indiana University, USA).

Preparation of RSF

RSF was prepared according to Yamada et al. (2001; Ajisawa, 1998) (44-45). Briefly, raw silk yarns of *Bombyx mori* were degummed twice by boiling in a 0.5 % (w/v) sodium carbonate solution for one hour to remove sericin. Then, the silk yarns were washed three times with warm reverse osmosis (RO) water and dried overnight at 40°C. The resulting degummed silk yarns were heated at 85-90°C in a solution of CaCl₂:H₂O:Ca(NO₃)₂:EtOH at 30:5:45:20 in gram ratio until a gel-like solution was formed. Next, the resultant gel is dialyzed (using a snakeskin pleated dialysis tube having a 10,000 MWCO) against RO water at room temperature for 3 days to remove residual salts, then centrifuged at 15300×g for 30 min to remove foreign particles. The RSF solution was lyophilized and kept in sealed plastic bags at -20°C until use.

Preparation of CS/RSF films

CS/RSF films were prepared by a casting method (37). Briefly, 2% (w/v) RSF aqueous solution, 2% (w/v) of CS solution, dissolved in 2% (v/v) acetic acid and PEG400 25 % w/w of polymer matrix were mixed using magnetic stirrer at 200 rpm for 30 min. The CS/RSF ratios were varied as 100/0, 90/10, 80/20 and 70/30 (w/w). The mixtures were then poured onto the polystyrene plates and dried in an oven at 40°C until completely dried. The dried films were immersed in 1M NaOH solution for 15 min, and then repeatedly rinsed with RO water until a neutral pH was obtained. The films were then soaked in 0.01M phosphate buffer saline (PBS) solution, pH 7.4 for 24 h and autoclaved at 121°C and 15 psi for 20 min. The autoclaved CS/RSF films were dried at room temperature and further stored in desiccators until used. All samples were prepared in triplicate.

Thickness measurements

The CS/RSF films thickness was measured with a thickness gauge (Mitutoyo 7301 Dial Thickness Gage, Kanagawa, Japan). The dried films were rehydrated by soaking them in 0.01M phosphate buffer saline (PBS), pH 7.4 for 24 h. Measurements were taken at the center and at four positions around the perimeter of the hydrated film and then the average thickness of films were calculated (46).

Morphology

A scanning electron microscope (SEM, Carl Zeiss AURIGA®, Thuringia, Germany) was employed to examine the morphology of surface and cross-section of RSF/CS films. The samples were sputter-coated with gold by plasma in order to minimize electron charging on the surface and to obtain fine images. Acceleration voltage of 5 kV was used to collect SEM images of the samples.

Light transparency

The light transparency of CS/RSF films were determined using UV-VIS spectrophotometer (Genesys 10S, Thermo scientific, Wisconsin, USA). A dried film was rehydrated by soaking it in 0.01M PBS, pH 7.4 for 24 h. Then the hydrated film with an average thickness of 0.09 mm was mounted on the outer surface of a quartz cuvette. The cuvette was placed in the spectrophotometer and the light transparency was measured at 280-780 nm (47).

Mechanical properties

The Young's modulus and elongation at break of the CS/RSF films were determined according to ASTM D882-12 using a texture analyzer (TA.XT-PLUS, London, UK) with a load cell of 5 kg, a crosshead speed of 20 mm/min, and a gauge length of 10 mm (48). A dried film was rehydrated by soaking it in 0.01M PBS, pH 7.4 for 24 h, and then the hydrated film with width of 3 mm and thickness of 0.09 mm was measured using the texture analyzer.

Water content

The CS/RSF films were soaked in 0.01M PBS, pH 7.4 for 24 h, and then water content of films were measured using a moisture analyzer (Sartorius MA 30, Sartorius lab instruments GmbH & Co. KG, Lower Saxony, Germany). The rehydrated film was weighed for its initial weight (W_{wet}). After that, the rehydrated film was dried at 105°C and weighed several times until the film's weight was

constant (W_{dried}) (49). The water content was calculated as shown in the following equation (1)

Water content (%) =
$$\frac{(W_{\text{wet}} - W_{\text{dried}})}{W_{\text{wet}}} \times 100$$
 (3.1)

Thermal properties

Differential scanning calorimetry (DSC) was performed to determine the thermal properties of the CS/RSF films using DSC 3⁺ STAR System (Mettler Toledo (Thailand), Bangkok, Thailand). Samples were heated from -20°C to 400°C at a heating rate of 20°C/min under a nitrogen atmosphere with a flow rate of 50 ml/min (36). Thermogravimetric analysis (TGA) was performed using TGA/DSC 3⁺ STAR System (Mettler Toledo (Thailand), Bangkok, Thailand). Thermal decomposition temperature of each sample was examined under a nitrogen atmosphere with a flow rate of 50 ml/min, in a temperature range of 30-600°C and at a heating rate of 20°C/min (36).

Ion permeability

The ion permeability was determined using a homemade horizontal diffusion cell, with an aperture a diameter of 35 mm, at 34±1°C. The receiving chamber was filled with 35 ml of deionized (DI) water. After soaking in DI water for 24 h, a hydrated film, 0.09 mm in thickness, was placed between the two compartments of the diffusion cell and then the donor chamber was filled with 18 ml of 154 mM NaCl solution. The conductivity of the solution in the receiving chamber was measured at time intervals by a conduct meter (Model 712 Conductometer, Metrohm UK Ltd., Cheshire, UK). The conductivity was converted to ion concentration using calibration curve of NaCl solution with a concentration range of 10-60 mM. The ion concentration was plot as a function of time. Then, the apparent ion permeability was calculated using a slope (F) at steady state (dc/dt) following Fick's law as shown in the following equation (2) (47, 50).

Apparent ion permeability (mm²/min) =
$$\left(\frac{F \times V}{A}\right) / \left(\frac{C_0}{T}\right)$$
 (3.2)

Where V is the volume of the receiving chamber solution, A is the area of the tested film, C_0 is the initial NaCl concentration in donor, and T is the film thickness.

Oxygen permeability

CS/RSF contact lenses for oxygen permeability testing were prepared by spinning casting method in an oven at 40°C until completely dried, The oxygen permeability of hydrated CS/RSF contact lenses, 0.2 mm of center thickness, were measured according to ISO 18369-4 (35°C and >98% relative humidity) using the polarographic amplifier (Model 201T Permeometer, Createch/Rehder development. CO., Indiana, USA).

In vitro enzymatic degradation

The degradation of CS/RSF films was analyzed following their incubation at 34±1°C in stimulated tear fluid (STF) containing lysozyme 1 mg/ml (pH 7.4). The compositions of STF were sodium chloride 0.67 g, sodium bicarbonate 0.2 g, calcium chloride 2H₂O 0.008 g, and deionized water added to 100 g. The film (2×2 cm²) after autoclaving and drying were weighed (initial weight, W₀). The films were immersed in 2 ml of STF containing lysozyme for 2, 5, 7, and 14 days. After that, the films were dried at 60°C overnight and weighed after degradation (W₁). The percentage of the remaining weight was calculated as shown in the following equation (3) (33, 51-53).

Remaining weight (%) =
$$\frac{W_1}{W_0} \times 100$$
 (3.3)

Cytotoxicity study

CS/RSF films cytotoxicity was determined by telomerase-immortalized human corneal epithelial cells line (HCECs) viability. The HCECs were seeded onto 96-well plates at 1.5 × 10⁴ cells per well in 100 μl of cell culture medium and incubated at 37°C, 5% CO₂ until reaching ~90% of cell confluence (3 days). The RSF/CS films, after soaking with PBS for 24 h, were cut into the same size of 96-well plates and were then autoclaved. Then, the films were placed gently on HCECs in 96-well plates and incubated for up to 24 h at 37°C, 5% CO₂. After 24 h, the films were carefully removed from the wells. Then, the cells were washed with PBS twice, and 100 μl of 3-(4, 5-Dimethylthiazol-2-yl)-2, 5-Diphenyltetrazolium Bromide (MTT) solution (0.5 mg MTT/ml of medium) was added. After a 2 h reaction time, MTT formazan was extracted with dimethyl sulfoxide (DMSO) for 10 min and the absorbance of the extract was measured at 595 nm with a microplate reader

(SynergyTM H1, BioTek Instruments, Inc., Vermont, USA) (54). All results were expressed as relative viability compared to cells grown in the absence of a film (control). The ratio (%) of MTT formazan absorbance for each sample to the absorbance of MTT formazan for control represented cell viability using the following formula (4).

Cell viability (%) =
$$\frac{\text{Absorbance of sample}}{\text{Absorbance of control}} \times 100$$
 (3.4)

Statistical analysis

The results were expressed as mean \pm standard deviation (SD). For all comparisons, statistical significant differences were analyzed with paired t-test or one-way ANOVA followed by Tukey's post hoc test, and P < 0.05 was considered statistically significant.

Results and discussion

The PEG400 content, 25% by weight of polymer content, and the 15 min NaOH treatment were selected based on the preliminary study. In the preliminary study, CS/RSF films prepared with PEG400 as a plasticizer were successfully developed. However, without NaOH treatment, they were extremely weak and brittle. On the other hand, with 15 min NaOH treatment, CS/RSF films showed high strength with homogeneous films. This is due to NaOH allowing new hydrogen bond formation which caused larger anhydrous crystal size and more compact structure in the films (55). In addition, the film prepared with PEG400 at 25% by weight of polymer content showed high oxygen permeability. Therefore, all the prepared films were composed of PEG400 25%w/w with 15 min NaOH treatment. Moreover, the blended films were prepared covering the whole range of CS/RSF weight ratio of 100/0 to 0/100 (w/w). Unfortunately, the pure RSF film and CS/RSF films at ratios of 30/70, 20/80, and 10/90 (w/w) were extremely brittle and could not be handled. In contrast, when increasing the CS content, CS/RSF ratios of 100/0, 90/10, 80/20, 70/30, 60/40, 50/50, and 40/60 (w/w), the obtained films showed to be non-brittle and were strong enough to handle without deformation. However, CS/RSF films at ratios of 60/40, 50/50, and 40/60 (w/w) showed visible light transparency of less than 90%, which did not satisfy the visual requirements. Typically, the visible light transparency of contact lenses

should be more than 90% (56). Therefore, only CS/RSF films at ratios of 100/0, 90/10, 80/20, and 70/30 (w/w) were selected to be further studied as they manifested high tensile strength with visible light transparency of > 90% which is similar to commercial contact lenses (47).

Appearances and morphology of CS/RSF films

The prepared CS/RSF films at ratios of 100/0, 90/10, 80/20 and 70/30 (w/w) were uniformly light transparent, non-brittle and were strong enough to handle without deformation. Typically, commercial contact lenses have thickness of 0.05-0.2 mm (20, 57). All prepared CS/RSF films showed no significant difference in thickness of 0.09 ± 0.01 mm, indicating they were suitable for contact lenses. SEM micrographs of topical surface of all CS/RSF films showed smooth surfaces without phase separation. Moreover, their cross-sections exhibited homogenous blending between CS and RSF without obvious phase disengagement as shown in Figure 3.1.

Light transparency of CS/RSF films

The light transparency of blended films is an important property of contact lenses. The optical transmittance spectra in the range 280 - 780 nm of CS/RSF films were displayed in Figure 3.2, while the mean light transparency of each spectral range were shown in Table 3.1. Typically, the visible light transparency (381-780 nm) of contact lenses should be more than 90% (56). All CS/RSF films showed excellent visible light transparency of > 90%, which meet the visual requirement, indicating a good compatibility of the blended film. According to the American National Standards Institute of Z80.20 standard, contact lenses shall satisfy Class II UV blocking, which transmittance for UV-B (280-315 nm) and UV-A (316-380 nm) less than 5% and 30%, respectively. Although UV-B and UV-A transmittance of all prepared CS/RSF films did not meet the Class II UV blocking standard. However, all films showed significant protection against UV-B and UV-A, especially when increasing the RSF content. 100CS/0RSF film showed UV-B and UV-A transmittance of 27% and 58% respectively while 70CS/30RSF was reduced to 12% and 50%, respectively. In addition, the blue visible light is considered unsafe to the eyes. It can be divided into the short-wavelength blue region (SWB, 381–460 nm) and the longwavelength blue region (LWB, 461-500 nm). Similarly to UV blocking ability, all films showed ability to reduce blue light transmittance suggesting some protection

against blue light, particularly when the amount of RSF was increased. 100CS/0RSF film showed SWB transmittance of 88%, while 70CS/30RSF film was reduced to 80%. These results suggested that the CS/RSF blended films showed greater potential in the protection from UV-B, UV-A, and blue light than CS film.

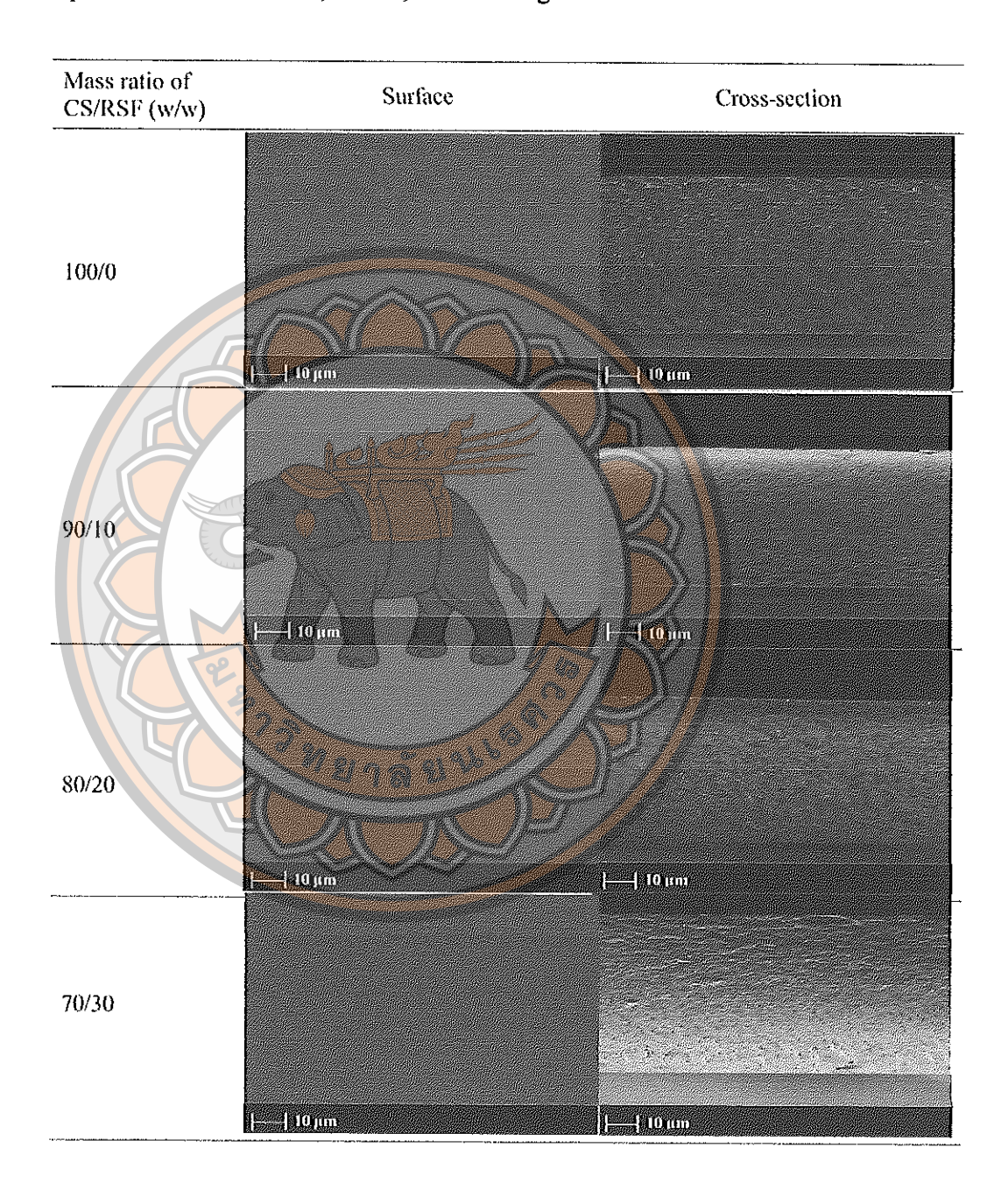


Figure 3.1 SEM micrographs of surface and cross-section of CS/RSF films (×1000 magnification)

Table 3.1 Light transparency of CS/RSF films

Mass ratio	Light transparency (%) ± SD					
of CS/RSF	UV-B	UV-A	SWB	LWB	Visible	
	(280-315	(316-380	(381-460	(461-500	(381-780	
(w/w)	nm)	nm)	nm)	nm)	nm)	
100/0	27 ± 2	58 ± 2	88 ± 1	95 ± 1	95 ± 1	
90/10	17 ± 0	52 ± 0	83 ± 1	91 ± 1	92 ± 1	
80/20	10 ± 1	48 ± 1	82 ± 0	90 ± 0	91 ± 0	
70/30	12 ± 2	50 ± 3	80 ± 2	88 ± 2	90 ± 2	

SD: standard deviation, n = 3

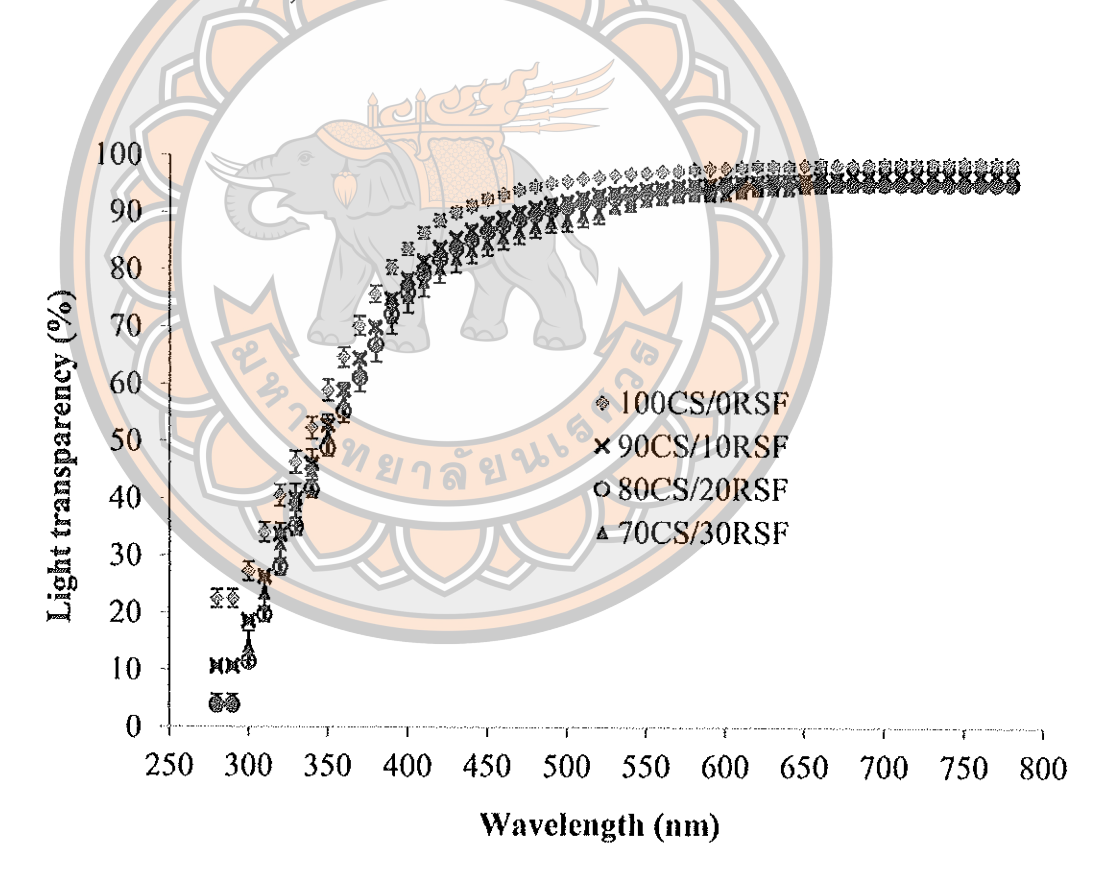


Figure 3.2 Light transparency of CS/RSF films with indicated blend ratios

Mechanical properties of CS/RSF films

The mechanical properties of contact lenses are important considerations with respect to durability and resistance to damage during handling. The stiffness and flexibility of contact lenses are expressed by Young's modulus and elongation at break, respectively. The Young's modulus of CS/RSF films was decreased by increasing RSF content, Table 3.2. 100CS/0RSF film showed Young's modulus of 6 Mpa, while 70CS/30RSF was reduced to 3.8 Mpa. The maximum Young's modulus of the various commercial soft contact lenses materials are reported to be at 1.5 Mpa (22-23, 48, 64). Clearly, the stiffness of CS/RSF films was slightly higher suggesting a more stiffness and thus are easier to handle and less likely to fold in on itself. Similarly, the RSF content affected the elongation at break. The elongations at break of 100CS/0RSF and 70CS/30RSF films were 135 and 113%, respectively (Table 3.2). Nevertheless, all prepared blended films possessed the elongation at break of > 50% which are considered to satisfy the flexibility requirement (48).

Water content of CS/RSF films

Water content is one of the key parameters to determine the comfort of wearing contact lenses wearing. Contact lenses with high water content would offer greater softness and comfortable wearing. According to FDA's classification, soft contact lenses with water content of < 50% by weight is considered as "low water content", while those with > 50% by weight is considered as "high water content". All prepared CS/RSF films showed high water content (59 to 65% by weight) as shown in Table 3.2. Nevertheless, the water content of CS/RSF films was slightly decreased as the content of silk fibroin increased. This phenomenon could be explained by the intermolecular hydrogen bonds between CS and RSF molecules, resulting in the reduced interaction between CS and water.

Table 3.2 Mechanical properties and water content of CS/RSF films

Mass ratio of	Young's Modulus	Elongation at	Water content
CS/RSF (w/w)	$(Mpa) \pm SD$	break (%) ± SD	(%) ± SD
100/0	6.0 ± 1.2	135 ± 17	65 ± 1.34
90/10	5.4 ± 0.6	116 ± 28	62 ± 1.38
80/20	4.6 ± 1.1	111 ± 26	59 ± 1.35
70/30	3.8 ± 0.5	113 ± 13	59 ± 0.92

SD: standard deviation, n = 3

Thermal properties of CS/RSF films

Thermal properties of CS/RSF films were investigated by DSC measurement as shown in Figure 3.3. Water evaporation temperature, glass transition temperature (Tg), thermal decomposition temperature were investigated. A broad endothermic peak below 110°C observed in all CS/RSF films was attributed to moisture evaporation. With increasing RSF content, the height and area under endothermic peak were decreased indicating the reduction of moisture in the films. This observation correlated to the water content of the film, the water content of CS/RSF films decreased with increasing RSF content, Table 3.2.

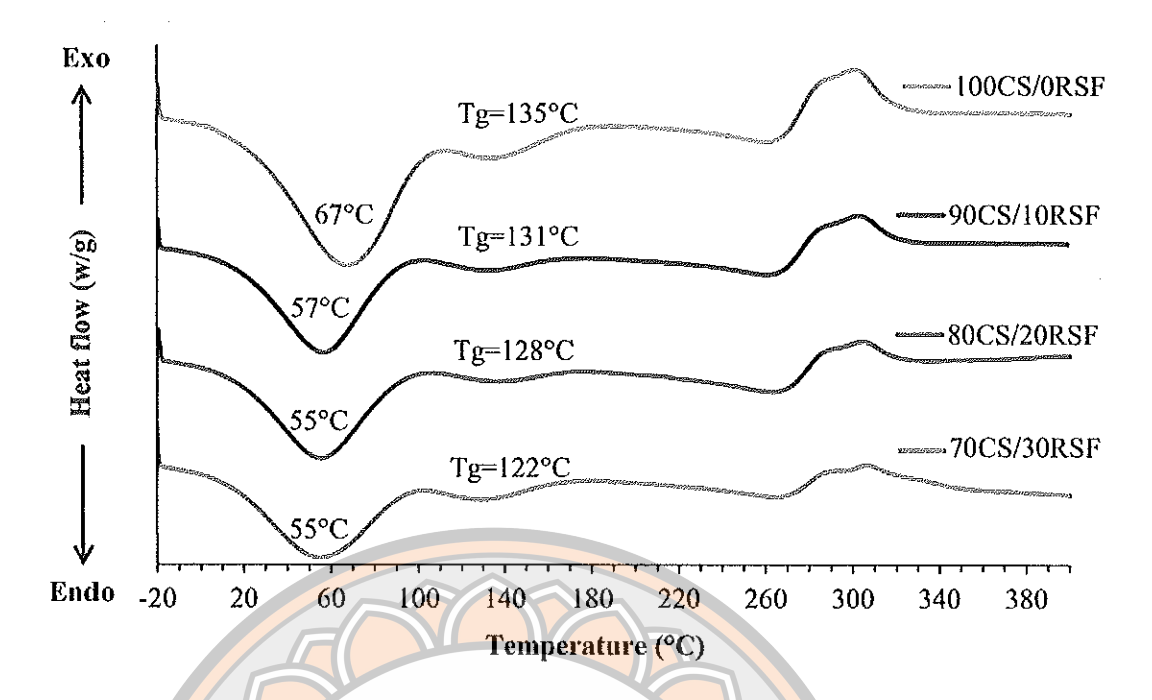


Figure 3.3 DSC curve of CS/RSF films with indicated blend ratios

The Tg of 100CS/0RSF film was observed at 135°C, while 70CS/30RSF film showed Tg at 122°C. Interestingly, with increasing RSF content, the decreasing Tg was observed indicating the increased amorphous portion of CS/RSF film (65). The increasing amorphous fraction could be attributed to decrease in the film strength. This result was in agreement with their mechanical properties. The Young's modulus of CS/RSF films decreased with increasing RSF content. From DSC peaks, the thermal decomposition temperature of CS/RSF films was ~ 265-330°C. The initial thermal decomposition temperature of CS/RSF films slightly increased from 265 to 270°C with increasing RSF content indicating that RSF could slightly increase thermal stability of CS/RSF films.

In addition, the thermal properties of blended film were also confirmed by TGA. The initial weight loss of CS/RSF films at below 170°C, ~5-20%, was due to water evaporation (Figure 3.4A). In accordance with DSC results, the moisture content of CS/RSF films decreased with increasing RSF contents. However, to determine the effect of RSF content on thermal decomposition temperature, the TGA curves of CS/RSF films were adjusted to avoid the interference from the moisture (Figure 3.4B). The thermal decomposition temperature of CS/RSF films was ~ 260-330°C similar to DSC results. At thermal decomposition temperature, the residual weight of CS/RSF

films slightly increased with increasing RSF. This indicated that increasing RSF slightly increased the thermal stability of CS/RSF films. Furthermore, both DSC and TGA techniques revealed that all CS/RSF films possessed high thermal stability with thermal decomposition temperature of > 260°C. This confirmed that CS/RSF films were able to be autoclaved at 121°C without deterioration.

Ion permeability of CS/RSF films

Ion permeability of contact lenses is a critical variable for lens motion on the eye (66). For sufficient on-eye-movement, typically, ion permeability of the lens should be greater than 12 × 10⁻⁶ mm²/min (67). The ion permeability of CS/RSF films was calculated using the slope obtained from the plots of NaCl concentration in the receiving chamber versus time (Figure 3.5). The ion permeability of 100CS/0RSF and 70CS/30RSF films showed no significant difference of 10.91 × 10⁻³ and 10.70 × 10⁻³ mm²/min, respectively. It is important to note that the ion permeability of CS/RSF films showed approximately 900 times higher than that of the minimum ion permeability requirement. Interestingly, comparing to commercial soft contact lenses, the ion permeability of CS/RSF films was likely an intermediate range of the ion permeability of various commercial contact lenses (0.6 to 26 × 10⁻³ mm²/min) (50). In general, the contact lens material with high water content usually gives high ion permeability. As a consequence, CS/RSF films showed high water content (59 to 65% by weight) that could lead to ion permeability enhancement.

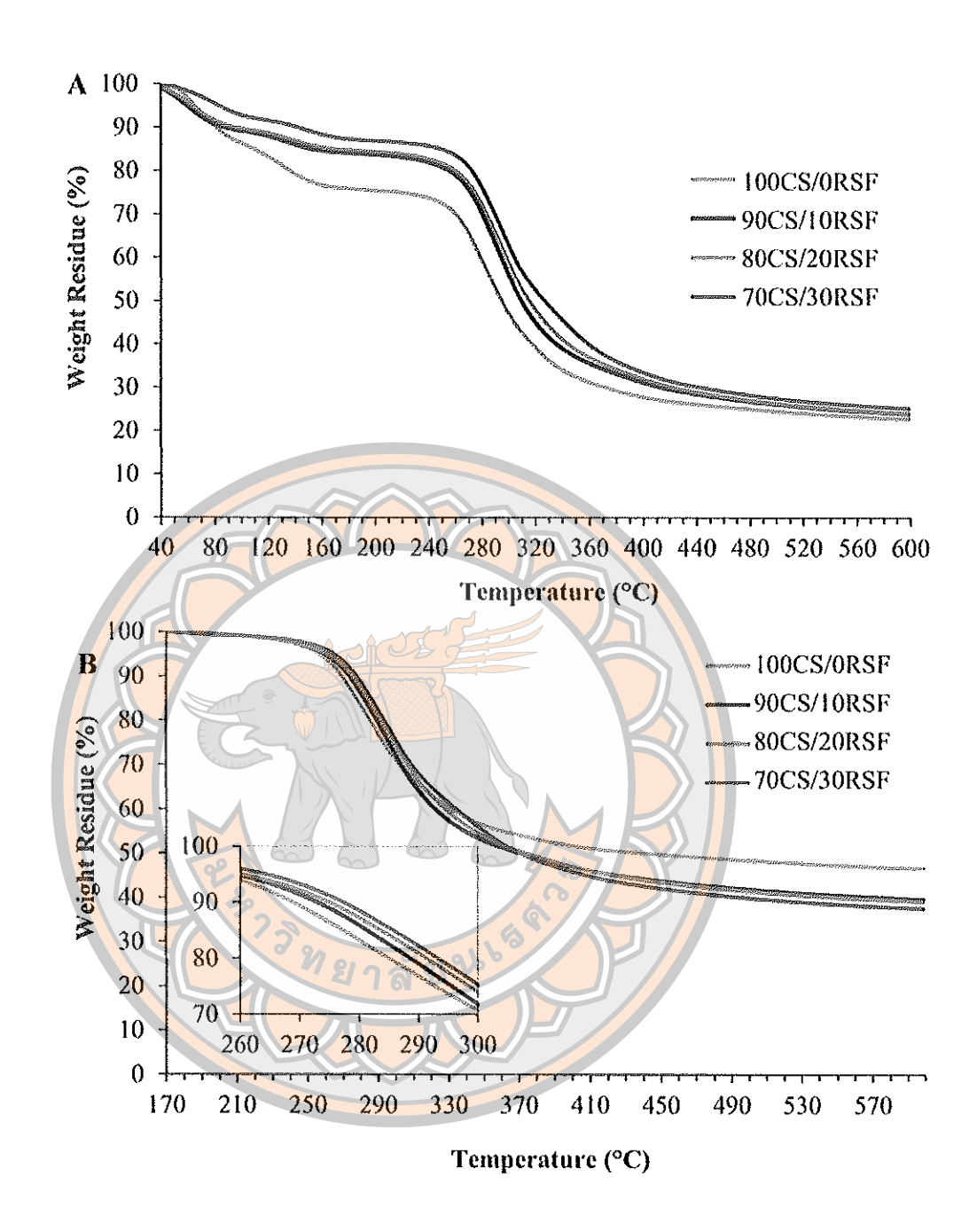


Figure 3.4 TGA curve of CS/RSF films with indicated blend ratios, (A) Original curve and (B) Adjusted curve after moisture removal

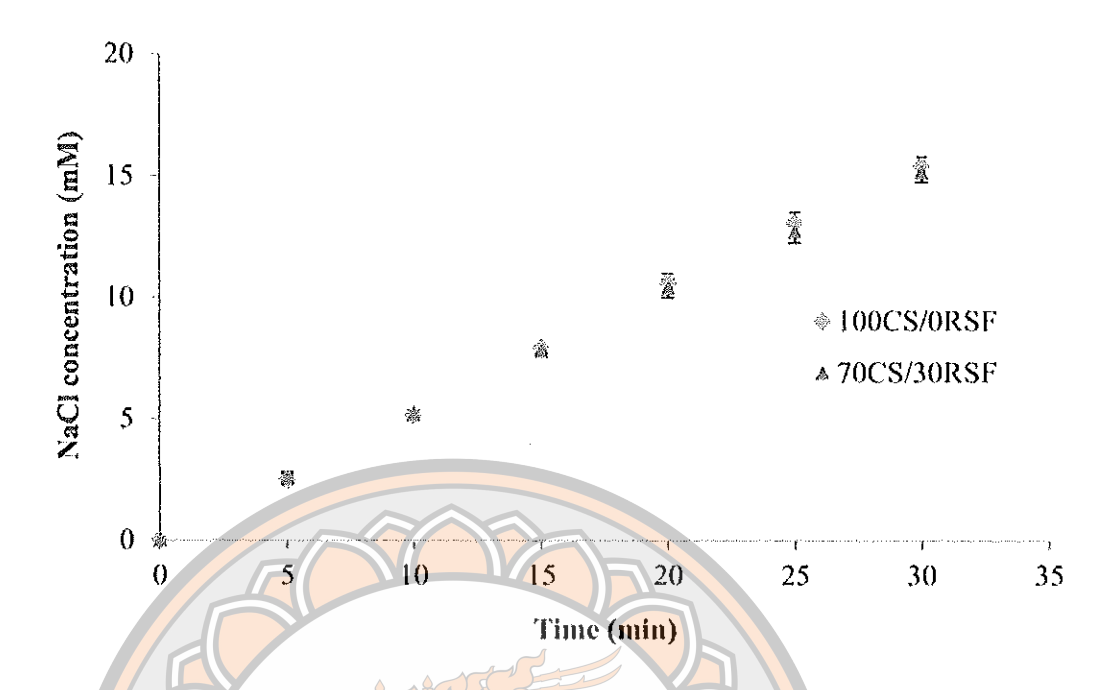


Figure 3.5 The plots of NaCl concentration in the receiving chamber versus time for CS/RSF films used in ion permeability study

Oxygen permeability of CS/RSF films

Oxygen permeability is an important parameter to characterize the contact lenses. Contact lenses with high oxygen permeability to the cornea tend to be safer, lower the risk of corneal hypoxia, and provide greater comfort of wearing. 100CS/0RSF and 70CS/30RSF contact lenses were successfully prepared by spinning casting method with 0.2 mm in thickness. The oxygen permeability of 100CS/0RSF contact lenses was 22 Barrers (10⁻¹¹(cm²/sec)(mlO₂(ml × mmHg))). In contrast, the 70CS/30RSF contact lenses showed greater oxygen permeability of 26 Barrers. This result indicated that oxygen permeability of CS/RSF films slightly increased with higher amount of RSF because it could be strongly related to the polymorphism of the film (68). As evident from DSC results, the amorphous portion of CS/RSF films slightly increased with increasing RSF content. Accordingly, oxygen permeability of CS/RSF contact lenses were shown to meet standards for use as daily disposable contact lenses as compared to the commercial contact lenses (10-33 Barrers) (20, 64).

In vitro enzymatic degradation study

Enzymatic degradation is a significant consideration in the design and quality control of the soft contact lenses materials. Biodegradable materials are not suitable for contact lenses application because the small residual may cause eye irritation. Thus, the stability of CS/RSF film in tear fluids containing important amounts of proteins and lysozyme is a crucial issue. The CS/RSF films are constructed from CS, which can be hydrolyzed by the lysozyme presenting in tear fluids. Therefore, the remaining weight of CS/RSF was determined upon their incubation in the STF containing lysozyme. After incubation in the STF containing lysozyme for 14 days, only 70CS/30RSF film showed no degradation with percentage of remaining weight of 100% (Table 3.3). In contrast, CS/RSF films at ratios of 100/0, 90/10, 80/20 (w/w) illustrated slight degradation as evidenced by from the remaining weight of 94, 97, and 99%, respectively. The degradation of CS/RSF films in the STF containing lysozyme increased by increasing the proportion of CS. This result could be attributed to a partial hydrolysis of CS by lysozyme. (43,51). Nevertheless, all CS/RSF films incubated with STF containing lysozyme for 7 days showed no degradation, with remaining weight of 100%.

Table 3.3 Percentage of remaining weight of CS/RSF films after incubation in STF Containing lysozyme

Mass ratio of	Mass ratio of Remaining Weight (%) ± SD			
CS/RSF (w/w)	2 days	5 days	7 days	14 days
100/0	100.30 ± 0.81	99.94 ± 0.31	100.46 ± 0.83	94.38 ± 2.13
90/10	100 .22 ±0.83	100.16 ± 0.75	100.36 ± 0.73	97.09 ± 2.68
80/20	100.08 ± 0.27	100.02 ± 0.42	100.02 ± 0.85	98.93 ± 2.68
70/30	100.51 ± 0.75	100.34 ± 0.88	100.41 ± 0.77	99.54 ± 1.31

SD: standard deviation, n = 3

Cytotoxicity study

The cell viability of HCECs after incubation with CS/RSF films for 24 h was approximately 100% (Figure 3.6) indicating that CS/RSF films are non-cytotoxic. In addition, non-cytotoxicity of CS/RSF films was further confirmed by microscopic observation (Figure 3.7). Upon treatment with CS/RSF films, the appearance of confluence HCECs showed no significant difference as compared to those treated without CS/RSF films (control). Similarly, after they were incubated with MTT, the appearance of HCECs treated with CS/RSF films showed similar morphology as those of control.

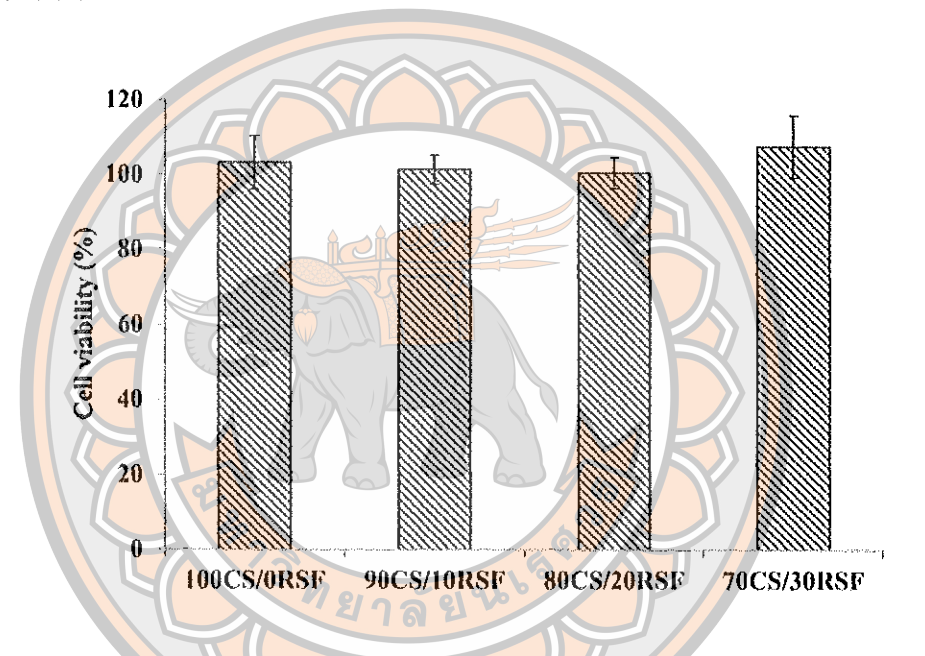


Figure 3.6 Cell viability of HCECs after exposed to CS/RSF films for 24 h

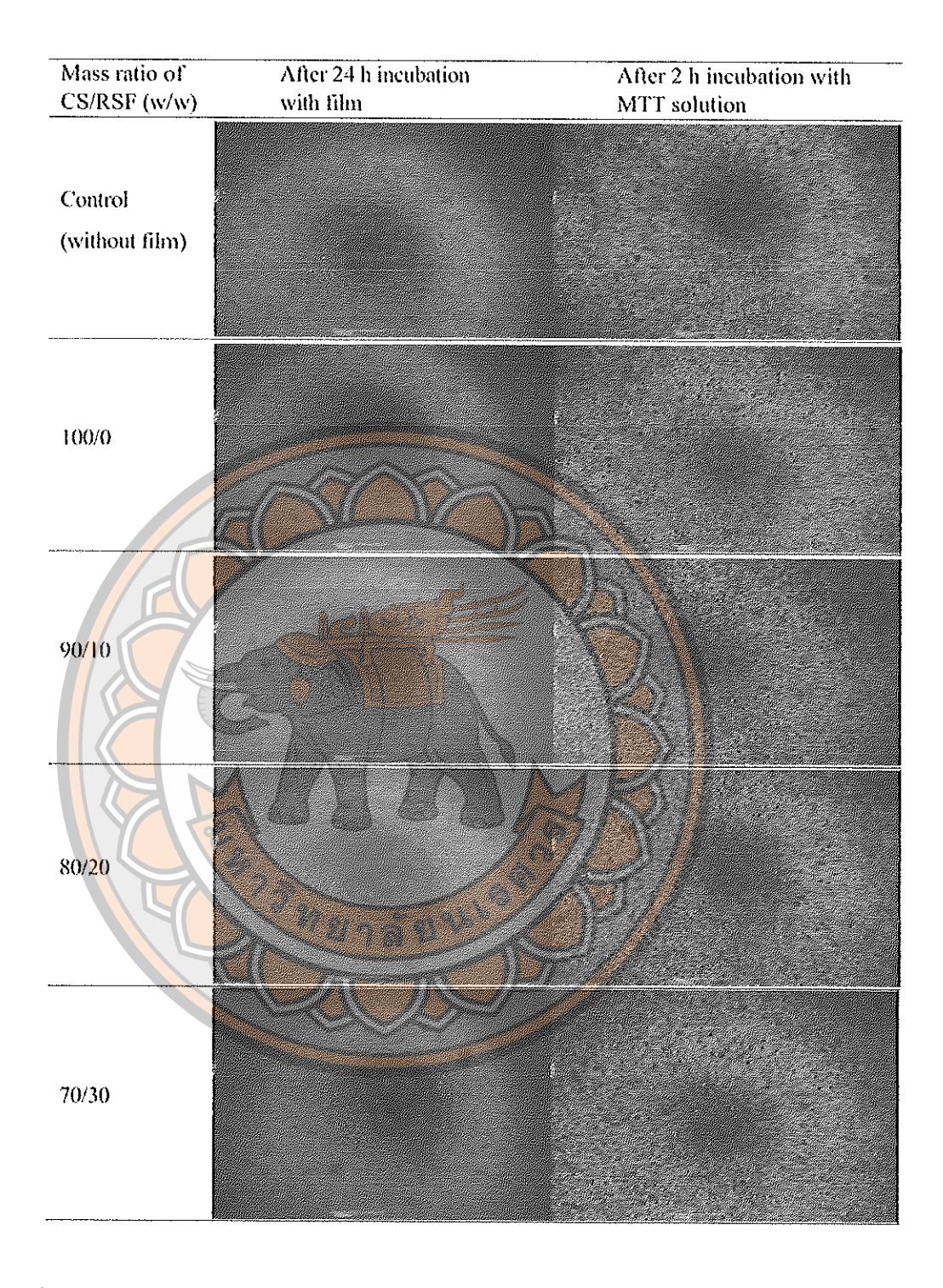


Figure 3.7 Optical micrographs of HCECs after 24 h incubation with film and after 2 h incubation with MTT solution (×4 magnification)

Conclusion

The CS/RSF films at ratios of 100/0, 90/10, 80/20 and 70/30 (w/w) showed high visible light transparency, smooth surface morphology and their cross-sections exhibited homogenous blending between CS and RSF without phase separation. With increasing RSF content, oxygen permeability, and thermal stability of the prepared films increased whereas the mechanical properties and water content of the prepared films slightly decreased. Moreover, all prepared films showed high thermal stability, high Young's modulus and elongation at brake. In conclusion, all prepared films were softness with high strength characteristics, good oxygen and ion permeability, high water content, no cytotoxicity and no degradation in STF containing lysozyme for 7 days implying that prepared films were biocompatible and could promote the comfort for wearing without irritation and grittiness in the eyes. Therefore, CS/RSF films showed excellent physicochemical properties and noncytotoxicity indicating their promising potential use as a biomaterial for daily disposable contact lenses-based ophthalmic drug delivery system.

References

- 1. Bourlais CL, Acar L, Zia H, Sado PA, Needham T, Leverge R. Ophthalmic drug delivery systems. Progress Retinal Eye Research. 1998;17(1):33-58.
- 2. Lang JC. Ocular drug delivery conventional ocular formulations. Advanced Drug Delivery Reviews. 1995;16(1):39-43.
- 3. Ali M, Byrne ME. Challenges and solutions in topical ocular drug delivery systems. Expert Opinion on Drug Delivery. 2008;1(1):145-61.
- 4. Deshpande SG, Shirolkar S. Sustained release ophthalmic formulations of pilocarpine. J Pharm Pharmacol. 1989;41(3):197-200.
- 5. Geroski DH, Edelhauser HF. Drug delivery for posterior segment eye disease. Investigative Ophthalmology & Visual Science. 2000;41(5):961-4.
- 6. Hyun JJ, Anuj C. Ophthalmic drug delivery by contact lenses. Expert Review of Ophthalmology. 2012;7(3):199-201.
- 7. Winfield AJ, Jessiman D, Williams A, Esakowitz L. A study of the causes of non-compliance by patients prescribed eyedrops. British Journal of Ophthalmology. 1990;74(8):477-80.

- 8. Barbu E, Verestiuc L, Nevell TG, Tsibouklis J. Polymericmaterials for ophthalmic drug delivery: trends and perspectives. Journal of Materials Chemistry. 2006;16(36):3439-43.
- 9. Lin HR, Sung KC. Carbopol/pluronic phasechange solutions for ophthalmic drug delivery. Journal of Controlled Release. 2000;69(3):379-88.
- 10. Maulvi FA, Soni TG, Shah DO. A review on therapeutic contact lenses for ocular drug delivery. Drug Deliv. 2016;23(8):3017-26.
- 11. Xinming L, Yingde C, Lloyd AW, Mikhalovsky SV, Sandeman SR, Howel CA, Liewen L. Polymeric hydrogels for novel contact lens-based ophthalmic drug delivery systems: a review. Cont Lens Anterior Eye. 2008;31(2):57-64.
- 12. Guzman-Aranguez A, Colligris B, Pintor J. Contact Lenses: Promising Devices for Ocular Drug Delivery. Journal of Ocular Pharmacology and Therapeutics. 2013;29(2):189-99.
- 13. Gulsen D, Chauhan A. Dispersion of microemulsion drops in HEMA hydrogel: a potential ophthalmic drug delivery vehicle. Int J Pharm. 2005;292(1-2):95-117.
- 14. Tieppo A, Pate KM, Byrne ME. In vitro controlled release of an anti-inflammatory from daily disposable therapeutic contact lenses under physiological ocular tear flow. European Journal of Pharmaceutics and Biopharmaceutics. 2012;81(1):170-7.
- 15. Karlgard CCS, Wong NS, Jones LW, Moresoli C. In vitro uptake and release studies of ocular pharmaceutical agents by silicon-containing and p-HEMA hydrogel contact lens materials. International Journal of Pharmaceutics. 2003;257(1):141-51.
- 16. Lee D, Cho S, Park HS, Kwon I. Ocular Drug Delivery through pHEMA-Hydrogel Contact Lenses Co-Loaded with Lipophilic Vitamins. Sci Rep. 2016;6:34194.
- 17. McDermott ML, Chandler JW. Therapeutic uses of contact lenses. Survey of Ophthalmology. 1989;33(5):381-94.
- 18. Henry VA, DeKinder JO. Soft lens material selection. In: Bennett ES, Henry VA, ed. Clinical Manual of Contact Lenses. Lippincott: Williams & Wilkins; 2014.
- 19. Lloyd AW, Faragher RGA, Denyer SP. Ocular biomaterials and implants. Biomaterials. 2001;22(8):769-85.

- 20. Lee SE, Kim SR, Park M. Oxygen permeability of soft contact lenses in different pH, osmolality and buffering solution. Int J Ophthalmol. 2015;8(5):1037-42.
- 21. Alava J, Garagorri N, Briz N, Mendicute J. Effects of bacterial adhesion with respect to the type of material, structure and design of intraocular lenses. Journal of Materials Science: Materials in Medicine. 2005;16(4):313-7.
- 22. Tighe BJ. A decade of silicone hydrogel development: surface properties, mechanical properties, and ocular compatibility. Eye Contact Lens. 2013;39(1):4-12.
- 23. Horst CR, Brodland B, Jones LW, Brodland GW. Measuring the modulus of silicone hydrogel contact lenses. Optom Vis Sci. 2012;89(10):1468-76.
- 24. Ho CH, Hlady V. Fluorescence assay for measuring lipid deposits on contact lens surfaces. Biomaterials. 1995;16(6):479-82.
- 25. Fornasiero F, Prausnitz JM, Radke CJ. Post-lens tear-film depletion due to evaporative dehydration of a soft contact lens. Journal of Membrane Science. 2006;275(1):229-43.
- 26. Minoura N, Tsukada M, Nagura M. Fine structure and oxygen permeability of silk fibroin membrane treated with methanol. Polymer. 1990;31(2):265-9.
- 27. Minoura N, Tsukada M, Nagura M. Physico-chemical properties of silk fibroin membrane as a biomaterial. Biomaterials. 1990;11(6):430-4.
- 28. Sashina ES, Golubikhin AY, Novoselov NP, Tsobkallo ES, Zaborskii M, Goralskii Y. Study of a possibility of applying the films of the silk fibroin and its mixtures with synthetic polymers for creating the materials of contact lenses. Russian Journal of Applied Chemistry. 2009;82(5):898-904.
- 29. Liu TL, Miao JC, Sheng WH, Xie YF, Huang Q, Shan YB, Yang JC. Cytocompatibility of regenerated silk fibroin film: a medical biomaterial applicable to wound healing. J Zhejiang Univ Sci B. 2010;11(1):10-6.
- 30. Ju HW, Lee OJ, Lee JM, Moon BM, Park HJ, Park YR, Lee MC, Kim SH, Chao JR, Ki CS and others. Wound healing effect of electrospun silk fibroin nanomatrix in burn-model. International Journal of Biological Macromolecules. 2016;85:29-39.
- 31. Li M, Lu S, Wu Z, Tan K, Minoura N, Kuga S. Structure and properties of silk fibroin–poly(vinyl alcohol) gel. International Journal of Biological Macromolecules. 2002;30(2):89-94.

- 32. Caner C, Vergano PJ, Wiles JL. Chitosan film mechanical and permeation properties as affected by acid, plasticizer, and storage. Journal of Food Science. 1998;63(6):1049-53.
- 33. Luangbudnark W, Viyoch J, Laupattarakasem W, Surakunprapha P, Laupattarakasem P. Properties and biocompatibility of chitosan and silk fibroin blend films for application in skin tissue engineering. ScientificWorldJournal. 2012;2012:697201.
- 34. Kweon H, Ha HC, Um IC, Park YH. Physical properties of silk fibroin/chitosan blend films. Journal of Applied Polymer Science. 2001;80(7):928-34.
- 35. Shi X-Y, Tan T-W. New Contact Lens Based on Chitosan/Gelatin Composites. Journal of Bioactive and Compatible Polymers. 2004;19(6):467-79.
- 36. Moraes MAd, Nogueira GM, Weska RF, Beppu MM. Preparation and Characterization of Insoluble Silk Fibroin/Chitosan Blend Films. Polymers. 2010;2(4):719.
- 37. Dalia MNA, Ahmed Abd E-b, Samia HS, Mohamed AEN. Chitosan mucoadhesive buccal films: Effect of different casting solvents on their physicochemical properties. International Journal of Pharmacy and Pharmaceutical Sciences. 2016;8(9):206-13.
- 38. Preethi GB, Prashanth K. Design and evaluation of controlled-release ocular inserts of brimonidine tartrate and timolol maleate. International Journal of Pharmacy and Pharmaceutical Sciences. 2016;9(1):79-82.
- 39. Aya MD, Hamdy MD, Amal SMAE-e, Maha KAK. Fabrication of bioadhesive ocusert with different polymers: Once a day dose. International Journal of Applied Pharmaceutics. 2018;10(6):309-17.
- 40. Sashina ES, Janowska G, Zaborski M, Vnuchkin AV. Compatibility of fibroin/chitosan and fibroin/cellulose blends studied by thermal analysis. Journal of Thermal Analysis and Calorimetry. 2007;89(3):887-91.
- 41. Bini E, Knight DP, Kaplan DL. Mapping Domain Structures in Silks from Insects and Spiders Related to Protein Assembly. Journal of Molecular Biology. 2004;335(1):27-40.

- 42. Mukhamedzhanova MY, Takhtaganova DB, Pak TS. Properties of Concentrated Solutions of Fibroin and Its Derivatives. Chemistry of Natural Compounds. 2001;37(4):377-80.
- 43. Verheul RJ, Amidi M, van Steenbergen MJ, van Riet E, Jiskoot W, Hennink WE. Influence of the degree of acetylation on the enzymatic degradation and in vitro biological properties of trimethylated chitosans. Biomaterials. 2009;30(18):3129-35.
- 44. Yamada H, Nakao H, Takasu Y, Tsubouchi K. Preparation of undegraded native molecular fibroin solution from silkworm cocoons. Materials Science and Engineering: C. 2001;14(1):41-6.
- 45. Akiyoshi A. Dissolution of silk fibroin with calcium chloride/ethanol aqueous solution. Journal of Sericology Science Japan. 1998;67(2):91-4.
- 46. Kim KM, Son JH, Kim SK, Weller C, Hanna M. Properties of chitosan films as a function of pH and solvent type. Journal of Food Science E: Food Engineering and Physical Properties. 2006;71(3):119-24.
- 47. Peng CC, Kim J, Chauhan A. Extended delivery of hydrophilic drugs from silicone-hydrogel contact lenses containing vitamin E diffusion barriers.

 Biomaterials. 2010;31(14):4032-47.
- 48. Tranoudis I, Efron N. Tensile properties of soft contact lens materials. Contact Lens and Anterior Eye. 2004;27(4):177-91.
- 49. Jung HJ, Abou-Jaoude M, Carbia BE, Plummer C, Chauhan A. Glaucoma therapy by extended release of timolol from nanoparticle loaded silicone-hydrogel contact lenses. Journal of Controlled Release. 2013;165(1):82-9.
- 50. Gavara R, Compan V. Oxygen, water, and sodium chloride transport in soft contact lenses materials. J Biomed Mater Res B Appl Biomater. 2017;105(8): 2218-31.
- 51. Chaiyasan W, Srinivas SP, Tiyaboonchai W. Mucoadhesive Chitosan–Dextran Sulfate Nanoparticles for Sustained Drug Delivery to the Ocular Surface. Journal of Ocular Pharmacology and Therapeutics. 2013;29(2):200-7.
- 52. Nwe N, Furuike T, Tamura H. The Mechanical and Biological Properties of Chitosan Scaffolds for Tissue Regeneration Templates Are Significantly Enhanced by Chitosan from Gongronella butleri. Materials. 2009;2(2):374-98.

- 53. She Z, Zhang B, Jin C, Feng Q, Xu Y. Preparation and in vitro degradation of porous three-dimensional silk fibroin/chitosan scaffold. Polymer Degradation and Stability. 2008;93(7):1316-22.
- 54. Gorbet MB, Tanti NC, Jones L, Sheardown H. Corneal epithelial cell biocompatibility to silicone hydrogel and conventional hydrogel contact lens packaging solutions. Mol Vis. 2010;16:272-82.
- 55. Takara EA, Marchese J, Ochoa NA. NaOH treatment of chitosan films: Impact on macromolecular structure and film properties. Carbohydrate Polymers. 2015;132:25-30.
- 56. Lai C-F, Li J-S, Fang Y-T, Chien C-J, Lee C-H. UV and blue-light antireflective structurally colored contact lenses based on a copolymer hydrogel with amorphous array nanostructures. RSC Advances. 2018;8(8):4006-13.
- 57. Gonzalez-Meijome JM, Compañ-Moreno V, Riande E. Determination of Oxygen Permeability in Soft Contact Lenses Using a Polarographic Method: Estimation of Relevant Physiological Parameters. Industrial & Engineering Chemistry Research. 2008;47(10):3619-29.
- Selby A, Maldonado-Codina C, Derby B. Influence of specimen thickness on the nanoindentation of hydrogels: measuring the mechanical properties of soft contact lenses. J Mech Behav Biomed Mater. 2014;35:144-56.
- 59. Khodaverdi E, Tekie FSM, Amoli SS, Sadeghi F. Comparison of Plasticizer Effect on Thermo-responsive Properties of Eudragit RS Films. AAPS PharmSciTech. 2012;13(3):1024-30.
- 60. Domschke A, Lohmann D, Winterton L. On-eye mobility of soft oxygen permeable contact lenses. Proceedings of the ACS Spring National Meeting, San Francisco: PMSE; 1997.
- 61. Nicolson PC, Vogt J. Soft contact lens polymers: an evolution. Biomaterials. 2001;22(24):3273-83.
- 62. Marelli B, Brenckle MA, Kaplan DL, Omenetto FG. Silk Fibroin as Edible Coating for Perishable Food Preservation. Scientific Reports. 2016;6:25263.

CHAPTER IV

OPHTHALMIC DRUG DELIVERY SYSTEM BASED ON BIOGENIC MATERIALS

This chapter is the manuscript currently being modified for submission to the Journal of Macromolecule Bioscience. It investigated the applicability of the biogenic materials with various formation approaches, CS/RSF films, RSS-coated CS/RSF films and multilayer films-based CS and RSF, as a contact lenses-based ophthalmic drug delivery system. The substances with various charged, non-charged acetaminophen (APAP), negatively charged 5(6)-carboxyfluorescein (CF) and zwitterion charged rhodamine B (RB) were used as a hydrophilic substance model.

Abstract

Chitosan/regenerated silk fibroin (CS/RSF) films were evaluated as a contact lenses-based ophthalmic drug delivery system. CS/RSF films were prepared by using a film casting technique and dip-coated with recombinant spider silk (RSS). Moreover, CS/RSF films were prepared using layer by layer (L-b-L) technique. Non-charged acetaminophen (APAP), negatively charged 5(6)-carboxyfluorescein (CF) and zwitterion rhodamine B (RB) were loaded as model drugs and their release was studies in vitro. Non-charged APAP cannot load in the CS/RSF films. Interestingly, negatively charged CF and zwitterion RB could be successfully loaded in the CS/RSF films. Essentially, the RSS coatings on the CS/RSF films significantly increased the loading efficiency of negatively charged CF as well as zwitterion RB. These films also showed prolonged release of CF and RB up to 12 h indicating their promising potential use as a biomaterial for daily disposable contact lenses-based ophthalmic drug delivery system. Furthermore, the multilayer films -based CS and RSF enhanced loading efficiency of zwitterion RB and also prolonged RB more than 12 h. Furthermore, L-b-L films made of CS and RSF also showed enhanced drug loading efficiency as well as prolonged release of RB for more than 12 h. However, these films revealed low oxygen permeability, thus being not appropriate for use as a therapeutic contact lenses.

Keywords: Chitosan, Regenerated silk fibroin, Recombinant spider silk, Films, Contact lenses, Ophthalmic drug delivery

Introduction

More than 90% commercially available of currently topical eye drops are solutions or suspensions because of their convenience and non-invasive administration (1-3). However, the main drawback of eye drops is the short residence time, only ~2 min in the tear film, leading to low ocular bioavailability with less than 5% of administered reaching the intraocular tissues (2, 4-6). Most of the drug is lost due to blinking, rapid tear turnover rate and drainage into the nasal cavity reaching the systemic circulation. Therefore, frequent administration of eye drops is required, which reduces patient compliance, increases local and systemic side effects (2, 7-9).

Recently, daily disposable contact lenses have been proposed as alternative ophthalmic drug delivery system (10-14). This approach offers several advantages including administration without any surgery, increased drug residence time on the ocular surface and reduced application frequency (12, 15-17). Prior studies focused on soaking commercial contact lenses in hydrophilic ocular drug solutions, such as diclofenae sodium, cysteamine, brimonidine, fluconazole, and moxifloxacin hydrochloride, followed by insertion into the eye (18-21). Contact lenses are placed directly on the cornea with a thin 5-10 micron thick post-lens tear film (POLTF) layer in between, which makes contacts a natural choice for delivering drugs to the cornea. The released drug by the contact towards the cornea surface is trapped in the POLTF for extended duration into the cornea leading to improved drug bioavailability, ~50% (22). However, these lenses have some limitations including low drug loading and a fast release characteristic within 1-3 h. This suggested that commercial contacts lenses are not ideal for drug delivery due to the short release durations which may necessitate wearing multiple lenses each day, reducing the viability of this approach. Therefore, developing a new daily disposable contact lenses to effectively deliver the hydrophilic drug in a prolonged drug release pattern is still a challenging task.

In a previous study, we successfully developed chitosan/regenerated silk fibroin (CS/RSF) blended films for the potential use in contact lens applications (23). The CS/RSF films showed high optical transparency, high wettability, high thermal stability,

high ion and oxygen permeability, good chemical and mechanical stabilities and noncytotoxicity, thus, meeting well the requirement of daily disposable contact lenses (23). Thus, in this study, we further explored the potential of CS/RSF to be used as contact lenses for ophthalmic delivery of hydrophilic drugs. Typically, the topical ophthalmic drugs for the treatment of eye disease are several of drugs charged (24-27). Consequently, the substances with various charged, non-charged acetaminophen (APAP), negatively charged 5(6)-carboxyfluorescein (CF) and zwitterion charged rhodamine B (RB) were used as a hydrophilic substance model. To broader the applicability of the drug delivery system, negatively and positively charged recombinant spider silk (RSS) proteins were used to coat the CS/RSF films. The used RSS variants are based on the consensus sequence of the repetitive part of the dragline silk protein ADF4 of the European garden spider (Araneus diadematus) and possess a well-dominated excellent biocompatibility, non-toxicity, and non-immune reactivity (28-35). The negatively and positively charged RSS effectively accommodated oppositely charged drugs. The variant eADF4(C16) is polyanionic consisting of 16 repeats of module C (sequence: GSSAAAAAAAAAGGPGGY GPENQGPSGPGGYGPGGP). In contrast, eADF4(κ16) is polycationic consisting of module k (sequence: GSSAAAAAAAASGPGGYGPKNQGPSGPGGYGPGGP) in which all glutamic acid residues are replaced by lysine ones (35-39). In addition, the development of the multilayer films-based CS and RSF was also investigated for contact lenses-based ophthalmic drug delivery system.

The aim of this study was to investigate the applicability of the biogenic biomaterials with various formation approaches, CS/RSF films, RSS-coated CS/RSF films and multilayer films-based CS and RSF, as a contact lenses-based ophthalmic drug delivery system.

Materials and methods

Materials

Shrimp chitosan (CS, > 90% deacetylation, mean molecular weight of 250 kDa) was obtained from Marine Bio Resources Co., Ltd (Samutsakhon, Thailand). Regenerated silk fibroin (RSF) was produced as previously reported (23). Polyethylene glycol 400 (PEG400) was purchased from Merck KGaA, (Darmstadt, Germany). The recombinant spider silk protein eADF4(C16) was obtained from

AMsilk GmbH (Munich, Germany) and eADF4(κ16) was produced as previously reported (40). 5(6)-carboxyfluorescein succinimidyl ester (NHS-fluoresceine) was purchased from Thermo Fischer Scientific GmbH (Darmstadt, Germany). Lysozyme from chicken egg, acetaminophen (APAP) and 5(6)-carboxyfluorescein (CF) were also purchased from Sigma-Aldrich Chemie GmbH (Munich, Germany). Rhodamine B (RB) was purchased from Carl Roth GmbH & Co. KG (Karlsruhe, Germany). All chemicals and solvents were of analytical grade.

Preparation of CS/RSF films

CS/RSF films were prepared by casting. Briefly, 2% (w/v) of CS solution in acetic acid, 2% (w/v) of RSF aqueous solution in deionized water and PEG400 25 % (w/w) of polymer matrix were mixed using magnetic stirrer at 200 rpm for 30 min. The CS/RSF ratios were varied as 100/0 (from only CS), 90/10, 80/20 and 70/30 (w/w). The mixtures were poured onto polystyrene plates and dried in an oven at 60 °C. The dried films were immersed in 1M NaOH solution for 15 min, and then repeatedly rinsed with deionized water until a neutral pH was obtained. The films were then soaked in 0.01M phosphate buffer saline (PBS) solution, pH 7.4 for 24 h and autoclaved at 121 °C and 15 psi for 20 min.

Preparation of RSS coated CS/RSF films

1 mg/ml of RSS solutions were prepared by dissolving the proteins in 6 M guanidinium isothiocynate (GdmSCN) and dialyzed three times against 20 mM Tris/HCl (pH7.5) buffer for 6 h. Then, the samples were centrifuged (30 min, 12,000 g, 4 °C). CS and CS/RSF: 70/30 films (2×2 cm²) were dipped in 5 ml of RSS solution at 1mg/ml for 5 s and then dried at room temperature for 2 h. The dried RSS-coated CS/RSF films were post-treated by water steaming at 60 °C for 30 min.

The homogeneity of RSS coatings on CS/RSF films was investigated by labelled RSS with NHS-fluorescein. Briefly, RSS-NHS-Fluorescein were prepared by adding 2.5x molar excess of NHS-fluorescein dissolved in DMSO (30 min, rotation, dark) into negatively charged eADF4(C16) or positively charge eADF4(κ16) solution and incubated for 1 h in darkness. Precipitation of RSS-NHS-fluorescein was initiated by 1 M of K₂HPO₄/KH₂PO₄ (pH7.4) and incubated for overnight. After centrifugation (30 min, 12,000 g, 4 °C), the pellet was washed twice with DMSO: H₂O (1:1) and twice with deionize water. The pellet was immersed in liquid nitrogen, lyophilized and

stored at -20 °C until further use. Then the RSS-NHS-fluorescein coated CS/RSF films were prepared as described above. Their coating appearances were determined by fluorescence microscope (Leica DMI 3000B, Wetzlar, Germany).

Preparation of L-b-L films

L-b-L films were prepared using layer-by-layer casting. Each of the solution type, neat CS and RSF as well as CS/RSF: 70/30 blended solution, were mixed with 25% w/w of PEG400. The solutions of CS, RSF and CS/RSF have been used in different combinations to process different layers as shown in Figure 2. Each of the solutions were then poured onto the polystyrene plates and dried in an oven at 60 °C until completely dried. The dried RSF layer was post-treated by water steaming at 60 °C for 30 min, whereas the dried CS layer was immersed in 1M NaOH solution for 15 min and then repeatedly rinsed with deionize water until the neutral pH was obtained. In case of the dried CS/RSF: 70/30 layer, both post-treatment methods were use sequentially starting with the water steaming. Finally, the L-b-L films were soaked in 0.01M phosphate buffer saline (PBS) solution, pH 7.4 for 24 h and autoclaved at 121 °C and 15 psi for 20 min.

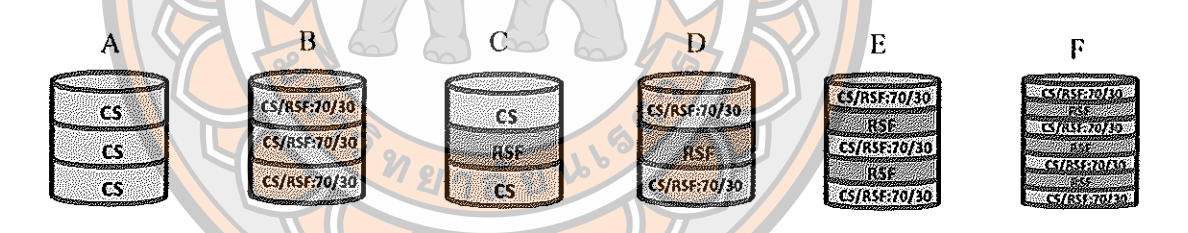


Figure 4.1 Formulation of L-b-L films-based CS and RSF

Physicochemical characterization

The film thickness was measured with a thickness gauge (Holex Digital Micrometer, Munich, Germany). The measurement was taken at the center and at four positions around the perimeter of the hydrated films, and then the average thickness was calculated as described previously (41).

The surface morphologies and cross-sections of films were determined using a scanning electron microscope (SEM, Carl Zeiss AURIGA®, Thuringia, Germany). The samples were sputter-coated with platinum by plasma in order to minimize electron charging on the surface and to obtain high resolution images.

The light transparency of films was determined using a UV-VIS spectrophotometer (Genesys 10S, Thermo scientific, Wisconsin, USA). The hydrated films with an average thickness of 100 ± 10 µm were mounted on the outer surface of a quartz cuvette. The cuvette was placed in the spectrophotometer, and the light transparency of films was measured at 280-780 nm (19).

The Young's modulus and elongation at break of films with a width of 3 mm and a thickness of 0.1 mm were determined according to ASTM D882-12 using a universal testing machine (Zwick/Roell Z2.5, Ulm, Germany) with a load cell of 2 kg, a crosshead speed of 20 mm/min, and a gauge length of 10 mm (42).

The water content of the films was determined using the weight of initially hydrated RSS-coated CS/RSF films (W_{wet}). Then, the films were allowed to dry at 105°C until the film's weight was constant (W_{dried}) (43). The water content of RSS-coated CS/RSF films was calculated according to equation (4.1)

Water content (%) =
$$((W_{wet} - W_{dried})/W_{wet}) \times 100$$
 (4.1)

Surface contact angle were measured to assess the wettability of films. Contact angle of deionize water on each hydrated films blotted with soft blotting paper were measured at room temperature for 60 s using a contact angle goniometer (Surftens Universal, OEG GmbH, Frankfurt, Germany) applying the sessile drop method (44).

Differential scanning calorimetry (DSC) was performed to determine the thermal properties of the films using a DSC 3⁺ STAR System (Mettler-Toledo GmbH, Giessen Germany). Samples were heated from -20°C to 400°C at a heating rate of 20°C/min under a nitrogen atmosphere with a flow rate of 50 ml/min (45). The thermal decomposition temperature of each sample was examined under a nitrogen atmosphere with a flow rate of 50 ml/min, in a temperature range of -20 - 400°C and at a heating rate of 20°C/min (45).

The oxygen permeability of multilayer films-based CS and RSF were measured according to ASTM D3985 (35°C and 50% relative humidity) using the Illinois model 8000 (Illinois, U.S.A).

In vitro enzymatic degradation study

The enzymatic degradation of the films were analyzed following their incubation at 34 ± 1 °C in stimulated tear fluid containing lysozyme (STF) 4.6 mg/ml (pH 7.4), sodium chloride 0.67 g, sodium bicarbonate 0.2 g, calcium chloride $2H_2O$ 0.008 g, and deionized water added to 100 g. The autoclaved films (2×2 cm²) were weighed (initial weight, W_0) before immersing in 2 ml of STF for 24 h. After that, films were dried at 60 °C overnight and weighed (W_1). Then, the lysozyme degradation was illustrated by the percentage of the remaining weight as shown in the following equation (4.2) (46-49).

Remaining weight (%) =
$$(W_1/W_0) \times 100$$
 (4.2)

Drug loading procedure

Non-charged APAP, negatively charged CF and zwitterion RB were used as model drugs. The model drug solutions (125 μg/ml) were prepared in 0.01M PBS. Then the CS/RSF blended films (10×10×0.1 mm) were soaked in at room temperature for a predetermined time. The loading parameters were varied as follows: the loading time was varied from 2 to 24 h; the pH of substance solution was varied from 6.5 to 8.5. The best condition was applied to load teADF4(κ16)-coated CS/RSF films (10×10×0.1 mm) in 1 ml of negatively charged CF solution andeADF4(C16)-coated CS/RSF films (10×10×0.1 mm) were soaked in 1 ml of zwitterion RB solution, respectively. In addition, the L-b-L films-based CS and RSF (10×10×0.1 mm) were also soaked in 1 ml of the model drug solutions at the best loading condition. After the film soaking, the amount of free substance remaining in the supernatant was determined using UV-VIS spectrophotometer at 241, 493 and 553 nm for APAP, CF and RB, respectively. All the experiments were carried out in triplicates.

In vitro drug release

In vitro substance release was carried out at 34 ± 1 °C. The substance-loaded films (10 mm × 10 mm × 0.1 mm) were placed a micropipette tip, with a fluid cavity of 30 μ l. Then, the micropipette tip was inserted into a microtube and subjected to stimulated tear fluid, pH 7.4, at a flow rate of 10 μ l/min. At predetermined time intervals, the microtube was taken and replaced with a new microtube. The amount of

released substance in the microtube was then determined using UV-VIS spectrophotometry at 241, 493 and 553 nm for APAP, CF and RB, respectively (50). All the experiments were carried out in triplicates.

Statistical analysis

The results were expressed as mean \pm standard deviation (SD). For all comparisons, statistical significant differences were analyzed with paired t-test or one-way ANOVA followed by Tukey's post-hoc test, and P < 0.05 was considered statistically significant.

Results and discussion

CS/RSF films

In our previous study, CS/RSF films at ratio of 100/0 (neat CS), 90/10, 80/20 and 70/30 (v/v) have met the necessary material standards for daily disposable contact lenses (23). The prepared films possessed smooth surfaces with a high visible light transparency (> 90%), high water content (59-65% by weight) and high oxygen permeability (22-26 bar). They were also easy to handle with a Young's modulus and elongation at break in the range of 3.8-6 MPa and 113-135%, respectively. In addition, the CS/RSF films could be autoclaved as they possessed a high glass transition temperature (> 158°C) and thermal decomposition temperature of > 260°C. In this study, we further explored the possibility of using those CS/RSF films for ophthalmic drug delivery.

Drug loading and in vitro release of CS/RSF films

One of the most conventional ways of loading a therapeutic drug into the contact lenses is the soaking method due to its cost-effectiveness and simplicity (51, 52). To this end, the preformed contact lenses are immersed in the drug solution and the drug molecules can be adsorbed into the lenses surfaces and/or inner core. The drug loading capacity depends on the drug loading time and pH of drug solution (11).

In this study, negatively charged CF and zwitterion RB were use as model drugs. In preliminary experiments, the non-charged APAP could not load in the CS/RSF films at different conditions tested. Probably lack of interactions between non-charged APAP with either of positively charged CS or negatively charged RSF

hindered the loading. Thus, the effects of drug loading parameters such as loading time and pH of loading solutions, were further studied with charged CF and RB.

To study the effects of drug loading time, the films were soaked into solutions of the model drugs (125 µg/ml) at pH 6.5, for 2 to 24 h. The amount of CF and RB loading reached equilibrium at 3 h for all blended films (Table 4.1). The short substance loading time of 3 h benefits manufacturing process in comparison to conventional contact lenses which require drug loading time of 12-24 h (21, 53).

To investigate the effect of pH, the drug solutions at pH 6.5, 7.4 and 8.5 were applied for 3 h. (Table 4.2). The increasing pH of the CS loading solutions resulted in decreased loading capacity of the CS/RSF blended films, presumably because successive deprotonation of the positively charged ammonium group in the CS matrix diminishing charge-charge interactions with negative CF, the importance of the interaction between CF drug and CS matrix is supported also by the observation, that the CF loading was increasing with the increasing CS content revealing the neat CS films with the highest loading capacity. Further, this result correlated well with SEM micrographs (Figure 4.2), where CF was administrated only on the outer surface in case of CS/RSF: 70/30 films, whereas increasing contend of the positive matrix up to neat CS films resulted in increasing amounts of CF found in the inner core.

Zwitterion RB could be loaded in CS/RSF films at ratios 70/30, 80/20 and 90/10. However, neat CS films (Table 4.1 and 4.2) revealed no loading at any time and pH value tested. The presence of negatively charged RSF in the blends was crucial for incorporation of RB (54). Moreover, lower pH values favored the protonation of the carboxylic group thus populating the positively charged form of the RB resulting into better interaction with the negatively charged RSF and higher loading efficiency in comparison to conditions at higher pH, which populate RB zwitterion form being in equilibrium with its tautomeric neutral form, resulting potentially into RB aggregation and lower loading efficiency. Interaction of the positively charged form of RB with negatively charged RSF is supported by the observation of RB loading increasing with increasing the film RSF content. This result also correlated well with SEM micrographs (Figure 4.3). RB disappeared on/in neat CS films while it was observed in both, the outer surface and the inner core of CS/RSF blended films, with increasing amount of RB in the inner core of films with the increasing RSF content.

From the drug loading study, the best conditions of substance loading parameters were determined at pH 6.5 and incubation time of 3 h for both model drugs, CF and RB.

In vitro drug release studies have shown CF release rates decreasing with increasing the CS content in the blended films nearly complete release of CF within 7 and 8 h was observed from the blended CS/RSF: 70/30 and CS/RSF: 80/20 films a, respectively, Figure 4.4(A). Contrary, the CS/RSF: 90/10 and neat CS films showed a prolonged CF release for more than 12 h. Vice versa, the films with higher ratio of RSF resulted in a prolongation of the RB release with the lowest rate observed for CS/RSF: 70/30 films, Figure 4.4(B). The CF and RB release profiles of all tested CS/RSF blends revealed the best fit to Higuchi's model with regression coefficient = 0.95-0.99. This implies that a diffusion-controlled mechanism of the substances release (55).

To explain this phenomenon, the substance locations and the ionic interaction effected the drug release profile significantly. Obviously, the drug located on the film surface fastly release into media, on the other hand, drug in the inner core requires longer time for dissolving and diffusion to outer surface, consequently attributed to the prolonged release phase. These results correlated well with the film SEM micrographs (Figure 4.2 and 4.3). Ionic interaction between the CS matrix and the negatively charged CF resulted in an increase drug amount in the film inner core (Figure 4.2), hence, longer time for the substance diffusion to outer surface were required. In case of RB release, the higher RSF ratio resulted in an increased RB amount in the film inner core (Figure 4.3), hence, resulting in longer time for RB diffusion to outer surface.

Table 4.1 Effect of drug loading time on loading capacity of CS/RSF films

Formulations	Substance loading (µg)/10 mm ³ of film					
	2h	3h	4h	24h		
5(6)-carboxyfluorescein (CF)						
CS	41.31 ± 1.73	60.74 ± 3.23	60.73 ± 3.18	60.95 ± 3.86		
CS/RSF: 90/10	31.18 ± 1.45	55.74 ± 3.07	54.27 ± 0.87	54.56 ± 1.29		
CS/RSF: 80/20	23.15 ± 1.58	37.88 ± 0.89	37.13 ± 1.05	37.30 ± 1.06		
CS/RSF: 70/30	20.43 ± 1.78	34.40 ± 1.66	34.68 ± 1.34	34.78 ± 1.93		
Rhodamine B (RB)						
CS	Not detected					
CS/RSF: 90/10	17.20 ± 1.31	24.92 ± 0.81	24.74 ± 1.43	25.04 ± 1.16		
CS/RSF: 80/20	40.76 ± 4.64	52.61 ± 1.00	52.07 ± 1.28	52.65 ± 1.08		
CS/RS <mark>F</mark> : 70/30	46.72 ± 1.31	61.27 ± 1.45	61.15 ± 1.27	60.89 ± 2.57		

Condition: substance solution pH6.5; SD: standard deviation, n = 3

Table 4.2 Effect of pH of drug solution on loading capacity of CS/RSF films

Ratio of	Substance loading (μg)/10 mm³ of film			
CS/RSF (v/v)	pH6.5	pH7.4	pH8,5	
5(6)-carboxyfluores	cein (CF)			
CS	60.74 ± 3.23	41.58 ± 1.15	19.93 ± 0.88	
CS/RSF: 90/10	55.74 ± 3.07	33.58 ± 1.50	16.80 ± 0.86	
CS/RSF: 80/20	37.88 ± 0.89	25.09 ± 2.63	16.57 ± 1.56	
CS/RSF: 70/30	34.40 ± 1.66	19.68 ± 0.70	13.61 ± 1.13	
Rhodamine B (RB)				
CS		Not detected		
CS/RSF: 90/10	24.92 ± 0.81	18.54 ± 1.42	16.31 ± 1.49	
CS/RSF: 80/20	52.61 ± 1.00	47.24 ± 2.52	45.37 ± 1.22	
CS/RSF: 70/30	61.27 ± 1.45	54.81 ± 0.71	50.47 ± 1.08	

Condition: loading time 3 h; SD: standard deviation, n = 3

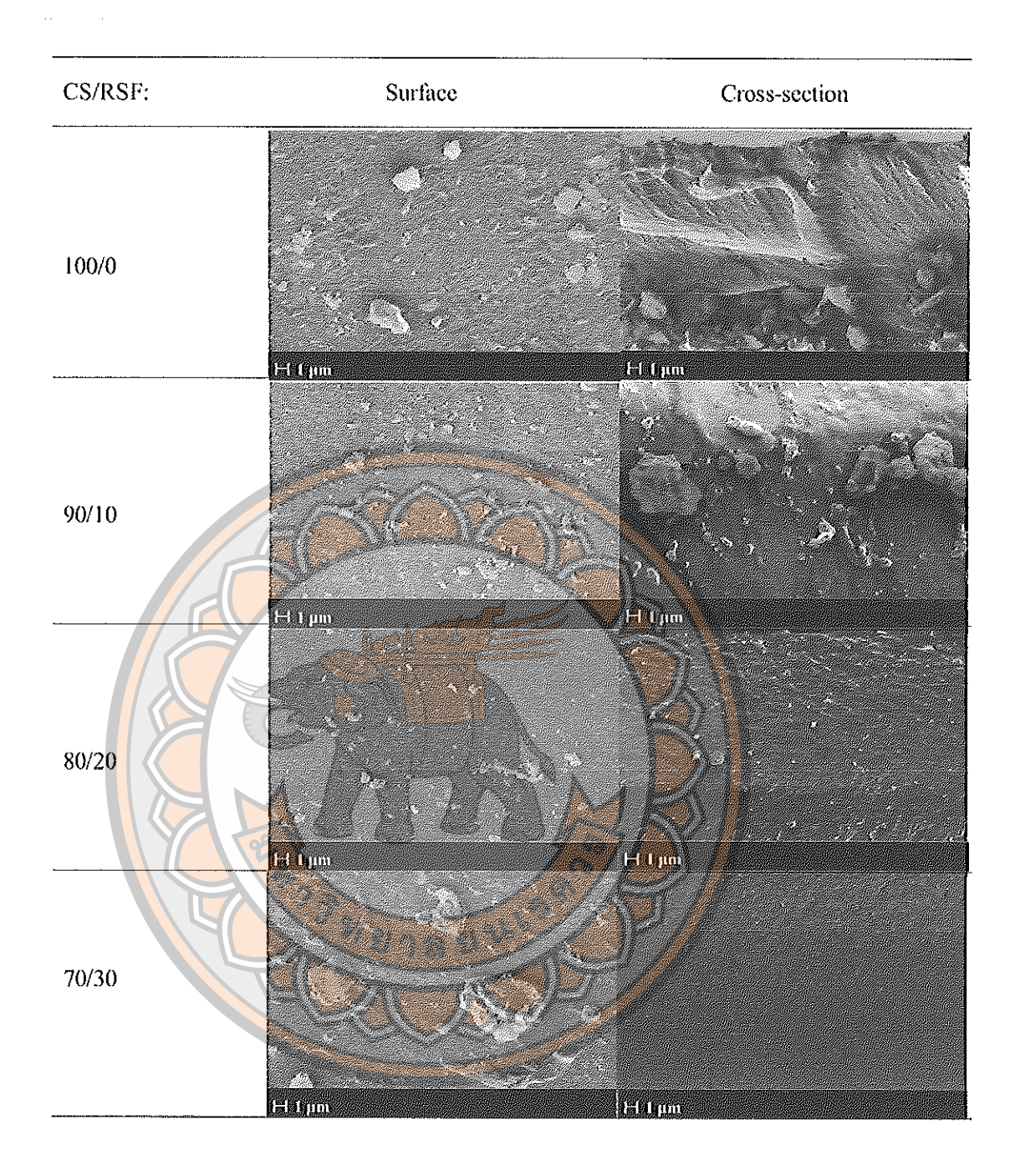


Figure 4.2 SEM micrographs of the surface and cross-section of negatively charged CF loaded CS/RSF films, pH 6.5, for 3 h (×3000 magnification)

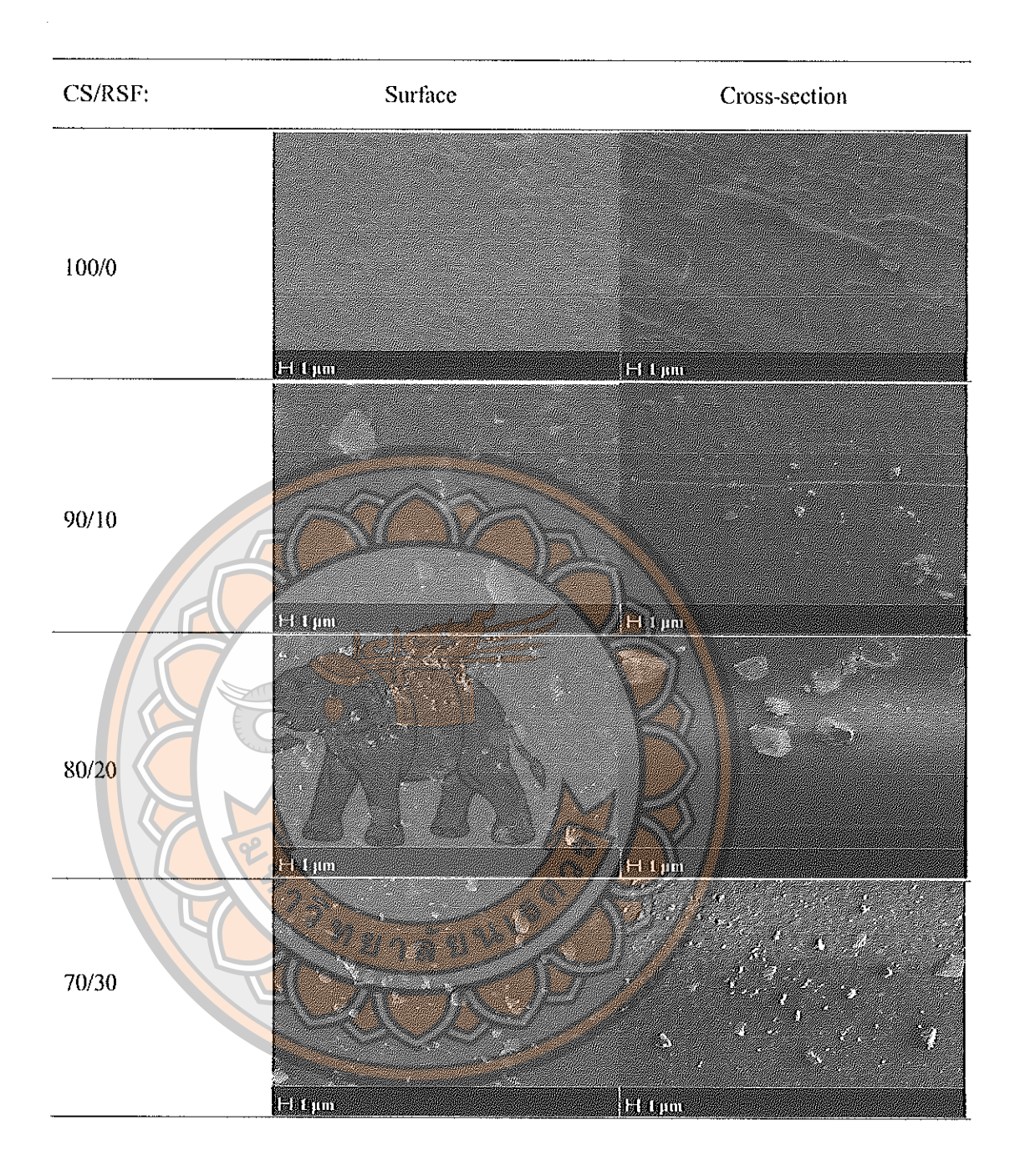


Figure 4.3 SEM micrographs of the surface and cross-section of zwitterion RB loaded CS/RSF films, pH 6.5, for 3 h (×3000 magnification)

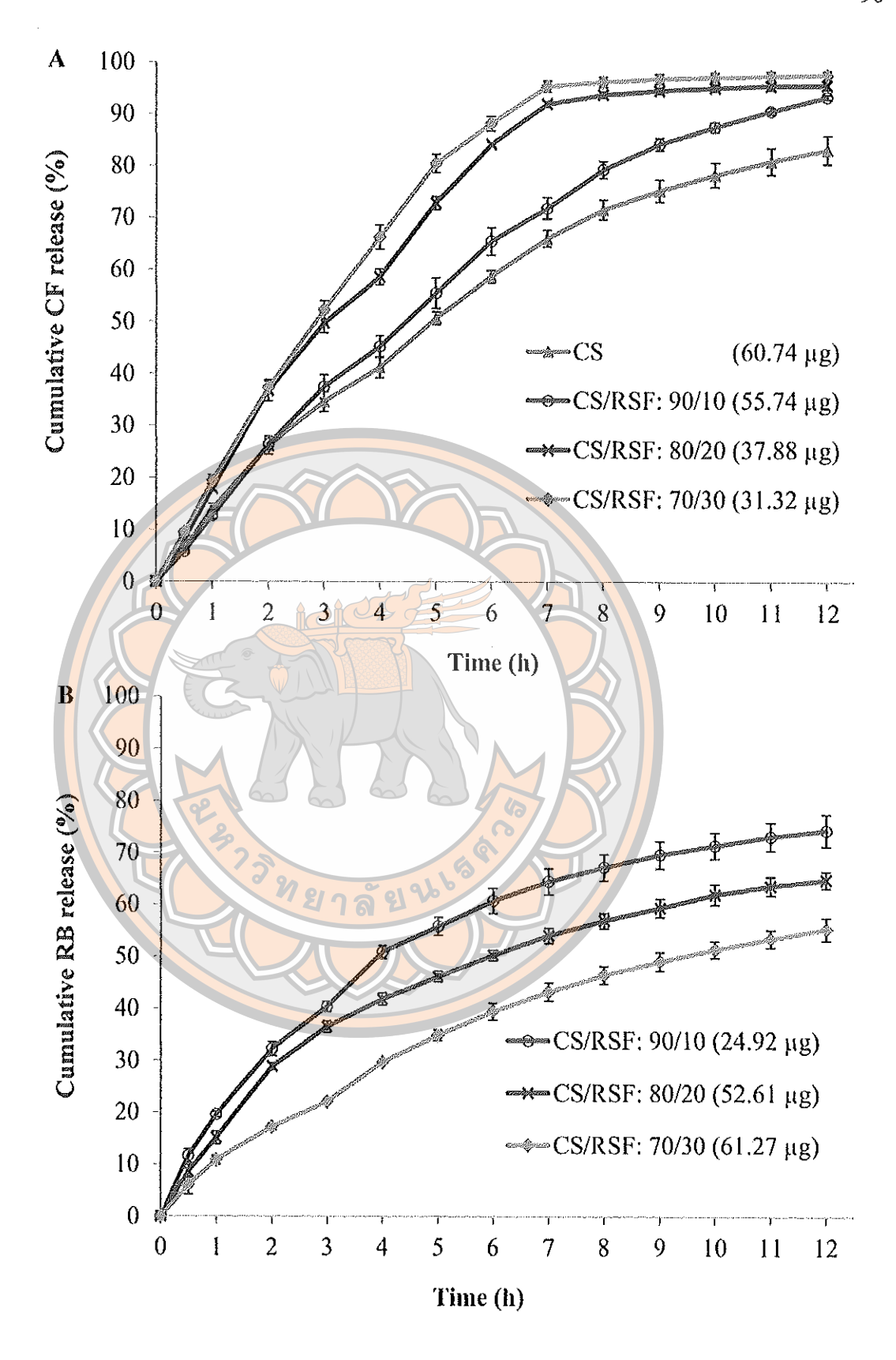


Figure 4.4 Cumulative release of CF (A) and RB (B) from CS/RSF blended films

Effect of drug loading on material properties of CS/RSF films

According to the best prolonged release times the neat CS and CS/RSF: 70/30 films loaded with CF and RB, respectively, were selected to study effects of substance loading on physical properties of the films. The physical properties of the unloaded and loaded films showed no significant difference (Table 4.3). They manifest similar thickness of ~100 μm, which comply with typical commercial contact lenses having thickness of 50-200 μm (56, 57). They possessed Young's modulus of > 1.5 MPa and the elongation at break of > 50% satisfying the stiffness and also the flexibility requirements for contact lens (42, 58-60). According to FDA's classification (61), they showed high water content (> 50% w/w) and good wettability (contact angle < 90%) implying that the lenses made of the films could promote the comfort for wearing. This indicated that the loading of substances model did not deteriorate the intrinsic contact lens physical properties of CS/RSF films. Thus, the drugs model-loaded CS/RSF films have met the requirements for daily disposable contact lenses.

To improve the drug loading efficiency and the drug release profile, RSS-coated CS/RSF films and L-b-L films-based CS and RSF were introduced and compared with the bended CS/RSF films.

Table 4.3 Physical properties of CS/RSF films and drug-loaded CS/RSF films

Formulations	Young's Modulus (Mpa) ± SD	Elongation at break (%) ± SD	Water content (%) ± SD	Contact angle (°) ± SD
CS	7.17 ± 0.89	104 ± 20	61 ± 0.50	70 ± 2.24
CF loaded CS	7.08 ± 0.73	101 ± 20	60 ± 0.64	69 ± 1.48
CS/RSF: 70/30	6.43 ± 1.00	72 ± 14	58 ± 0.84	75 ± 1.74
RB loaded CS/RSF: 70/30	6.52 ± 1.00	72 ± 18	58 ± 1.36	74 ± 1.55

SD: standard deviation, n = 3

RSS-coated CS/RSF films

Material properties of RSS-coated CS/RSF films

RSS covalently labeled with NHS-fluorescein has been applied to assess the impact of coating procedures onto homogeneity RSS layers on CS/RSF films using a fluorescence microscopy (Figure 4.5). Three repetitions of the dip-coating were required to obtain homogenously covered surfaces. All RSS-coated CS/RSF films showed no significant difference in thickness of $100 \pm 10 \mu m$ if compared with uncoated CS/RSF films and the RSS coating of \sim 2 μm as estimated from SEM images. SEM micrographs of RSS-coated CS/RSF films showed smooth surfaces without phase separation. Moreover, their cross-sections exhibited homogenous core of blended CS and RSF as well as a good interaction between RSS layer and CS/RSF film (Figure 4.6B-E). The analysis of the coated film has shown no significand changes of the physicochemical properties in comparison to the uncoated blended films. Light optical transmittance spectra of the coated and uncoated films showed high light transparency of > 90% in the visible range (381-780 nm) and a significant protection against UV-B (280-315 nm) and UV-A (316-380 nm) wavelengths (Figure 4.6A). The Young's modulus of CS and CS/RSF: 70/30 films slightly increased upon the coating from approximately 7 to 9 MPa and 6 to 8 MPa, respectively, due to the higher stiffness of RSS films (62-65). Interestingly, the RSS coating did not influence ductility of the films (Table 4.4), showing the elongation at break of > 50%. The RSS coated films (Table 4.4) showed a high water content (58 to 62% by weight) according to FDA's classification (61), which implies potential wearing comfort. Surface wettability of the films increased upon coating (Table 4.4), which is important for the tear fluids to spread well over the lens surface allowing more stable tear films. Thermal properties of the films, as analyzed by DSC (Figure 4.7), resulted in an identical glass transition (Tg) and decomposition temperature (Td) of both, uncoated and coated films. Importantly, the Tg values of tested films were ~ 160 °C indicating that RSS-coated CS/RSF films are suitable for decontamination in autoclaves at 121°C.

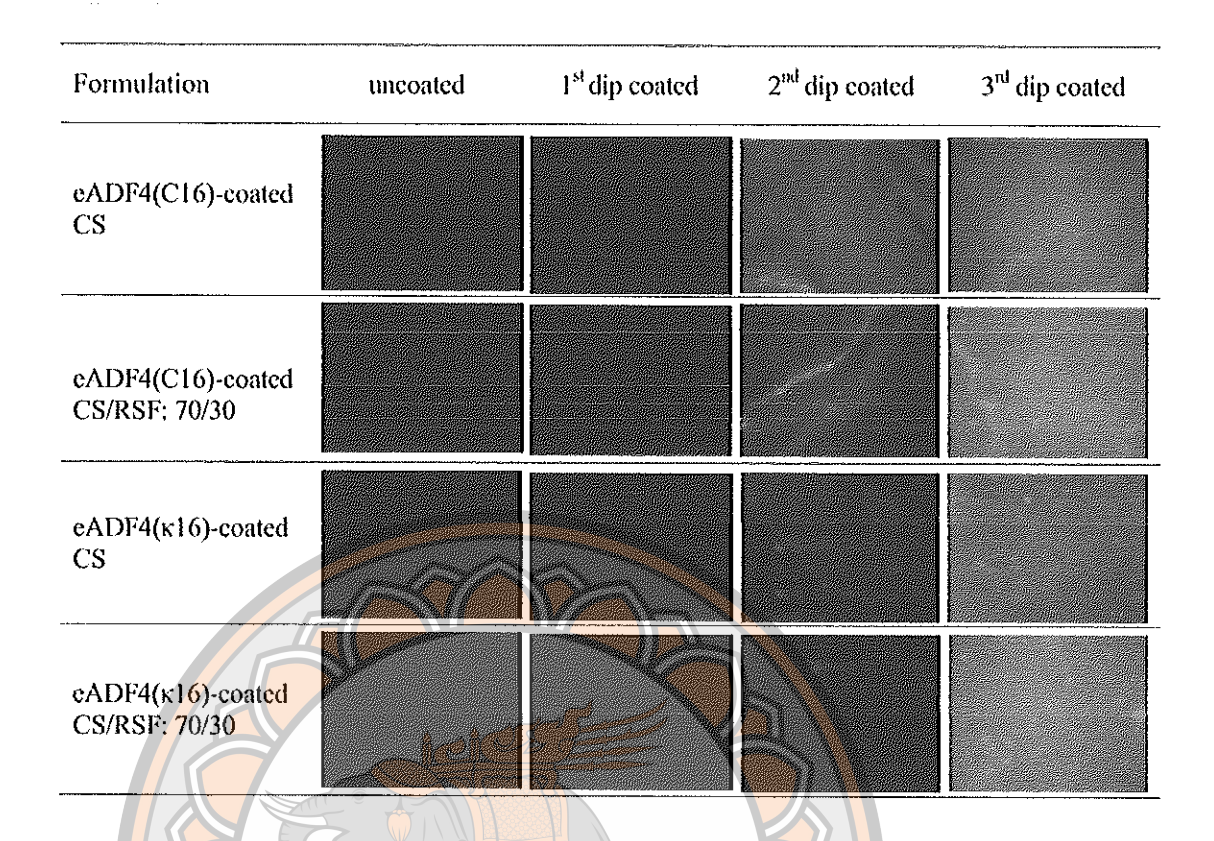


Figure 4.5 Fluorescence micrographs of RSS coated CS/RSF films
(×10 magnification)

Table 4.4 Properties of uncoated and RSS coated CS/RSF films

	Young's	Elongation	Water	Contact
Formulations	Modulus	at break (%)	content (%)	angle (°)
	$(MPa) \pm SD$	± SD	\pm SD	\pm SD
CS	7.17 ± 0.89	104 ± 20	61 ± 0.50	70 ± 2.24
eADF4(C16)-coated CS	8.91 ± 1.49	100 ± 23	62 ± 0.76	69 ± 1.24
eADF4(κ16)-coated CS	8.86 ± 1.69	102 ± 22	61 ± 1.50	69 ± 2.52
CS/RSF: 70/30	6.43 ± 0.99	72 ± 14	58 ± 0.84	75 ± 1.74
eADF4(C16)-coated	7.75 ± 0.67	73 ± 21	59 ± 0.69	69 ± 1.35
CS/RSF: 70/30				
eADF4(κ16)-coated	7.83 ± 0.91	70 ± 18	58 ± 0.82	68 ± 1.57
CS/RSF: 70/30				

SD: standard deviation, n = 3

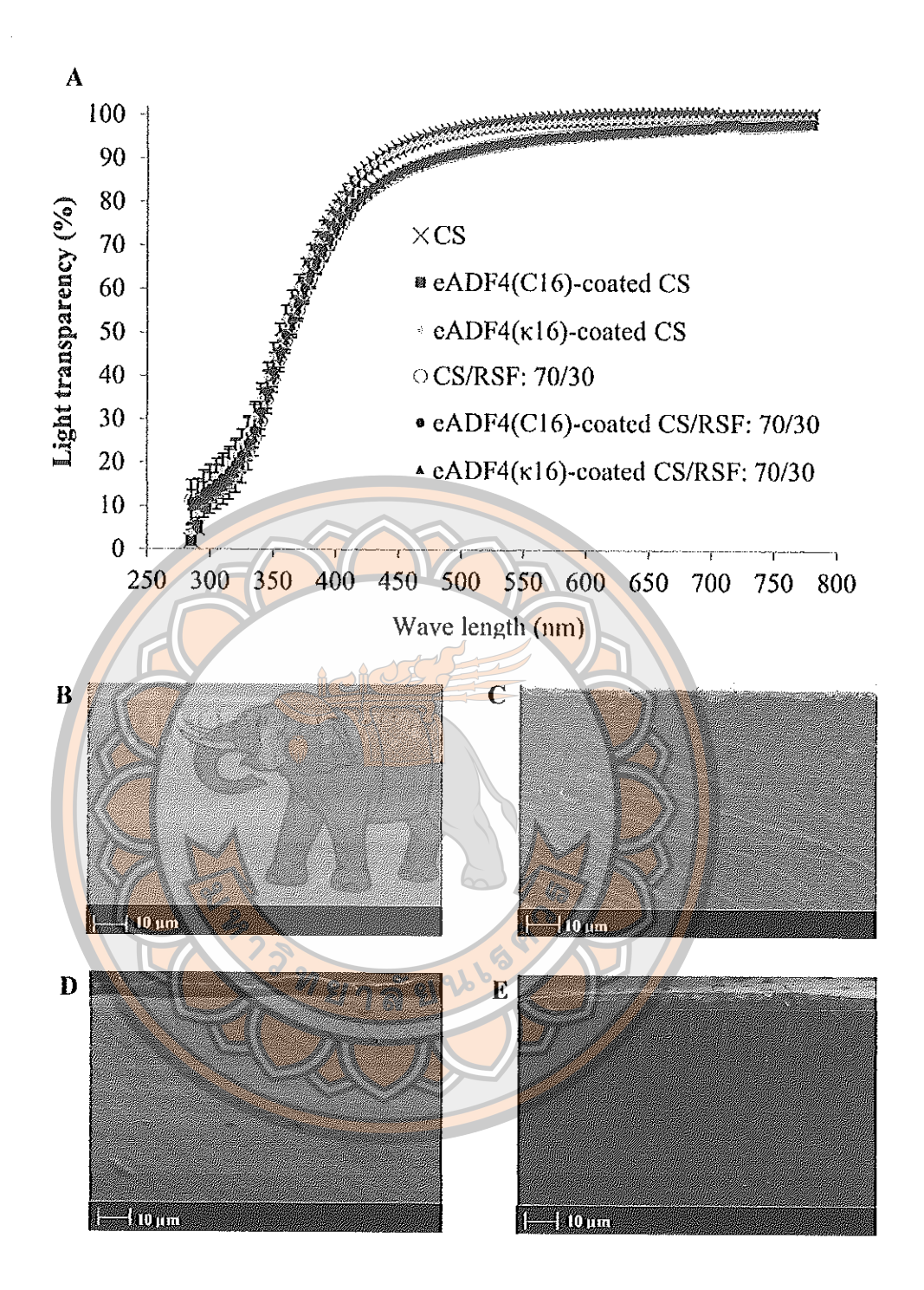


Figure 4.6 (A) Light transparency of uncoated and RSS-coated CS/RSF films, SEM micrographs of cross-section of RSS-coated CS/RSF films:

(B) eADF4(C16)-coated CS, (C) eADF4(C16)-coated CS/RSF: 70/30, (D) eADF4(κ16)-coated-CS, (E) eADF4(κ16)-coated CS/RSF: 70/30 (×3000 magnification)

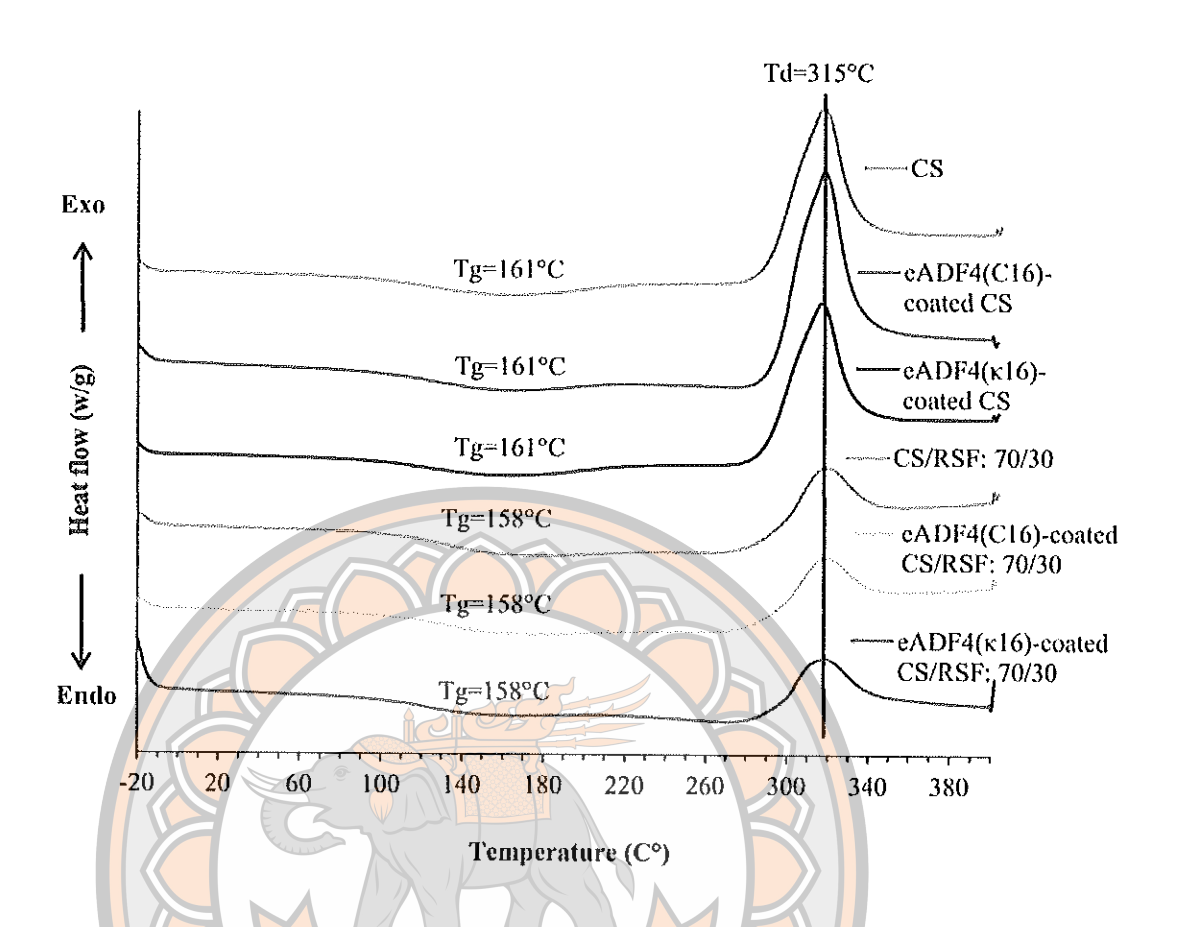


Figure 4.7 DSC curve of uncoated and RSS coated CS/RSF films

Biodegradation of RSS-coated CS/RSF films

Several hundred proteins have been identified in the tear film (68). Among these, lysozyme is an enzymatic protein found at a high concentration (4.6 mg/ml) which could significantly deposit onto soft contact lens materials (68-69). Enzymatic degradation is in this context an important consideration in the design and quality control of soft contact lenses, to avoid residuals causing eye irritation. In general, CS can be degraded by lysozyme (70). Interestingly, uncoated and coated CS/RSF films showed no degradation after incubation in model STF containing lysozyme for 24 h. This could be based on the difficulties of lysozyme to hydrolyze insoluble CS matrices after NaOH treatment (23, 68-69).

Drug loading and in vitro release of RSS-coated CS/RSF films

Positively charged eADF4(C16) and negatively charged eADF4(k16) were used as complementary charged RSS coatings on the CS/RSF films. From the drug

loading study of uncoated CS/RSF films, the best parameters, soaking in drug solutions at pH 6.5 for 3 h, were chosen for evaluation of the drug loading capacity. The eADF4(κ 16) and eADF4(C16) coatings improved significantly CF and RB loading of the CS/RSF films, respectively, (Table 4.5), clearly due to respective ionic interactions of oppositely charged RSS coatings and drugs (35-39).

The improvements were observed in the release profiles of CS and RB model drugs as well. eADF4(k16)-coating decreased release of negatively charged CF from 83% to 60% in case of CS films and from 96% to 82% in case of CS/RSF: 70/30 films after 12 h, when compared to non-coated films (Figure 4.8A). The release rates of the model substances from the coated films were decreased due to additional oppositely charged diffusion barrier in relation to the released drug. The drug release profiles from uncoated and RSS coated CS/RSF films well fitted to Higuchi's model with regression coefficient = 0.97-0.99, which implies that the charged model drugs released from RSS coated and uncoated CS/RSF films by a diffusion-controlled mechanism (55). The utilization of RSS coatings shows potential for establishing a prolonged drug release and development of weekly wear contact lenses for ophthalmic drug delivery.

Table 4.5 Drug loading into uncoated and RSS-coated CS/RSF films

Formulation	Drug loading (μg)/10 mm ³ of film
5(6)-carboxyfluorescein (CF)	
CS	60.74 ± 3.23
eADF4(κ16)-coated CS	75.30 ± 0.95
CS/RSF: 70/30	34.40 ± 1.66
eADF4(κ16)-coated CS/RSF: 70/30	49.42 ± 2.82
Rhodamine B (RB)	
CS	Not detected
eADF4(C16)-coated CS	4.32 ± 1.23
CS/RSF: 70/30	61.27 ± 1.45
eADF4(C16)-coated CS/RSF: 70/30	70.29 ± 0.62

Condition: substance solution pH6.5 and loading time 3 h; SD: standard deviation, n = 3

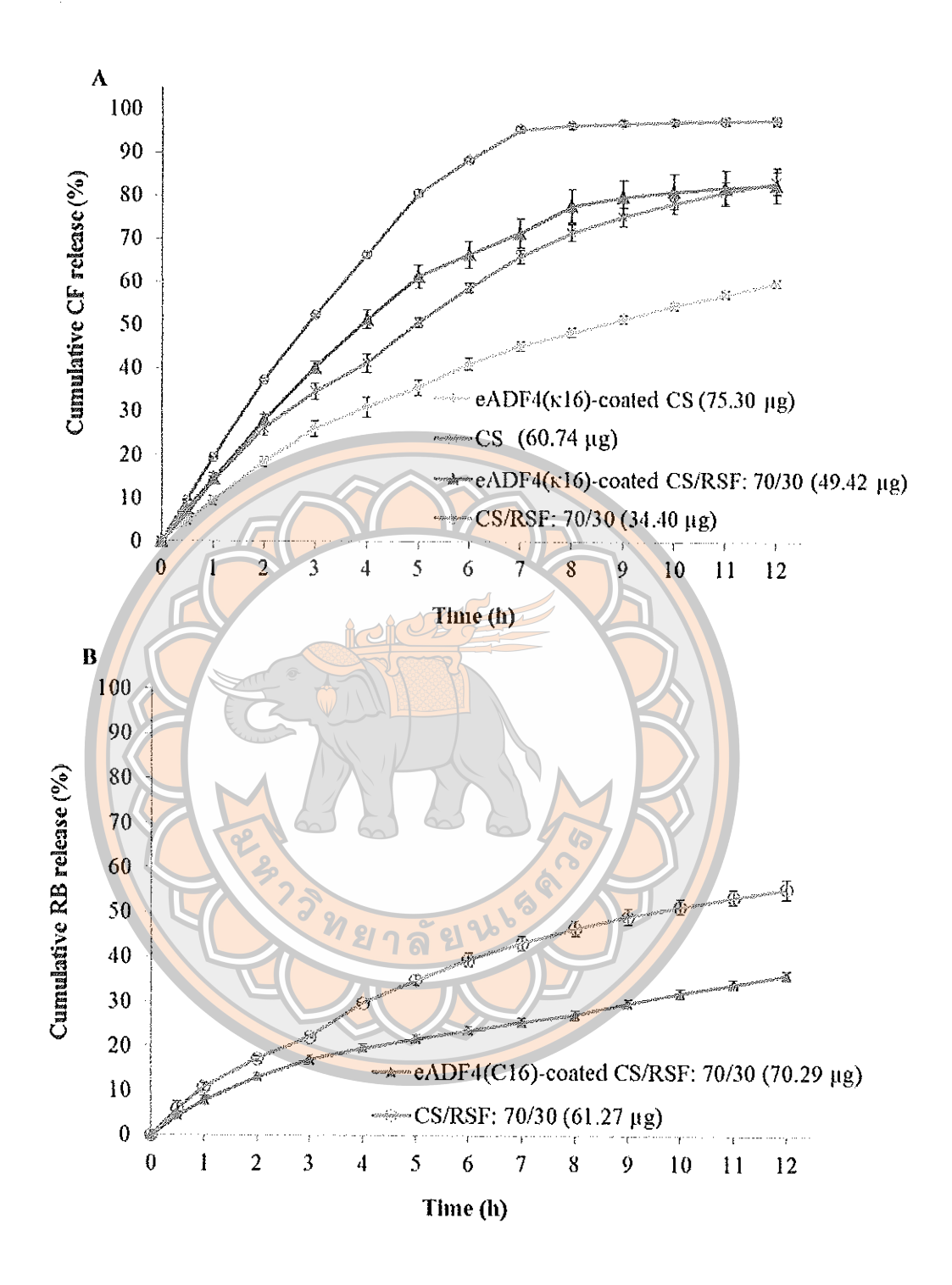


Figure 4.8 Cumulative release of CF (A) and RB (B) from uncoated and RSS coated CS/RSF blended films

L-b-L films-based CS and RSF

Material properties of L-b-L films-based CS and RSF

Several approaches have been tested to cast L-b-L films from CS and RSF, as represented in Figure 4.1. From the visual appearance, the L-b-L film formulations A, B, C and F showed a surfaces deformation due to film shrinkage. This is because the dried and post treated CS or CS/RSF layers could partially re-dissolve in acetic acid-based of CS or CS/RSF solutions in subsequent layer casting process in cases A and B. The films of formulation C deformed probably due to a surface tension between the relatively thick CS and RSF layers. On the other hand, formulation D and E (Figure 4.1) comprising layering of CS/RSF mixture (70/30) and neat RSF, respectively, showed smooth surface in SEM micrographs (Figure 4.9A) and were not brittle. Moreover, their cross-sectional analyses exhibited homogenous blending between CS and RSF matrix and no phase separation between the layers. However, the increasing number of the layers up to 7 (formulation F) resulted into rough surfaces again. It is likely possible that acetic acid in CS/RSF solution penetrated through thin RSF layer and re-dissolved the dried CS/RSF layer below. Therefore, only formulation D and E-based (CS/RSF)-RSF were further investigated.

Both types, D and E films, showed thickness of ~100 μm with similar thickness of each layer. Their light transparency in the visible range (381-780 nm) was > 90% and showed a significant protection against UV-B (280-315 nm) and UV-A (316-380 nm) light (Figure 4.9B). The Young's modulus of the L-b-L films were 7 and 6 MPa, respectively and their elongation at break of > 50% (Table 4.6) similarly to the blended films (42, 58-60). These films also showed high water content of 52 and 51 % by weight, respectively, and surface wettability similar to the blended CS/RSF films with contact angles of approximately 75° (Table 4.6)

Although the Tg values at 152°C were lower than those of the coated and uncoated blended films, the films are still suitable for autoclaving at 121°C (Figure 4.10) Oxygen permeability is an important parameter of contact lenses, decreasing the risk of corneal hypoxia, and providing wearing comfort. However, the oxygen permeability of 3 layer-(CS/RSF)-RSF films was 0.46 bar, which is very low in comparison with the blended CS/RSF films as well as commercial daily disposable contact lenses (10-33 bar) (57, 60). Nevertheless, due to the good mechanic and high

drug loading efficiency these L-b-L films could be suitable biogenic material formulations for development of drug delivery systems for occlusive dressings to treat burn wounds and scars.

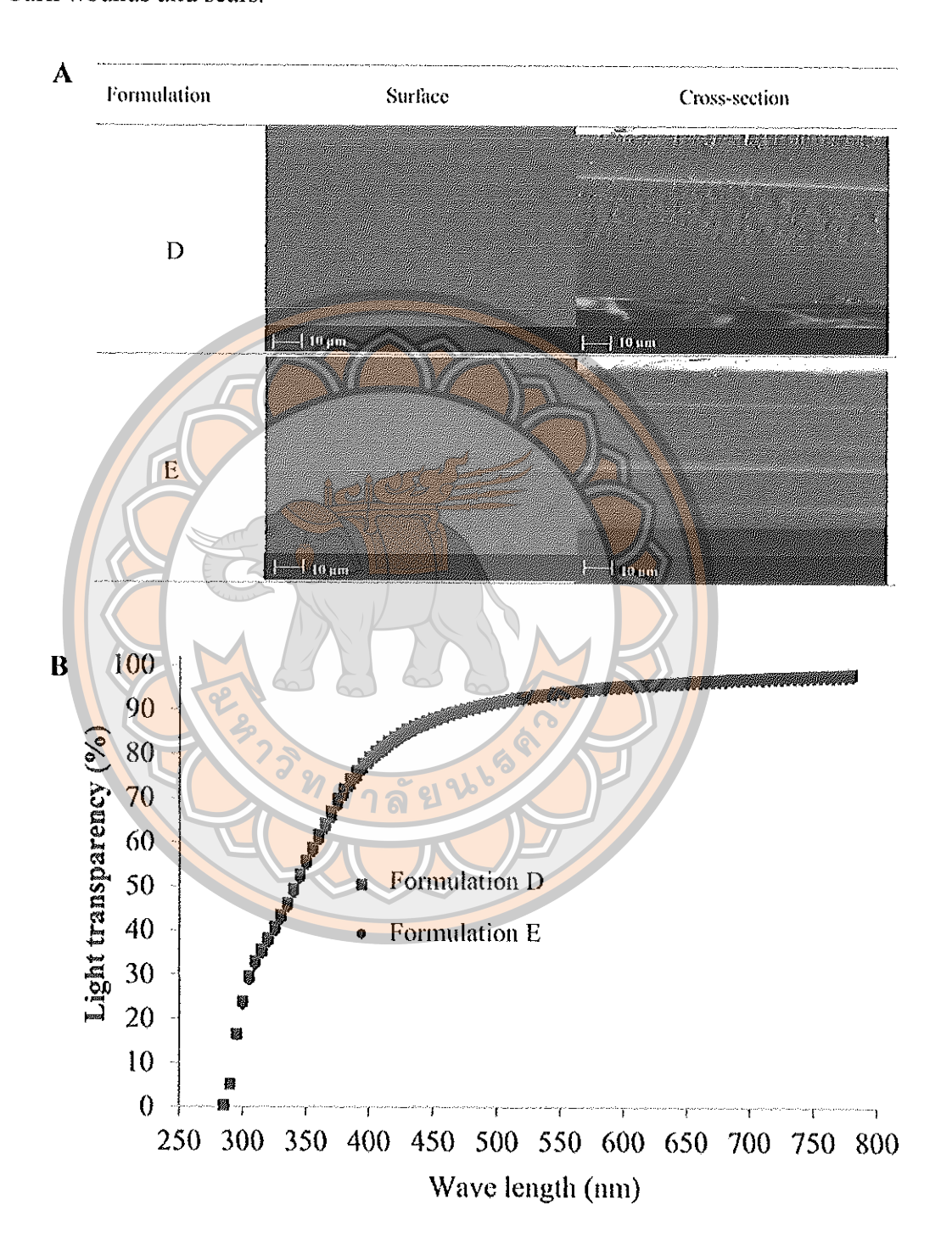


Figure 4.9 (A) SEM micrographs of surface and cross-section of L-b-L films (×1000 magnification) (B) Light transparency of L-b-L films

Table 4.6 Properties of L-b-L films-based CS and RSF

WZZALI ZAZI ZAZI ZAZI ZAZI ZAZI ZAZI ZAZI	Young's	Elongation at	Water content	Contact angle
Formulation	Modulus (Mpa)	break (%) ± SD	$(\%) \pm SD$	(°) ± SD
	± SD			
D	6.94 ± 0.94	55.54 ± 8.21	52 ± 0.92	75 ± 1.52
Е	6.08 ± 1.58	51.63 ± 6.80	51 ± 0.85	75 ± 1.65

SD: standard deviation, n = 3

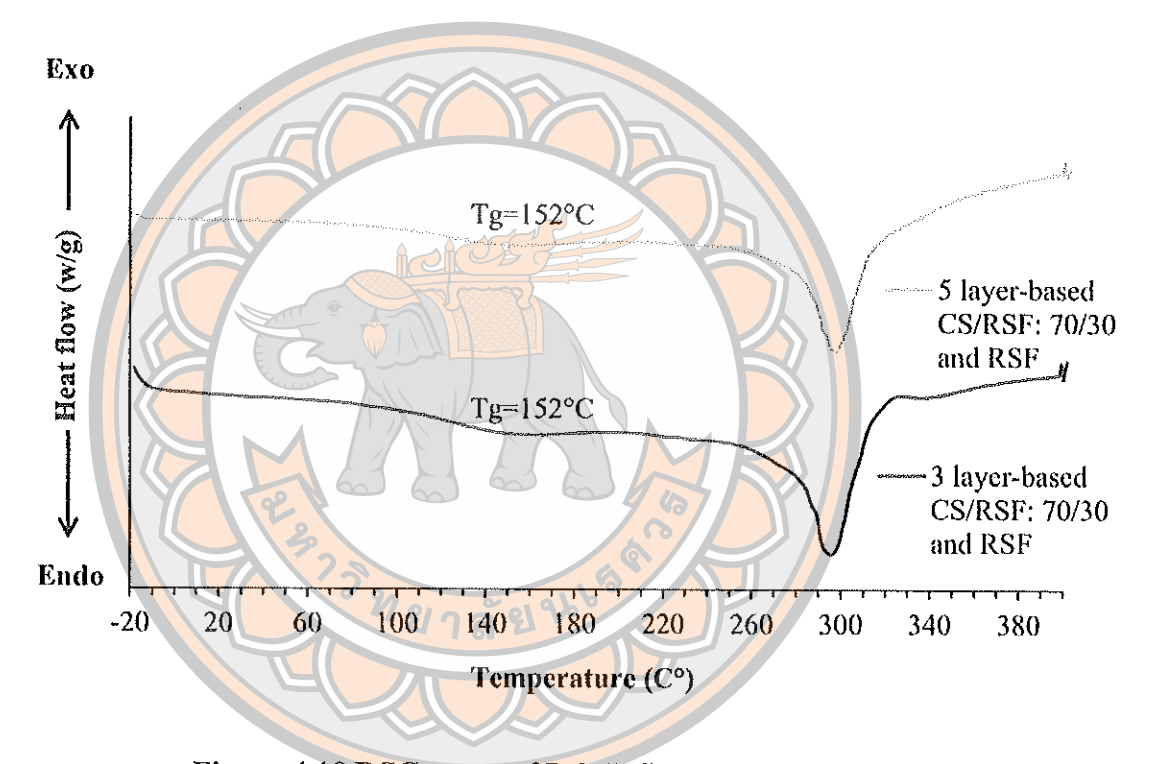


Figure 4.10 DSC curve of L-b-L films-based CS and RSF

Biodegradation of L-b-L films-based CS and RSF

The L-b-L film-based CS/RSF: 70/30 and RSF are constructed from CS, which can be hydrolyzed by the lysozyme presenting in tear fluids. Therefore, the remaining weight of 3 and 5 layer-based RSF and CS/RSF: 70/30 was determined upon their incubation in the STF containing lysozyme. Interestingly, all multilayer film-based CS/RSF: 70/30 and RSF showed no degradation after incubation in model STF containing lysozyme for 24 h.

Drug loading and in vitro release of L-b-L films-based CS and RSF

The 3- and 5-layer-films (D and E, Figure 4.1) showed the CF loading of 31.25 and 26.36 µg/10 mm³ of film, and RB loading of 81.81 and 86.28, µg/10 mm³ of film, respectively (Table 4.7). The combination of the layers in the formulation D and E increased the RSF content up to 53 and 58% (v/v), respectively, in comparison to blended films (highest content 30% in CS/RSF: 70/30 films). Thus the higher content of negatively charged RSF allowed increased RB loading in comparison to the blended films. Figure 4.11A illustrated the 3- and 5-layer-films resulted into fast release of negatively charged CF with nearly 100% released within 7 h. The CF release profiles from 3 layer and 5 layered films fit well to the Higuchi's model with regression coefficient = 0.90-0.95 supporting diffusion-controlled mechanism. Contrary, the L-b-L films showed prolonged release of zwitterion RB (42% and 36% for 3 and 5 layers, respectively) for 12 h, similarly to the eADF4(C16) coated CS/RSF blends (Figure 4.11A). The RB release profile revealed best fit to zero order model with regression coefficient = 0.98 with implying beneficial constant drug release rate.

Table 4.7 Drug loading into multilayer films-based CS and RSF

Formulation	5(6) carboxyfluorescein loading	Rhodamine B loading
	$(\mu g/10 \text{ mm}^3 \text{ of film}) \pm SD$	$(\mu g/10 \text{ mm}^3 \text{ of film}) \pm SD$
D	31.25 ± 0.55	81.81 ± 2.83
E	26.39 ± 0.46	86.28 ± 1.80

Condition: substance solution pH6.5 and loading time 3 h; SD: standard deviation,

n = 3

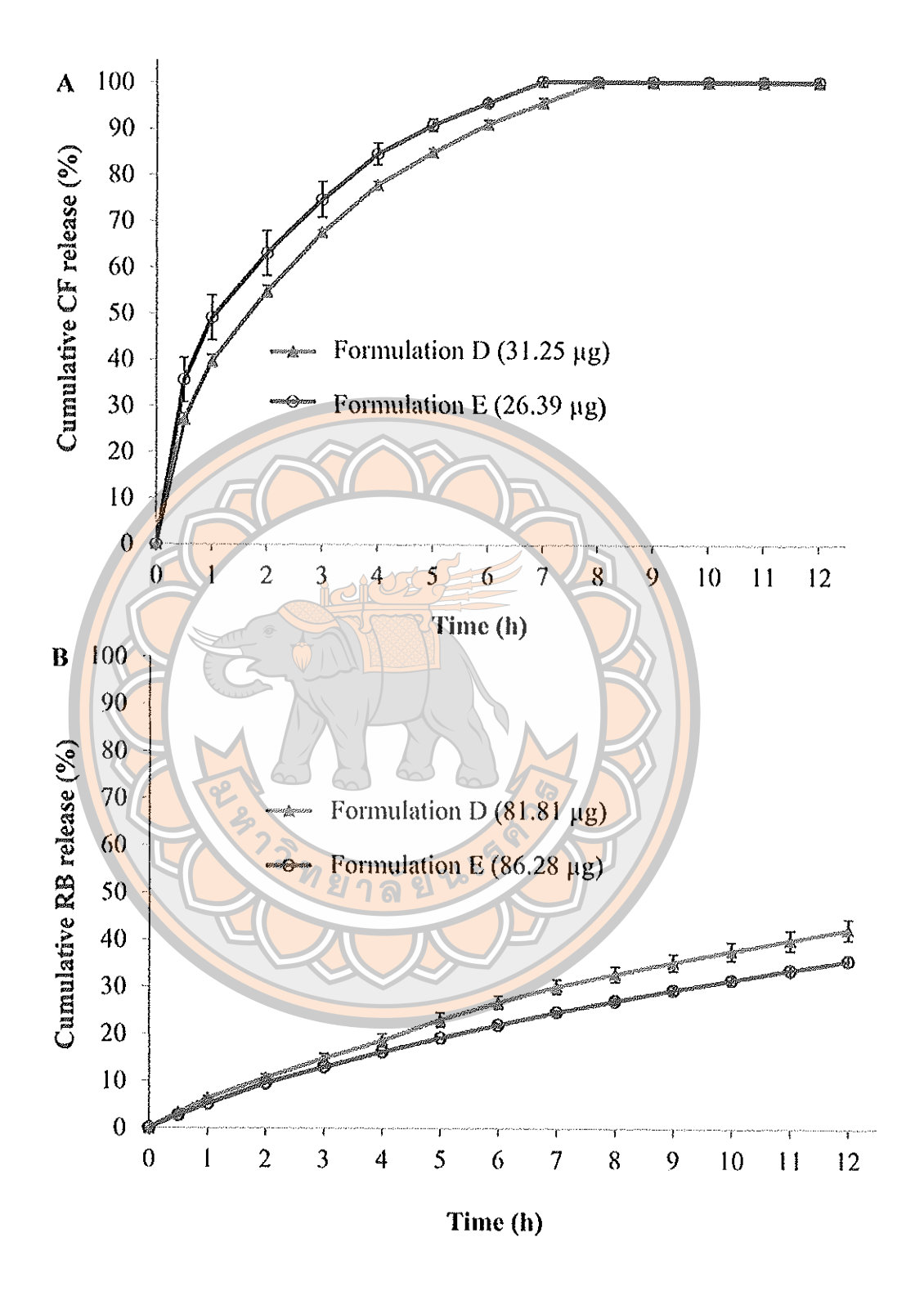


Figure 4.11 Cumulative release of CF in (A) and RB in (B) from the L-b-L films

Conclusion

The blended films prepared from CS/RSF mixtures have been shown as promising combination of biogenic materials for developments of daily disposable contact lenses-suitable for ophthalmic delivery of various charged drugs, which is beneficial for reducing drug side effects and administration frequency as compared to conventional contact lenses. The films fulfill physicochemical requirements in terms of VIS transparency, UV-A and B protection, mechanical properties, water contend and wettability. High glass transition at 150-160 °C allows decontaminations via autoclaving. In general, increased presence of CS in the films was supportive for the improved loading and release kinetics of negatively charged model drugs, whereas similar effects were observed also for negatively charged RSF and positively charged drugs in the films. Further improvements were achieved via positively and negatively charged variants of recombinant spider silk proteins used as coatings on the CS/RSF-based films. The negatively charged coating made of eADF4(C16) and positively charged coatings made of eADF4(k16) were advantageous for loading efficiency and long-term releases of positively and negatively charged drugs, respectively.

References

- 1. Bourlais CL, Acar L, Zia H, Sado PA, Needham T, Leverge R. Ophthalmic drug delivery systems. Progress Retinal Eye Research. 1998;17(1):33-58.
- 2. Lang JC. Ocular drug delivery conventional ocular formulations. Advanced Drug Delivery Reviews. 1995;16(1):39-43.
- 3. Ali M, Byrne ME. Challenges and solutions in topical ocular drug delivery systems. Expert Opinion on Drug Delivery. 2008;1(1):145-61.
- 4. Deshpande SG, Shirolkar S. Sustained release ophthalmic formulations of pilocarpine. J Pharm Pharmacol. 1989;41(3):197-200.
- 5. Geroski DH, Edelhauser HF. Drug delivery for posterior segment eye disease. Investigative Ophthalmology & Visual Science. 2000;41(5):961-4.
- 6. Hyun JJ, Anuj C. Ophthalmic drug delivery by contact lenses. Expert Review of Ophthalmology. 2012;7(3):199-201.

- 7. Winfield AJ, Jessiman D, Williams A, Esakowitz L. A study of the causes of non-compliance by patients prescribed eyedrops. British Journal of Ophthalmology. 1990;74(8):477-80.
- 8. Barbu E, Verestiuc L, Nevell TG, Tsibouklis J. Polymericmaterials for ophthalmic drug delivery: trends and perspectives. Journal of Materials Chemistry. 2006;16(36):3439-43.
- 9. Lin HR, Sung KC. Carbopol/pluronic phasechange solutions for ophthalmic drug delivery. Journal of Controlled Release. 2000;69(3):379-88.
- 10. Maulvi FA, Soni TG, Shah DO. A review on therapeutic contact lenses for ocular drug delivery. Drug Deliv. 2016;23(8):3017-026.
- 11. Xinming L, Yingde C, Lloyd AW, Mikhalovsky SV, Sandeman SR, Howel CA, Liewen L. Polymeric hydrogels for novel contact lens-based ophthalmic drug delivery systems: a review. Cont Lens Anterior Eye. 2008;31(2):57-64.
- 12. Guzman-Aranguez A, Colligris B, Pintor J. Contact Lenses: Promising Devices for Ocular Drug Delivery. Journal of Ocular Pharmacology and Therapeutics. 2013;29(2):189-99.
- 13. Gulsen D, Chauhan A. Dispersion of microemulsion drops in HEMA hydrogel: a potential ophthalmic drug delivery vehicle. Int J Pharm. 2005;292(1-2):95-117.
- 14. Tieppo A, Pate KM, Byrne ME. In vitro controlled release of an anti-inflammatory from daily disposable therapeutic contact lenses under physiological ocular tear flow. European Journal of Pharmaceutics and Biopharmaceutics. 2012;81(1):170-7.
- 15. Karlgard CCS, Wong NS, Jones LW, Moresoli C. In vitro uptake and release studies of ocular pharmaceutical agents by silicon-containing and p-HEMA hydrogel contact lens materials. International Journal of Pharmaceutics. 2003;257(1):141-51.
- 16. Lee D, Cho S, Park HS, Kwon I. Ocular Drug Delivery through pHEMA-Hydrogel Contact Lenses Co-Loaded with Lipophilic Vitamins. Sci Rep. 2016;6:34194.
- 17. McDermott ML, Chandler JW. Therapeutic uses of contact lenses. Survey of Ophthalmology. 1989;33(5):381-94.

- 18. Hsu K-H, Fentzke RC, Chauhan A. Feasibility of corneal drug delivery of cysteamine using vitamin E modified silicone hydrogel contact lenses. European Journal of Pharmaceutics and Biopharmaceutics. 2013;85(3, Part A):531-40.
- 19. Peng CC, Kim J, Chauhan A. Extended delivery of hydrophilic drugs from silicone-hydrogel contact lenses containing vitamin E diffusion barriers. Biomaterials. 2010;31(14):4032-47.
- 20. Sharma J. Moxifloxacin loaded contact lens for ocular delivery an in vitro study; 2018.
- 21. Lee D, Cho S, Park HS, Kwon I. Ocular Drug Delivery through pHEMA-Hydrogel Contact Lenses Co-Loaded with Lipophilic Vitamins. Scientific Reports. 2016;6:34194.
- 22. Gause S, Hsu KH, Shafor C, Dixon P, Powell KC, Chauhan A. Mechanistic modeling of ophthalmic drug delivery to the anterior chamber by eye drops and contact lenses. Adv Colloid Interface Sci. 2016;233:139-54.
- 23. Rachasit J, Manote S, Waree T. Preparation and characterization of chitosan/regenerated silk fibroin (CS/RSF) films as a biomaterial for contact lenses-based ophthalmic drug delivery system. International Journal of Applied Pharmaceutics. 2019;11(4):275-84.
- 24. Lindell K, Engblom J, Engström S, Jonströmer M, Carlsson A. Influence of a charged phospholipid on the release pattern of timolol maleate from cubic liquid crystalline phases. In: Lindman B, Ninham BW, editors. Darmstadt (pp. 111-8). N.P.: Steinkopff; 1998.
- 25. Hirano T, Yasuda S, Osaka Y, Kobayashi M, Itagaki S, Iseki K. Mechanism of the inhibitory effect of zwitterionic drugs (levofloxacin and grepafloxacin) on carnitine transporter (OCTN2) in Caco-2 cells. Biochimica et Biophysica Acta (BBA) Biomembranes. 2006;1758(11):1743-50.
- 26. Suzuki T, Yamamoto T, Ohashi Y. The antibacterial activity of levofloxacin eye drops against staphylococci using an in vitro pharmacokinetic model in the bulbar conjunctiva. Journal of Infection and Chemotherapy. 2016;22(6):360-5.

- 27. Patidar N, Rathore MS, Sharma DK, Middha A, Gupta VB. Transcorneal permeation of ciprofloxacin and diclofenac from marketed eye drops. Indian journal of pharmaceutical sciences. 2008;70(5):651-4.
- 28. Römer L, Scheibel T. Spinnenseidenproteine: Grundlage für neue Materialien. Chemie in unserer Zeit. 2007;41(4):306-14.
- 29. Vollrath F, Barth P, Basedow A, Engstrom W, List H. Local tolerance to spider silks and protein polymers in vivo. In Vivo. 2002;16(4):229-34.
- 30. Leal-Egana A, Scheibel T. Silk-based materials for biomedical applications. Biotechnol Appl Biochem. 2010;55(3):155-67.
- 31. Allmeling C, Jokuszies A, Reimers K, Kall S, Choi CY, Brandes G, Kasper C, Scheper T, Guggenheim M, Vogt PM. Spider silk fibres in artificial nerve constructs promote peripheral nerve regeneration. Cell Prolif. 2008;41(3):408-20.
- 32. Spiess K, Lammel A, Scheibel T. Recombinant spider silk proteins for applications in biomaterials. Macromol Biosci. 2010; 10(9):998-1007.
- 33. Humenik M, Smith A, Thomas S. Recombinant Spider Silks—Biopolymers with Potential for Future Applications; 2011.
- 34. Slotta U, Tammer M, Kremer F, Koelsch P, Scheibel T. Structural Analysis of Spider Silk Films. Supramolecular Chemistry. 2006;18(5):465-71.
- 35. Blum C, Scheibel T. Control of Drug Loading and Release Properties of Spider Silk Sub-Microparticles; 2012.
- 36. Huemmerich D, Helsen CW, Quedzuweit S, Oschmann J, Rudolph R, Scheibel T. Primary structure elements of spider dragline silks and their contribution to protein solubility. Biochemistry. 2004;43(42):13604-12.
- 37. Lammel A, Schwab M, Hofer M, Winter G, Scheibel T. Recombinant spider silk particles as drug delivery vehicles. Biomaterials. 2011;32(8):2233-40.
- 38. Hofer M, Winter G, Myschik J. Recombinant spider silk particles for controlled delivery of protein drugs. Biomaterials. 2012;33(5):1554-62.
- 39. Doblhofer E, Scheibel T. Engineering of recombinant spider silk proteins allows defined uptake and release of substances. J Pharm Sci. 2015;104(3):988-94.
- 40. Borkner CB, Elsner MB, Scheibel T. Coatings and Films Made of Silk Proteins. ACS Applied Materials & Interfaces. 2014;6(18):15611-25.

- 41. Kim KM, Son JH, Kim SK, Weller C, Hanna M. Properties of chitosan films as a function of pH and solvent type. Journal of Food Science E: Food Engineering and Physical Properties. 2006;71(3):119-24.
- 42. Tranoudis I, Efron N. Tensile properties of soft contact lens materials. Contact Lens and Anterior Eye. 2004;27(4):177-91.
- 43. Jung HJ, Abou-Jaoude M, Carbia BE, Plummer C, Chauhan A. Glaucoma therapy by extended release of timolol from nanoparticle loaded silicone-hydrogel contact lenses. Journal of Controlled Release. 2013;165(1):82-9.
- 44. Spelt JK, Rotenberg Y, Absolom DR, Neumann AW. Sessile-drop contact angle measurements using axisymmetric drop shape analysis. Colloids and Surfaces. 1987;24(2):127-37.
- 45. Moraes MAd, Nogueira GM, Weska RF, Beppu MM. Preparation and Characterization of Insoluble Silk Fibroin/Chitosan Blend Films. Polymers. 2010;2(4):719.
- 46. Chaiyasan W, Srinivas SP, Tiyaboonchai W. Mucoadhesive Chitosan–Dextran Sulfate Nanoparticles for Sustained Drug Delivery to the Ocular Surface. Journal of Ocular Pharmacology and Therapeutics. 2013;29(2):200-7.
- 47. Nwe N, Furuike T, Tamura H. The Mechanical and Biological Properties of Chitosan Scaffolds for Tissue Regeneration Templates Are Significantly Enhanced by Chitosan from Gongronella butleri. Materials. 2009;2(2):374-98.
- 48. Luangbudnark W, Viyoch J, Laupattarakasem W, Surakunprapha P, Laupattarakasem P. Properties and biocompatibility of chitosan and silk fibroin blend films for application in skin tissue engineering. ScientificWorldJournal. 2012;2012:697201.
- 49. She Z, Zhang B, Jin C, Feng Q, Xu Y. Preparation and in vitro degradation of porous three-dimensional silk fibroin/chitosan scaffold. Polymer Degradation and Stability. 2008;93(7):1316-22.
- 50. Maulvi FA, Mangukiya MA, Patel PA, Vaidya RJ, Koli AR, Ranch KM, Shah DO. Extended release of ketotifen from silica shell nanoparticle-laden hydrogel contact lenses: in vitro and in vivo evaluation. J Mater Sci Mater Med. 2016;27(6):113.

- 51. Bengani LC, Hsu KH, Gause S, Chauhan A. Contact lenses as a platform for ocular drug delivery. Expert Opin Drug Deliv. 2013;10(11):1483-96.
- 52. Peterson RC, Wolffsohn JS, Nick J, Winterton L, Lally J. Clinical performance of daily disposable soft contact lenses using sustained release technology. Contact Lens and Anterior Eye. 2006;29(3):127-34.
- 53. Maulvi DF. Effect of Timolol Maleate Concentration on Uptake and Release from Hydrogel Contact Lenses using Soaking Method. Journal of Pharmacy and Applied Sciences. 2014;1:16-22.
- 54. Lammel AS, Hu X, Park S-H, Kaplan DL, Scheibel TR. Controlling silk fibroin particle features for drug delivery. Biomaterials. 2010;31(16):4583-91.
- 55. Salome Amarachi C, Onunkwo G, Onyishi I. Kinetics and mechanisms of drug release from swellable and non swellable matrices: A review. Research Journal of Pharmaceutical, Biological and Chemical Sciences. 2013;4:97-103.
- Gonzalez-Meijome JM, Compañ-Moreno V, Riande E. Determination of Oxygen Permeability in Soft Contact Lenses Using a Polarographic Method: Estimation of Relevant Physiological Parameters. Industrial & Engineering Chemistry Research. 2008;47(10):3619-29.
- 57. Lee SE, Kim SR, Park M. Oxygen permeability of soft contact lenses in different pH, osmolality and buffering solution. Int J Ophthalmol. 2015;8(5):1037-42.
- 58. Horst CR, Brodland B, Jones LW, Brodland GW. Measuring the modulus of silicone hydrogel contact lenses. Optom Vis Sci. 2012;89(10):1468-76.
- 59. Tighe BJ. A decade of silicone hydrogel development: surface properties, mechanical properties, and ocular compatibility. Eye Contact Lens. 2013;39(1):4-12.
- 60. Selby A, Maldonado-Codina C, Derby B. Influence of specimen thickness on the nanoindentation of hydrogels: measuring the mechanical properties of soft contact lenses. J Mech Behav Biomed Mater. 2014;35:144-56.
- 61. Reynalyn M, Asim T, Raid G A, Amr E. Contact lenses: clinical evaluation, associated challenges and perspectives. Pharm Pharmacol Int J. 2017;5(3):78-88.
- 62. Scheibel T. Production and Processing of Spider Silk Proteins. Biopolymers with Application Potential for the Future. International Polymer Science and Technology. 2012;39(7):1-3.

- 63. Koev ST, Dykstra PH, Luo X, Rubloff GW, Bentley WE, Payne GF, Ghodssi R. Chitosan: an integrative biomaterial for lab-on-a-chip devices. Lab Chip. 2010;10(22):3026-42.
- 64. Bai J, Ma T, Chu W, Wang R, Silva L, Michal C, Chiao JC, Chiao M. Regenerated spider silk as a new biomaterial for MEMS. Biomed Microdevices. 2006;8(4):317-23.
- 65. Spiess K, Ene R, Keenan CD, Senker J, Kremer F, Scheibel T. Impact of initial solvent on thermal stability and mechanical properties of recombinant spider silk films. Journal of Materials Chemistry. 2011;21(35):13594-604.
- 66. Sack RA, Tan KO, Tan A. Diurnal tear cycle: evidence for a nocturnal inflammatory constitutive tear fluid. Invest Ophthalmol Vis Sci. 1992;33(3):626-40.
- 67. Carney FP, Morris CA, Willcox MDP. Effect of hydrogel lens wear on the major tear proteins during extended wear. Australian and New Zealand Journal of Ophthalmology. 1997;25(4):36-8.
- 68. Kadhm A, Alameer Z, Zubaidi A. Enzymatic degradation of chitosan blend for tissue engineering application. In AIP Conference Proceedings (p. 020017).

 USA: American Institute of Physics; 2019.
- 69. Takara EA, Marchese J, Ochoa NA. NaOH treatment of chitosan films: Impact on macromolecular structure and film properties. Carbohydrate Polymers. 2015;132:25-30.
- 70. Shi C, Zhu Y, Ran X, Wang M, Su Y, Cheng T. Therapeutic potential of chitosan and its derivatives in regenerative medicine. J Surg Res. 2006;133(2):185-92.

CHAPTER V

DAILY DISPOSABLE CONTACT LENSE BASED ON CHITOSAN AND REGENERATED SILK FIBROIN FOR THE OPHTHALMIC DELIVERY OF DICLOFENAC SODIUM

This chapter was published in Drug Delivery, volume 27, issue 1, page 782-790, accepted on 3 May 2020. It investigated to investigate the possibility of CS/RSF films as biomaterials for contact lenses based ophthalmic delivery for hydrophilic anti-inflammatory drug, diclofenac sodium (DS). The effects of drug loading parameters, loading time and pH drug solution, on drug loading of the films was studied. The effects of the film RSF content and the loaded drug content on drug loading and drug release characteristics of the films were observed. Moreover, the effects of DS loading on intrinsic contact lens properties, such as optical transparency and mechanical property, were also investigated.

Abstract

The aim of this study was to investigate the possibility of chitosan and regenerated silk fibroin (CS/RSF) blended films as novel biomaterials for daily disposable therapeutic contact lenses based ophthalmic drug delivery system. Diclofenac sodium (DS), a hydrophilic anti-inflammatory agent, was loaded into CS/RSF films by a soaking method. The best conditions of DS loading manifested the loading time of 2 h and pH 6.5 of drug solution. The drug loading capacity and the drug release profile could be controlled by varying the film RSF content. With increasing the film RSF content from 0 to 30%, the amount of loaded DS increased from 12 to 23 µg. Furthermore, the prolong drug released within therapeutic level was obtained with increasing the film RSF content. Consequently, a fast released characteristic within a therapeutic level up to 3 h was observed with the 100CS/0RSF film. On the other hand, the 70CS/30RSF film demonstrated a significant prolonged drug release within therapeutic level up to 11 h. In conclusion, the CS/RSF films are

promising as novel biomaterials for daily disposable therapeutic contact lenses-based ophthalmic delivery.

Keywords: Contact lenses, chitosan, regenerated silk fibroin, diclofenac sodium, drug release

Introduction

Topical eye drops in the form of solutions and suspensions are a common approach to treat ocular disorders because of their convenient and non-invasive application (1-3). However, a rapid drug clearance induced by a blink action leads to poor drug bioavailability with less than 5% of administered drugs entering the intraocular tissues (2, 4-6). Therefore, to maintain sustained therapeutic drug levels, frequent administration or large doses of eye drops are commonly required. However, this may reduce patient compliance, increase local and systemic side effects (2, 7-9).

To overcome these limitations, daily disposable contact lenses could be an interesting alternative approach (10-14). The daily disposable therapeutic contact lenses could increase the residence time of the drug leading to improved drug bioavailability, ~50%, and minimized drug side effects. In addition, they can be administered without surgery. Therefore, the platform of therapeutic contact lenses is considered as a non-invasive application that could enhance the patient compliance by elimination of multiple drug administration (12, 15-17).

Generally, most conventional hydrogel contact lenses based on poly (2-hydroxyethyl methacrylate) (pHEMA) was examined to deliver the hydrophilic ophthalmic drug by soaking the contact lenses in drug solution before insertion into the eyes (18-21). Although, more effective than eye drops in theory, but in practice, the conventional contact lenses have some limitations including low drug loading and a fast release characteristic within 1-3 h. Therefore, developing a new daily disposable contact lenses to effectively deliver the hydrophilic drug in a prolonged drug release pattern is still a challenging task.

In previous study, we successfully developed chitosan/regenerated silk fibroin (CS/RSF) blended films as the sustainable biomaterials for daily disposable contact lenses. The films have met material standards for daily disposable contact lenses (22). We propose that the incorporation of RSF into CS/RSF films with increasing

amorphous portion of the films would enhance the drug loading capacity and prolong the drugs release time. To test this hypothesis, diclofenac sodium (DS) was use as a hydrophilic model drug for drug loading and drug release study. DS is a non-steroidal anti-inflammatory drug which acts specifically on inflammatory sites and there by decreases the inflammation. It is also used as 0.1% eye drops to prevent post-operative inflammation in surgery and reduce the inflammation from corneal ulcer.

The aim of this study was to investigate the possibility of CS/RSF films as biomaterials for contact lenses based ophthalmic delivery for hydrophilic drug, DS. The effects of drug loading parameters, loading time and pH drug solution, on drug loading of the films was studied. The effects of the film RSF content and the loaded drug content on drug loading and drug release characteristics of the films were observed. Moreover, the effects of DS loading on intrinsic contact lens properties, such as optical transparency and mechanical property, were also investigated.

Materials and Methods

Materials

Chitosan shrimp (CS, > 90% deacetylation with mean molecular weight of 250 kDa) was obtained from Marine Bio Resources Co., Ltd (Samutsakhon, Thailand). Regenerated silk fibroin (RSF) was produced as previously reported (22). Polyethylene glycol 400 (PEG400) was purchased from Merck KGaA, (Darmstadt, Germany). Snakeskin pleated dialysis tube with MWCO at 10,000 Daltons was obtained from Thermo Fisher Scientific, Inc. (Illinois, USA). Diclofenac sodium (DS) was purchased from Sigma-Aldrich Co., Ltd (MO, USA.). All other chemicals and solvents were of analytical grade.

Preparation of CS/RSF films

CS/RSF films were prepared according to the optimum condition in our previous study (22). The films were prepared by a casting method. Briefly, 2% (w/v) of CS solution in acetic acid, 2% (w/v) of RSF aqueous solution in deionize water and PEG400 25 % (w/w) of polymer matrix were mixed using magnetic stirrer at 200 rpm for 30 min. The CS/RSF ratios were varied as 100/0, 90/10, 80/20 and 70/30 (v/v). The mixtures were then poured onto the polystyrene plates and dried in an oven at 60 °C. The dried films were immersed in 1M NaOH solution for 15 min, and then

repeatedly rinsed with deionize water until the neutral pH was obtained. The films were then soaked in 0.01M phosphate buffer saline (PBS) solution, pH 7.4 for 24 h and autoclaved at 121 °C and 15 psi for 20 min.

Drug loading by soaking method

DS solution was prepared by dissolving in 0.01M PBS. The DS solution was sterilized by filtration method using cellulose acetate membrane filter (pore size 0.22 μ m). Then the autoclaved film ($10\times10\times0.1~\text{mm}^3$) was soaked in 1 ml of DS solution for a predetermined time at room temperature in a laminar flow hood through UV light disinfection. After film soaking, the amount of free drug remaining in the DS solution was determined using UV-VIS spectrophotometer at 276 nm. Then, the amount of DS loading into the films was determined from the difference between the amount of initial drug and drug remaining in solution after film soaking. The loading parameters were varied as follows: the loading time was varied from 1 to 24 h; the pH of drug solution was varied from 6.5 to 8.5; and the concentration of initial DS solution was varied from 62.5 to 250 μ g/ml.

To confirm drug loading into the films, the morphology of the surface and cross-section of the DS loaded CS/RSF films were examined by a scanning electron microscope (SEM, Carl Zeiss AURIGA®, Thuringia, Germany). The samples were sputter-coated with platinum using a plasma sputter coater in order to obtain fine images via minimize electron charging on the surface.

In vitro drug release studies

In vitro drug release studies were carried out at 34 ± 1 °C. The DS loaded CS/RSF film ($10 \times 10 \times 0.1 \text{ mm}^3$) was placed into a micropipette tip, which fluid cavity of 30 µl. Then, the micropipette tip was inserted into a microtube and subjected to stimulated tear fluid (STF), pH 7.4, at a flow rate of 10 µl/min. The compositions of STF were sodium chloride 0.67 g, sodium bicarbonate 0.2 g, calcium chloride $^{\circ}2H_2O$ 0.008 g, and deionized water added to 100 g. At predetermined time intervals, the microtube was taken and replaced with a new microtube. The amount of DS released in microtube was then determined using UV-VIS spectrophotometer at 276 nm (23). The release profile of DS was evaluated by plotting graphs of cumulative drug release (µg) versus time and drug release rate (ng/h) versus time. All the experiments were carried out in triplicates.

Mathematical model for release kinetics and diffusion coefficient

The *in vitro* drug release results were fitted with different kinetic models, such as zero order, first order, and Higuchi, to understand the kinetics and mechanism of drug release. The plots of above models were analyzed by regression analysis and the regression coefficient (R²) values were calculated for the obtained linear curve (24- (24-26)).

Diffusion coefficient (D) of DS into CS/RSF films was observed by using Fickian diffusion model. Theoretical model was applied to determine diffusion of drug from the films. We considered the case in which the films are shaped like slab. The aspect ratio of the exposed surface diameter to the thickness is greater than 10, so we can assume diffusion is occurring in one dimension. The films immersed in an aqueous environment, the concentration of the diffusing drug is negligible in the bulk fluid outside the contact lens. The diffusion of drug from soaked films can be calculated according to equation (5.1) (27-28).

$$M = \frac{2AC_{p,o} \sqrt{Dt/\pi}}{}$$
(5.1)

In these equations, M is the mass of drug leached from film to STF medium (μg), A represents the area of films in contact with liquid (cm²), Cp,o is the initial concentration of drug in the film (μg /cm³), D is the diffusion coefficient of the drug from film to STF medium (cm²/s) and t is the migration time (s).

Estimation of therapeutic dose

The estimated therapeutic dose of DS was calculated based on Maulvi et al. (2016). DS eye drop solution (0.1% w/v) commonly recommended dose is one drop four time a day (29). Considering 1 drop \approx 50 μ l, thus the daily DS eye drop dose is 200 μ g (30). However, the ocular bioavailability through eye drop therapy is only ~1%, which suggests that the therapeutic requirement is ~2 μ g/day (31). Nevertheless, many scientific studies have proved that the bioavailability of drug to target tissue is more than 50 % through contact lenses (32-34). Assuming 50 % bioavailability, the therapeutic requirement of DS from contact lens is 4 μ g/day or 166 ng/h.

Physical properties of DS loaded CS/RSF films

The film thickness was measured with a thickness gauge (Holex Digital Micrometer, Munich, Germany). The measurement was taken at the center and at four positions around the perimeter of the hydrated films and then the average thickness was calculated (35).

The light transparency of the films were determined using UV-VIS spectrophotometer (Genesys 10S, Thermo scientific, Wisconsin, USA). The hydrated film with an average thickness of 100 µm was mounted on the outer surface of a quartz cuvette. The cuvette was placed in the spectrophotometer and the visible light transparency was measured at 381-780 nm (19).

The Young's modulus and elongation at break of the films with width of 3 mm and thickness of 0.1 mm were determined according to ASTM D882-12 using a universal testing machine (Zwick/Roell Z2.5, Ulm, Germany) with a load cell of 2 kg, a crosshead speed of 20 mm/min, and a gauge length of 10 mm (36).

The water content of the films was determined by measurement the weight of initial hydrated films (W_{wet}). Then, the films were allowed to dry at 105°C until weight constant (W_{dried}) (32). The water content of CS/RSF films were calculated according to equation (5.2)

Water content (%) =
$$((W_{wet} - W_{dried})/W_{wet}) \times 100$$
 (5.2)

The water content of drug loaded film was determined by measurement the weight of hydrated film after drying at 105° C until constant weight (W_{dried)}. The amount of drug loaded films was obtained from drug loading study (W_{drug)}. The hydrated drug loaded films was weighed for its initial weight (W_{wet}) (32). The water content of drug loaded film was calculated as shown in the following equation (5.3)

Water content (%) =
$$((W_{\text{wet}} - W_{\text{dried}} - W_{\text{drug}})/W_{\text{wet}}) \times 100$$
 (5.3)

Statistical analysis

The results were expressed as mean ± standard deviation (SD). For all comparisons, statistical significant differences were analyzed with paired t-test or one-

way ANOVA followed by Tukey's post hoc test, and P < 0.05 was considered statistically significant.

Results and discussion

The CS/RSF films were prepared following the optimum condition in our previous study (22). The derived CS/RSF films have met the material standards for daily disposable contact lenses requirement. The films possessed smooth surface with a high visible light transparency (> 90%) and high water content (59-65% by weight). They were also easy to handle with Young's modulus and elongation at break in the range of 6.4-7.2 MPa and 70-100%, respectively, and showed no degradation in STF containing lysozyme for 24 h. The films also showed high ion permeability of 11×10⁻³ mm²/min and oxygen permeability of 22-26 Barrers. Thus we further explored the possibility of using CS/RSF films as biomaterials for contact lenses based ophthalmic delivery of diclofenac sodium.

Drug loading capacity

One of the most conventional ways of loading a therapeutic drug into the contact lenses is the soaking method due to its cost-effectiveness and simplicity (37-38). To this end, the preformed contact lenses are immersed in the drug solution and the drug molecules can be adsorbed into the lenses surfaces and/or inner core. The drug loading capacity depends on the drug loading time, pH of drug solution and concentration of initial drug solution (11).

To study the effect of drug loading time, the films were soaked in 125 μ g/ml of DS solution, pH 6.5, with varying soaking time from 1 to 24 h. Table 5.1 illustrated that the amount of DS loading increased with increasing soaking time from 1 to 2 h and reached equilibrium at 2 h for all films ratios. Thus, the short drug loading time of 2 h suggesting its benefit for manufacturing process, comparing to conventional contact lenses which require drug loading time of 12-24 h (21, 39).

To investigate the effect of the drug solution pH on drug loading capacity, the films were soaked in 125 μ g/ml of DS solution with varying pH at 6.5, 7.4 and 8.5 for 2 h. When increasing the drug solution pH, the DS loading capacity was decreased (Table 5.2). All film ratios showed maximum drug loading at pH 6.5 and the minimum drug loading at pH 8.5. This could be explained by the pKa of DS. With increasing the

DS solution pH from 6.5 to 8.5 (>> pKa of DS = 4.15), the drug becomes more ionize from DS carboxylic acid groups leading to drug favors to diffuse from the films to aqueous solution.

The results indicated that DS can be loaded in all ratios of CS/RSF films. This could be explained by the intermolecular interaction, possible via hydrogen bonding and ionic interaction, between DS and CS or RSF. However, the amount of DS loading was increased with increasing the film RSF content. The 100CS/0RSF film gave the lowest DS loading capacity. On the other hand, the 70CS/30RSF film showed the highest DS loading capacity, which could be a result from its higher amorphous portion than 100CS/0RSF film, confirmed by DSC as discussed in our previous study (22). Thus, the high amorphous portion provides more space in the film, which could enhance drug adsorption in the film. This result was also correlated well with SEM micrographs, Figure 5.1. From SEM micrographs, DS was only illustrated on the outer surface of 100CS/0RSF, while DS was observed both outer surface and inner core of CS/RSF blended films. Notably, the higher ratios of RSF resulted in higher drug found in the inner core of films.

Therefore, the 70CS/30RSF film was selected to study the effect of drug concentration on drug loading capacity. The 70CS/30RSF film was soaked in three different DS concentrations (62.50, 125 and 250 µg/ml), pH 6.5, for 2 h. It can be seen that the drug loading capacity significantly increased proportionally with increasing the initial drug concentration, Table 5.3.

Table 5.1 Effect of drug loading time on drug loading capacity

Mass ratio of	Malayeyinin marana a sasasa sana sasasa s	Drug loading (μg)/10 mm³ of film				
CS/RSF (w/w)	1h	2h	3h	24h		
100/0	8.72 ± 0.63	11.82 ± 0.66	11.32 ± 0.42	11.85 ± 0.48		
90/10	10.36 ± 1.71	14.92 ± 1.55	14.70 ± 1.46	14.42 ± 1.33		
80/20	16.84 ± 1.79	18.69 ± 1.97	18.51 ± 1.80	18.30 ± 1.21		
70/30	16.91 ± 2.01	23.46 ± 0.57	23.46 ± 0.35	23.35 ± 1.04		

Condition: DS solution pH6.5, SD: standard deviation, n = 3

Table 5.2 Effect of pH of drug solution on drug loading capacity

Mass ratio of	Drug lo	ading (μg)/10 mm³ of	film
CS/RSF (w/w)	pH6.5	pH7.4	pH8.5
100/0	11.82 ± 0.66	5.84 ± 1.54	4.91 ± 1.10
90/10	14.92 ± 1.55	9.57 ± 1.25	5.70 ± 0.64
80/20	18.69 ± 1.97	10.61 ± 1.11	6.34 ± 0.91
70/30	23.46 ± 0.57	14.38 ± 2.12	10.68 ± 0.65

Condition: loading time 2 h, SD: standard deviation, n = 3

Table 5.3 Effect of concentration of initial drug solution on drug loading capacity

Concentration	of Division 3 cci.
DS sol <mark>u</mark> tion (µ	Drug loading (µg)/10 mm ³ of film
62.5	10.75 ± 1.33
125.0	23.46 ± 0.57
250.0	45.64 ± 0.67

Condition: DS solution pH6.5; loading time 2 h, n = 3

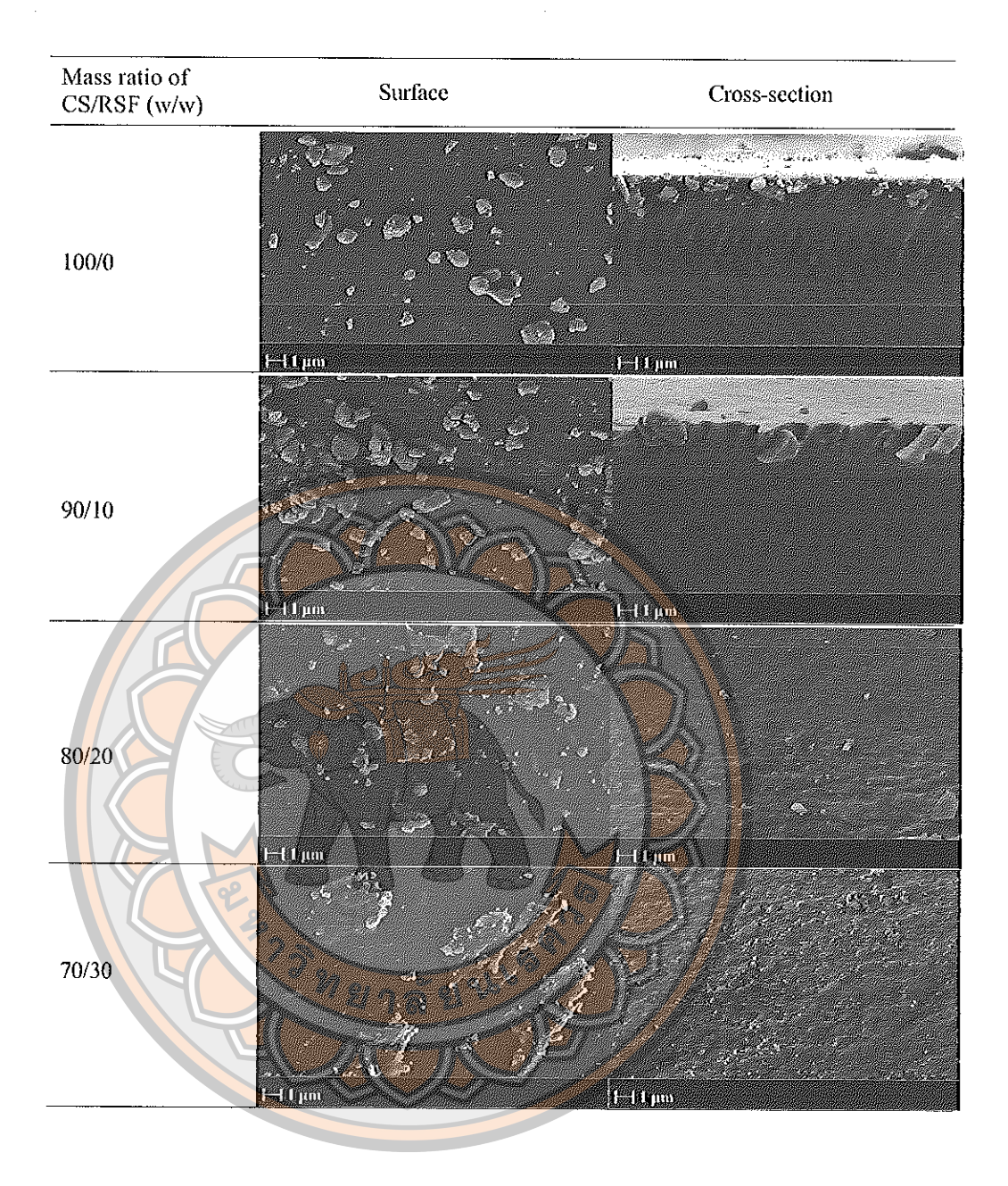


Figure 5.1 SEM micrographs of the surface and cross-section of DS loaded CS/RSF films, soaking in 125 μg/ml of DS solution, pH 6.5, for 2 h (×5000 magnification)

In vitro drug release studies

From the drug loading study, the best conditions of DS loading parameters were chosen. Therefore, all films ratios were soaked in 125 μ g/ml of DS solution, pH 6.5, for 2 h before performing the *in vitro* drug release studies.

The results illustrated that the 100CS/0RSF film showed a fast release characteristics with nearly 100% released within 3 h. On the contrary, a prolonged drug release characteristics was observed with increasing the film RSF content. The 90CS/10RSF, 80CS/20RSF, and 70CS/30RSF films showed a fast release during initial hours followed by a prolonged drug release up to 6, 9 and 11 h, respectively (Figure 5.2). Nevertheless, the drug release profiles of all tested CS/RSF films were best fitted to the Higuchi's model as shown in Table 5.4. This implies that the DS released from the films by a diffusion controlled mechanism. As expected, the 100CS/0RSF film manifested the highest diffusion coefficient of 1.63 × 10⁻⁸ (Table 5.4). Thus, the released DS was maintained within therapeutic level, 166 ng/h for only 3 h (Figure 5.3). This short acting time, although better than the eye drops, was not significantly different comparing to the conventional contact lenses. On the other hand, 90CS/10RSF, 80CS/20RSF, and 70CS/30RSF films showed a lower diffusion coefficient of 0.50×10^{-8} , 0.20×10^{-8} and 0.15×10^{-8} cm²/s, respectively (Table 4). Consequently, their drug therapeutic level was extended to 5, 9 and 11 h, respectively (Figure 5.3). To explain this phenomenon, the adsorbed drug locations effected the drug release profile significantly. Obviously, the drug located in the film surface immediately release into the media, contributing to the fast release phase. On the other hand, drug stayed in the inner core used longer time for dissolving and diffusion to outer surface, consequently attributed to the prolong release phase. These results correlated well with the film SEM micrographs (Figure 5.1). Thus, the higher RSF content resulted in an increase drug amount in the film inner core, hence, prolonging the drug release time.

To further extend the drug release duration, we hypothesized that it could be achieved by increasing the loaded drug content in the film. Thus, the 70CS/30RSF film was selected to study the effect of different amount of loaded drug, ~11, 24 and 46 μg, on the drug release profile. All films displayed similar drug release profiles, Figure 5.4. Accordingly, their diffusion coefficient of DS from the films was not significantly different, 0.14 -0.16×10⁻⁸ cm²/s (Table 5.5). These results suggested that the drug release duration was not extended with increasing amount of loaded drug in the film. Interestingly, the amount of drug release increased with increasing loaded drug content, Figure 5.5. The DS loaded film, 11 μg of DS, showed prolonged drug

release within the therapeutic window of 8 h, whereas the both DS loaded films, 23 and 46 μg of DS, showed prolonged drug release within the therapeutic window of 11 h. This result was in agreement with the Maulvi et al. They reported that the drug release duration within the therapeutic window of pHEMA-hydrogel contact lenses showed no significant enhancement with increasing amount of timolol maleate into the lenses (39).

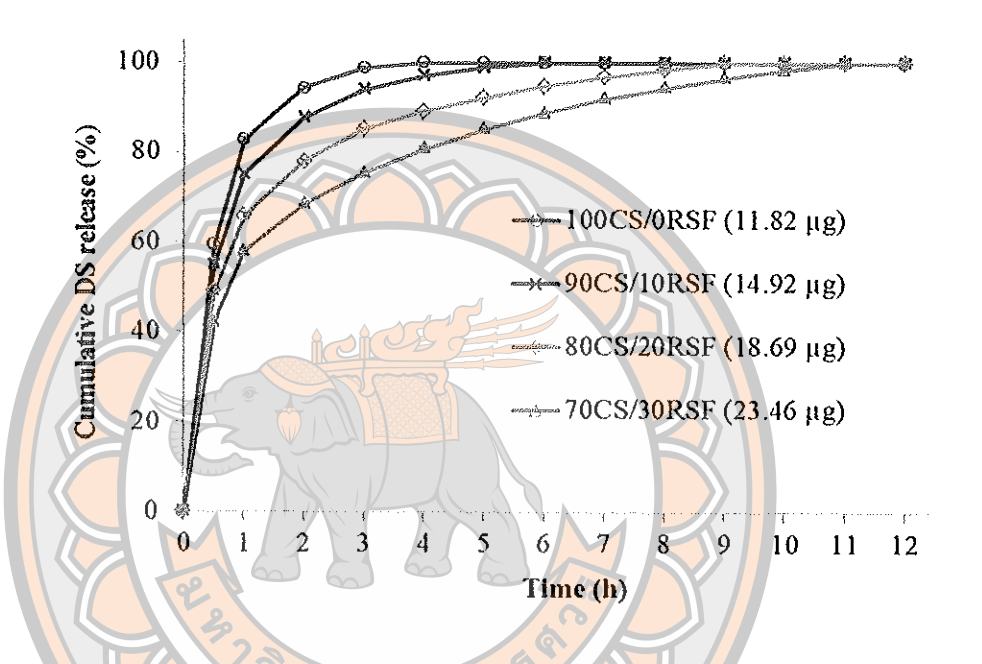


Figure 5.2 Cumulative DS release from CS/RSF films

Table 5.4 Drug release kinetic data of DS loaded CS/RSF films

Mass ratio CS/RSF (w/w)	Release time within therapeutic level (h)	Diffusion coefficient (×10 ⁻⁸ cm ² /s)	Regression coefficient, R ²
100/0	3	1.63	0.93
90/10	5	0.50	0.94
80/20	9	0.20	0.97
70/30	11	0.15	0.99

SD: standard deviation, n = 3

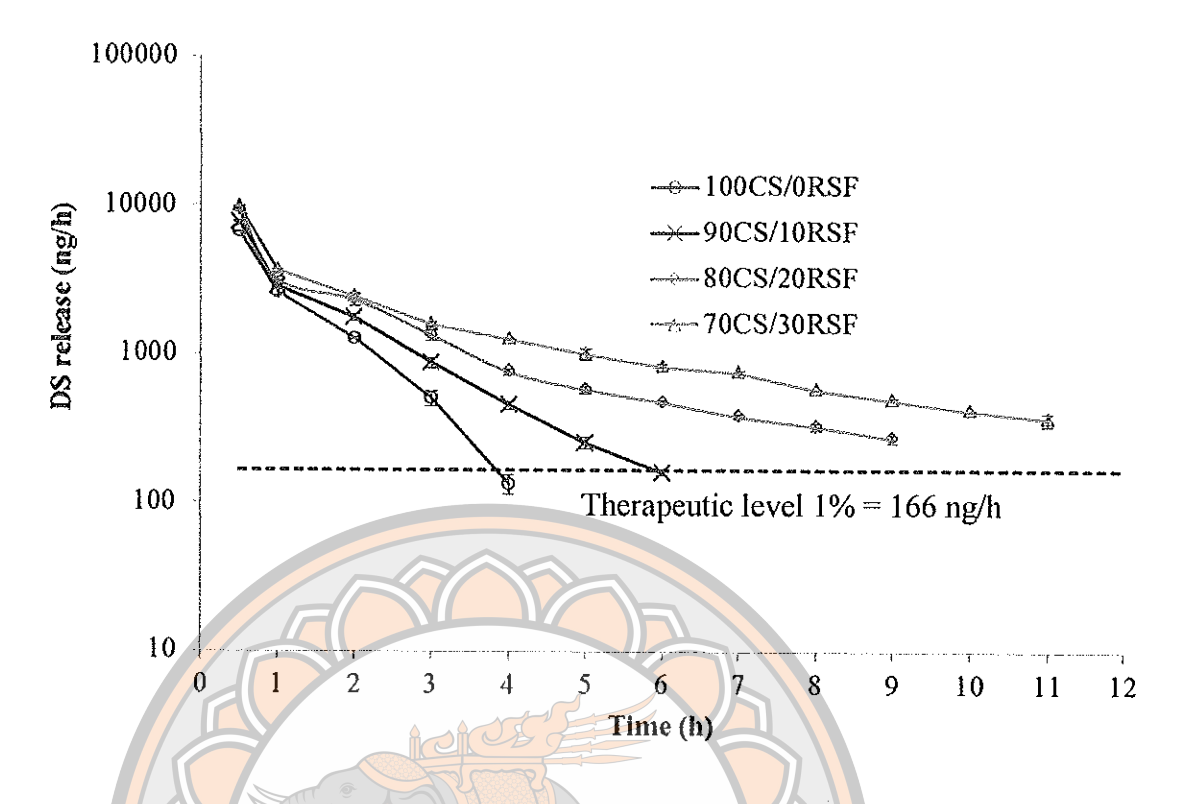


Figure 5.3 DS release from CS/RSF films compared with therapeutic level

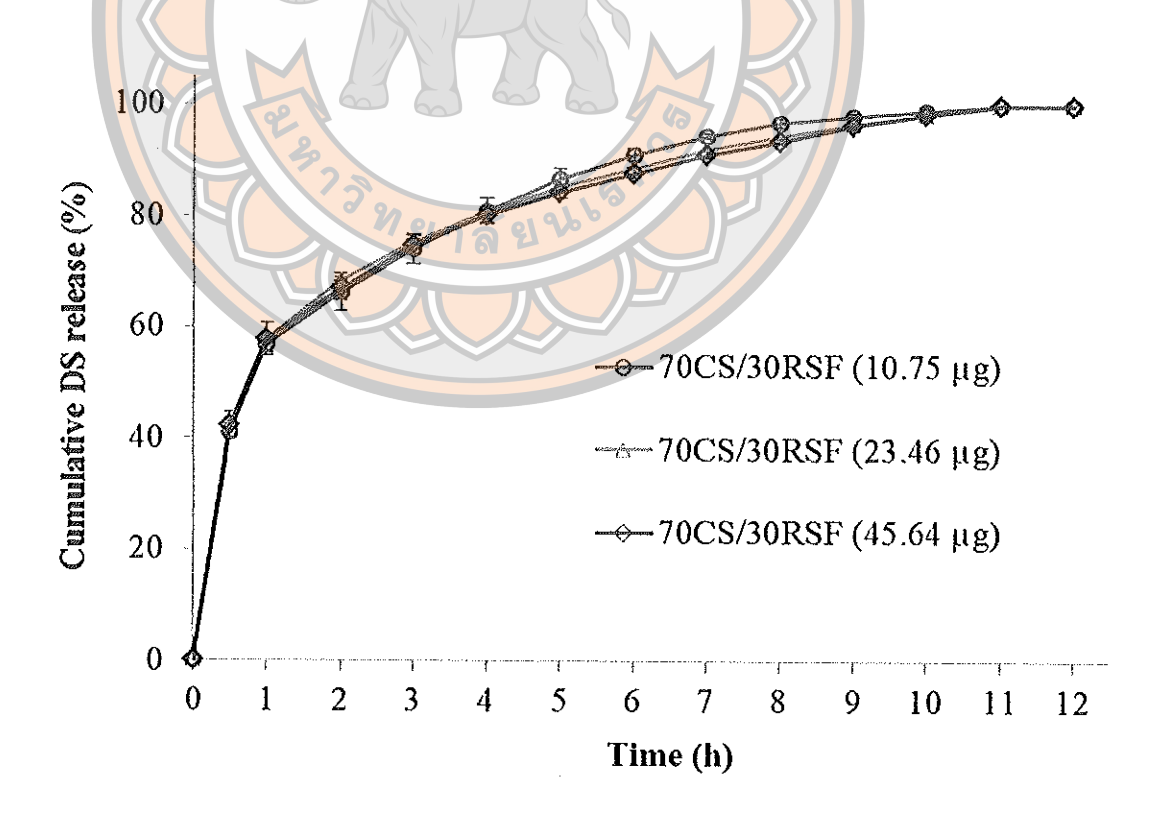


Figure 5.4 Cumulative DS release from 30CS/70RSF films with different loaded DS content

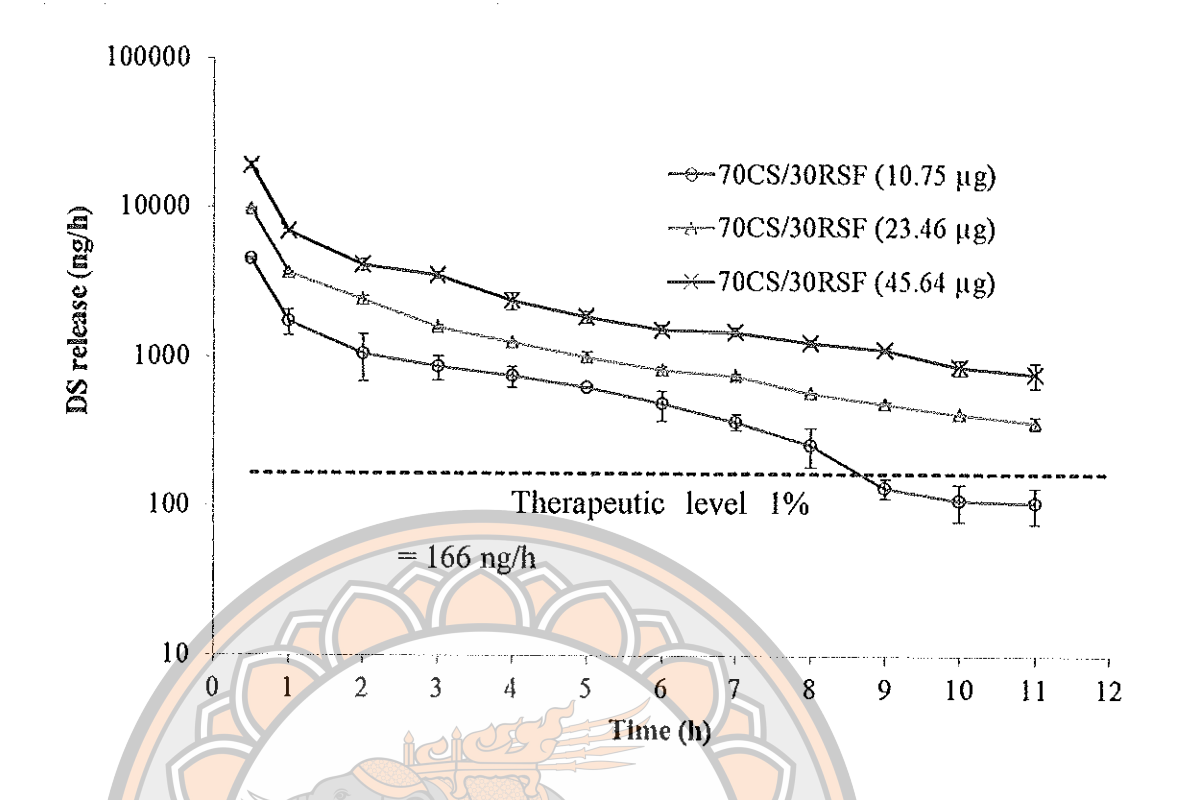


Figure 5.5 DS release from 70CS/30RSF films with different loaded DS content compared with therapeutic level

Table 5.5 Drug release kinetic data of 30CS/70RSF films with different loaded DS content

DS concentration	Drug loading (μg)/10 mm ³	Release time within	Diffusion coefficient	Regression coefficient (R ²)
(µg/ml)	of film ± SD	therapeutic level (h)	$(D\times10^{-8} \text{ cm}^2/\text{s})$	Higuchi
62.50	10.75 ± 1.33	8	0.16	0.95
125	23.46 ± 0.57	11	0.15	0.99
250	45.64 ± 0.67	11	0.14	0.99

SD: standard deviation, n = 3

Physical properties of DS loaded CS/RSF films

According to the drug release results, 70CS/30RSF film soaking in125 μg/ml of DS solution, pH 6.5 for 2 h was selected to further study the effect of drug loading on physical properties of films. The physical properties of the film and DS loaded-film showed no significant difference, Table 5.6. They manifest similar thickness of 100 ± 10 μm, which comply with typical commercial contact lenses having thickness of 50-200 μm (40-41). They showed high visible light transparency of > 90% which meet the visual requirement (42). They possessed Young's modulus of > 1.5 Mpa and the elongation at break of > 50% satisfying the stiffness and flexibility requirement of contact lens (36, 43-45). According to FDA's classification (46), they showed high water content implying that these films could promote the comfort for wearing. In summary, DS loading did not affect the intrinsic contact lens physical properties. Thus, the developed DS loaded CS/RSF films comply with the requirements for daily disposable contact lenses.

Table 5.6 Physical properties of 30CS/70RSF films and DS-loaded 30CS/70RSF films

AMPHANISH MATERIAL PROPERTY OF THE PROPERTY OF	Thickness	Light	Young's	Elongation	Water
Formulations	$(\mu m) \pm SD$	transparency	Modulus	at break	content
	TEC	(%) ± SD	$(Mpa) \pm SD$	(%) ± SD	(%) ± SD
70CS/30RSF	100 ± 10	93 ± 2	6.43 ± 1.00	72 ± 14	58 ± 0.84
DS loaded 70CS/30RSF	100 ± 10	92 ± 0	6.52 ± 1.00	72 ± 18	58 ± 1.36

SD: standard deviation, n = 3

Conclusion

DS as a hydrophilic model drug could be successfully loaded in the prepared CS/RSF films by the soaking method with a short drug loading time of 2 h. The DS loading did not affect the intrinsic contact lens properties of CS/RSF films. Essentially, the drug loading capacity and the drug released profile could be altered

favorable by varying the film RSF content. The drug loading capacity was increased with increasing the film RSF content. As the film RSF content increased, the more DS could be found in the inner core of the film. Consequently, a fast released characteristic within a therapeutic level up to 3 h was observed with the 100CS/0RSF film. On the contrary, the 70CS/30RSF film demonstrated a significant prolonged drug release within therapeutic level up to 11 h. In conclusion, the developed CS/RSF films are promising biomaterial for daily disposable contact lenses-based ophthalmic delivery, which is beneficial for reducing drug side effects and administration frequency as compared to conventional contact lenses.

References

- 1. Bourlais CL, Acar L, Zia H, Sado PA, Needham T, Leverge R. Ophthalmic drug delivery systems. Progress Retinal Eye Research. 1998;17(1):33-58.
- 2. Lang JC. Ocular drug delivery conventional ocular formulations. Advanced Drug Delivery Reviews. 1995;16(1):39-43.
- 3. Ali M, Byrne ME. Challenges and solutions in topical ocular drug delivery systems. Expert Opinion on Drug Delivery. 2008;1(1):145-61.
- 4. Deshpande SG, Shirolkar S. Sustained release ophthalmic formulations of pilocarpine. J Pharm Pharmacol. 1989;41(3):197-200.
- 5. Geroski DH, Edelhauser HF. Drug delivery for posterior segment eye disease. Investigative Ophthalmology & Visual Science. 2000;41(5):961-4.
- 6. Hyun JJ, Anuj C. Ophthalmic drug delivery by contact lenses. Expert Review of Ophthalmology. 2012;7(3):199-201.
- 7. Winfield AJ, Jessiman D, Williams A, Esakowitz L. A study of the causes of non-compliance by patients prescribed eyedrops. British Journal of Ophthalmology. 1990;74(8):477-80.
- 8. Barbu E, Verestiuc L, Nevell TG, Tsibouklis J. Polymericmaterials for ophthalmic drug delivery: trends and perspectives. Journal of Materials Chemistry. 2006;16(36):3439-43.
- 9. Lin HR, Sung KC. Carbopol/pluronic phasechange solutions for ophthalmic drug delivery. Journal of Controlled Release. 2000;69(3):379-88.

- 10. Maulvi FA, Soni TG, Shah DO. A review on therapeutic contact lenses for ocular drug delivery. Drug Deliv. 2016;23(8):3017-26.
- 11. Xinming L, Yingde C, Lloyd AW, Mikhalovsky SV, Sandeman SR, Howel CA, Liewen L. Polymeric hydrogels for novel contact lens-based ophthalmic drug delivery systems: a review. Cont Lens Anterior Eye. 2008;31(2):57-64.
- 12. Guzman-Aranguez A, Colligris B, Pintor J. Contact Lenses: Promising Devices for Ocular Drug Delivery. Journal of Ocular Pharmacology and Therapeutics. 2013;29(2):189-99.
- 13. Gulsen D, Chauhan A. Dispersion of microemulsion drops in HEMA hydrogel: a potential ophthalmic drug delivery vehicle. Int J Pharm. 2005;292(1-2): 95-117.
- 14. Tieppo A, Pate KM, Byrne ME. In vitro controlled release of an anti-inflammatory from daily disposable therapeutic contact lenses under physiological ocular tear flow. European Journal of Pharmaceutics and Biopharmaceutics. 2012;81(1):170-7.
- 15. Karlgard CCS, Wong NS, Jones LW, Moresoli C. In vitro uptake and release studies of ocular pharmaceutical agents by silicon-containing and p-HEMA hydrogel contact lens materials. International Journal of Pharmaceutics. 2003;257(1):141-51.
- 16. Lee D, Cho S, Park HS, Kwon I. Ocular Drug Delivery through pHEMA-Hydrogel Contact Lenses Co-Loaded with Lipophilic Vitamins. Sci Rep. 2016;6:34194.
- 17. McDermott ML, Chandler JW. Therapeutic uses of contact lenses. Survey of Ophthalmology. 1989;33(5):381-394.
- 18. Hsu K-H, Fentzke RC, Chauhan A. Feasibility of corneal drug delivery of cysteamine using vitamin E modified silicone hydrogel contact lenses. European Journal of Pharmaceutics and Biopharmaceutics. 2013;85(3, Part A):531-40.
- 19. Peng CC, Kim J, Chauhan A. Extended delivery of hydrophilic drugs from silicone-hydrogel contact lenses containing vitamin E diffusion barriers. Biomaterials. 2010;31(14):4032-47.
- 20. Sharma J. Moxifloxacin loaded contact lens for ocular delivery an in vitro study; 2018.

- 21. Lee D, Cho S, Park HS, Kwon I. Ocular Drug Delivery through pHEMA-Hydrogel Contact Lenses Co-Loaded with Lipophilic Vitamins. Scientific Reports. 2016;6:34194.
- 22. Rachasit J, Manote S, Waree T. Preparation and characterization of chitosan/regenerated silk fibroin (CS/RSF) films as a biomaterial for contact lenses-based ophthalmic drug delivery system International Journal of Applied Pharmaceutics. 2019;11(4):275-84.
- 23. Maulvi FA, Mangukiya MA, Patel PA, Vaidya RJ, Koli AR, Ranch KM, Shah DO. Extended release of ketotifen from silica shell nanoparticle-laden hydrogel contact lenses: in vitro and in vivo evaluation. J Mater Sci Mater Med. 2016;27(6):113.
- 24. Higuchi T. Mechanism of sustained-action medication. Theoretical analysis of rate of release of solid drugs dispersed in solid matrices. Journal of Pharmaceutical Sciences. 1963;52(12):1145-9.
- 25. Brazel CS, Peppas NA. Modeling of drug release from swellable polymers. European Journal of Pharmaceutics and Biopharmaceutics. 2000;49(1):47-58.
- Lapidus H, Lordi NG. Some factors affecting the release of a water-soluble drug from a compressed hydrophilic matrix. Journal of Pharmaceutical Sciences. 1966;55(8):840-3.
- 27. Piringer OG, Baner AL. Plastic Packaging: Interactions with Food and Pharmaceuticals (2nd ed.). USA: Wiley; 2008.
- 28. Rungchang S, Numthuam S, Qiu X, Li Y, Satake T. Diffusion coefficient of antimony leaching from polyethylene terephthalate bottles into beverages. Journal of Food Engineering. 2013;115(3):322-9.
- 29. Bodaghi B. Diclofenac sodium 0.1% ophthalmic solution: update on pharmacodynamics, clinical interest and safety profile. Expert Review of Ophthalmology. 2008;3(2):139-48.
- 30. Maulvi FA, Lakdawala DH, Shaikh AA, Desai AR, Choksi HH, Vaidya RJ, Ranch KM, Koli AR, Vyas BA, Shah DO. In vitro and in vivo evaluation of novel implantation technology in hydrogel contact lenses for controlled drug delivery. J Control Release. 2016;226:47-56.

- 31. Kearns VR, Williams RL. Drug delivery systems for the eye. Expert Rev Med Devices. 2009;6(3):277-90.
- 32. Jung HJ, Abou-Jaoude M, Carbia BE, Plummer C, Chauhan A. Glaucoma therapy by extended release of timolol from nanoparticle loaded silicone-hydrogel contact lenses. Journal of Controlled Release. 2013;165(1):82-9.
- 33. Bengani L, Chauhan A. Are contact lenses the solution for effective ophthalmic drug delivery? Future Medicinal Chemistry. 2012;4(17):2141-3.
- 34. Li C-C, Chauhan A. Modeling Ophthalmic Drug Delivery by Soaked Contact Lenses. Industrial & Engineering Chemistry Research. 2006;45(10):3718-34.
- 35. Kim KM, Son JH, Kim SK, Weller C, Hanna M. Properties of chitosan films as a function of pH and solvent type. Journal of Food Science E: Food Engineering and Physical Properties. 2006;71(3):119-24.
- 36. Tranoudis I, Efron N. Tensile properties of soft contact lens materials. Contact Lens and Anterior Eye. 2004;27(4):177-91.
- 37. Bengani LC, Hsu KH, Gause S, Chauhan A. Contact lenses as a platform for ocular drug delivery. Expert Opin Drug Deliv. 2013;10(11):1483-96.
- Peterson RC, Wolffsohn JS, Nick J, Winterton L, Lally J. Clinical performance of daily disposable soft contact lenses using sustained release technology. Contact Lens and Anterior Eye. 2006;29(3):127-34.
- 39. Maulvi DF. Effect of Timolol Maleate Concentration on Uptake and Release from Hydrogel Contact Lenses using Soaking Method. Journal of Pharmacy and Applied Sciences. 2014;1:16-22.
- 40. Gonzalez-Meijome JM, Compañ-Moreno V, Riande E. Determination of Oxygen Permeability in Soft Contact Lenses Using a Polarographic Method: Estimation of Relevant Physiological Parameters. Industrial & Engineering Chemistry Research. 2008;47(10):3619-29.
- 41. Lee SE, Kim SR, Park M. Oxygen permeability of soft contact lenses in different pH, osmolality and buffering solution. Int J Ophthalmol. 2015;8(5):1037-42.
- 42. Lai C-F, Li J-S, Fang Y-T, Chien C-J, Lee C-H. UV and blue-light antireflective structurally colored contact lenses based on a copolymer hydrogel with amorphous array nanostructures. RSC Advances. 2018;8(8):4006-13.

- 43. Horst CR, Brodland B, Jones LW, Brodland GW. Measuring the modulus of silicone hydrogel contact lenses. Optom Vis Sci. 2012;89(10):1468-76.
- 44. Tighe BJ. A decade of silicone hydrogel development: surface properties, mechanical properties, and ocular compatibility. Eye Contact Lens. 2013;39(1):4-12.
- 45. Selby A, Maldonado-Codina C, Derby B. Influence of specimen thickness on the nanoindentation of hydrogels: measuring the mechanical properties of soft contact lenses. J Mech Behav Biomed Mater. 2014;35:144-56.
- 46. Reynalyn M, Asim T, Raid G A, Amr E. Contact lenses: clinical evaluation, associated challenges and perspectives. Pharm Pharmacol Int J. 2017;5(3):78-88.



CHAPTER VI

CONCLUSION

This study introduced the development, characterizations, drug loading and drug release characteristics studies of chitosan/regenerated silk fibroin (CS/RSF) films as a biomaterial for contact lenses-based ophthalmic drug delivery system.

Firstly, the CS/RSF films at ratios of 100/0, 90/10, 80/20 and 70/30 (w/w) showed high visible light transparency, smooth surface morphology and their cross-sections exhibited homogenous blending between CS and RSF without phase separation. With increasing RSF content, oxygen permeability, and thermal stability of the prepared films increased whereas the mechanical properties and water content of the prepared films slightly decreased. Moreover, all prepared films showed high thermal stability, high Young's modulus and elongation at brake. All prepared films were softness with high strength characteristics, good oxygen and ion permeability, high water content, no cytotoxicity and no degradation in STF containing lysozyme for 7 days implying that prepared films were biocompatible and could promote the comfort for wearing without irritation and grittiness in the eyes.

Secondly, non-charged APAP, negatively charged CF and zwitterion RB were use as hydrophilic model drug. Non-charged APAP cannot load in the CS/RSF films. Interestingly, negatively charged CF and zwitterion RB could be successfully loaded in the films. The best conditions of CF and RB loading is the loading time of 3 h and pH 6.5 of drug solution. The substance loading did not affect the intrinsic contact lens properties of films. The CS/RSF ratio significantly affected the substance loading capacity. The negatively charged CF loading capacity was increased with increasing the CS ratio. In contrast, the zwitterion RB loading capacity was increased with increasing the RSF ratio. Thus, the CS and CS/RSF: 70/30 films showed the highest substance loading of negatively charged CF and zwitterion RB, respectively and prolonged released more than 12 h. Essentially, RSS coatings on CS/RSF films significantly increased the substances loading efficiency and also decreased drug released rate with prolonged substance release more than 12 h. In addition, the L-b-L

films-based CS/RSF: 70/30 and RSF enhanced loading capacity of positive charge RB and also prolonged this substance more than 12 h. Unfortunately, L-b-L layer films were not appropriate for use as a material for therapeutic daily disposable contact lenses because of low oxygen permeability. Nevertheless, these films could be potential as a drug delivery system for applications which require oxygen barrier or occlusive dressing.

Thirdly, diclofenac sodium (DS), a hydrophilic anti-inflammatory agent, could be successfully loaded in the prepared CS/RSF films by the soaking method with a short drug loading time of 2 h. The DS loading did not affect the intrinsic contact lens properties of CS/RSF films. Essentially, the drug loading capacity and the drug released profile could be altered favorable by varying the film RSF content. The drug loading capacity was increased with increasing the film RSF content. As the film RSF content increased, the more DS could be found in the inner core of the film. Consequently, a fast released characteristic within a therapeutic level up to 3 h was observed with the 100CS/0RSF film. On the contrary, the 70CS/30RSF film demonstrated a significant prolonged drug release within therapeutic level up to 11 h.

In conclusion, the developed CS/RSF films are promising biomaterial for daily disposable contact lenses-based ophthalmic delivery, which is beneficial for reducing drug side effects and administration frequency as compared to conventional contact lenses.